UNIVERSITY OF CALIFORNIA
RIVERSIDE

Perturbation of Protein Ubiquitination and Mechanisms of Arsenic Toxicity

A Dissertation submitted in partial satisfaction
of the requirements for the degree of

Doctor of Philosophy

in

Cell, Molecular, and Developmental Biology

by

Ji Jiang

March 2018

Dissertation Committee:
Dr. Yinsheng Wang, Chairperson
Dr. Frances M. Sladek
Dr. Quan Jason Cheng

The Dissertation of Ji Jiang is approved:

Committee Chairperson

University of California, Riverside

ACKNOWLEGEMENT

I could never complete my dissertation without help and support from all the lovely people around me. I'm so grateful to have all of them in my life during my PhD study at UC-Riverside.

First of all, I would like to thank my advisor, Professor Yinsheng Wang, for all that he has done to help me throughout my PhD period. I always remember that he accepted me without any doubt when I decided to switch a lab at the first year, and financially supported me to help me get through the difficult time. His guidance and mentorship has always been leading me in the scientific world, which encourages me to become well-trained scientist with independent thinking. Not only in the scientific world, his warm personality and passionate attitudes also inspired me to become a better person in my whole life.

I would also like to acknowledge Professor France M. Sladek and Professor Quan Jason Cheng for being my committee for my dissertation, and giving me precious suggestions and comments on my research. I also thank Professor France M. Sladek, Professor Xuemei Chen, Professor Xin Ge and Professor Aihui Huang for being my committee for my oral qualification exam and offering me guidance. I appreciate Professor France M. Sladek, Professor Xuemei Chen, Professor Jeff Bachant, Professor Karine Le Roch, Professor Morris Maduro, Professor Manuela Martins-Green and Professor Shou-Wei Ding for being my teachers and teaching me knowledge in the class.

I would also thank the stuff members in CMDB program, Kathy Redd and Julio E Sosa for helping me deal with all the documents and procedures, Dr. Star Lee and Dr. Kevin Simpson for training me as a teaching assistant, Dr. David Carter for the confocal microscopy training, Dr. Holly Eckelhoefer for her help with flow cytometry, and Dr. Ronald New for his guidance n using MALDI-TOF mass spectrometer.

In addition, I feel so lucky working in Dr. Wang's lab with all my group members. I would like to thank Dr. Fan Zhang, Dr. Qian Cai, Dr. Shuo Liu and Dr. Lijuan Fu for their generous help and patience in teaching me doing all the research experiments when I first came to the lab. I thank Dr. Lin li, Dr. Xiaoxia Dai, Dr. Pengcheng Wang and Mr. Lok Ming Tam for their help with my research projects. I would also like to thank all the other members in Wang's lab for their consistent support and friendship.

In the end, I would like to thank my family and all my friends for their unconditional love and support for me during all these years.

COPYRIGHT ACKNOWLEDGEMENTS

The text and figures of this dissertation in chapter 2, in part or in full, is a reprint of the material as it appears in ACS Chemical Biology, 2017, 12 (7), pp 1858–1866. The co-author Dr. Yinsheng Wang listed in that publication directed and supervised the research, which forms the basis for this dissertation. The co-author Dr. Marina Bellani and Dr. Michael M. Seidman helped with the immunofluorescent microscopy experiments in this publication. Dr. Lin Li provided valuable advise for the biotin-As pull down experiments in this publication. Dr. Pengcheng Wang helped with the synthesis of biotin-As probe in this publication.

ABSTRACT OF THE DISSERTATION

Perturbation of Protein Ubiquitination and Mechanisms of Arsenic Toxicity

by

Ji Jiang

Doctor of Philosophy, Graduate Program in Cell, Molecular and Developmental Biology, University of California, Riverside, March 2018
Dr. Yinsheng Wang, Chairperson

Arsenite exposure through drinking water and food has long been a health concern because of its cellular toxicity and carcinogenic effects in inducing various cancers and cardiovascular diseases. This dissertation research focused on exploring the underlying mechanisms accounting for arsenite toxicity. In particular, I explored the binding of trivalent arsenic to E3 ubiquitin ligases to suppress ubiquitination of their substrate proteins, where ubiquitination serve as important signals in multiple functional pathways and proteasome-mediated degradation of proteins.

In chapter 1, I briefly described the background of arsenite toxicity and the role of ubiquitination in cells. I also introduced the application of LC-MS for proteomic analysis, especially the ubiquitin-modified proteome. By employing LC-MS/MS couple with SILAC labeling and affinity enrichment, I was able to identify ~1500 ubiquitinated peptides, of which ~40% peptides were decreased upon arsenite exposure. I conducted a KEGG pathway analysis and functional categories of the identified proteins and was able to find some

interested protein targets, including FANCD2 and HMGCR that were studied in chapters 2 and 3, respectively.

The LC-MS/MS results showed a 50% decrease of FANCD2-K561 ubiquitination upon arsenite treatment. I further demonstrated, for the first time, that arsenite targets the RING finger domain of the E3 ubiquitin ligase, FANCL, to suppress FANCD2 ubiquitination, using MALDI-TOF mass spectrometry, and biotin-As pull down coupled with Western blot analysis. This interaction was also found to impair chromatin localization of FANCD2, which is crucial for recruiting downstream repair factors for DNA interstrand crosslink repair. Therefore, I revealed, for the first time, a role of arsenite in perturbing the Fanconi anemia pathway for DNA interstrand crosslink repair by targeting the RING finger of FANCL E3 ubiquitin ligase and inhibiting FANCD2 monoubiquitination.

The LC-MS/MS results also detected a 70% decrease of HMGCR-K248 ubiquitination upon arsenite treatment, which is important for HMGCR degradation and for maintaining cholesterol homeostasis in mammalian cells. Indeed I found that arsenite could stabilize HMGCR protein level by inhibiting its ubiquitination. This finding suggests a role of arsenite in affecting the cholesterol biosynthesis pathway.

In chapter 4, I further expanded the role of arsenite in targeting E3 ubiquitin ligase by measuring the interaction between arsenite and the E3 ubiquitin ligase RBX1, which is responsible for Nrf2 ubiquitination. This provides a novel insight in arsenite-mediated activation of antioxidant response.

Together, the research in this thesis provided novel insights into the

mechanisms of arsenic toxicity.

Table of Content

LIST OF FIGURES

The P values were calculated using two-tailed, unpaired Student's t test.

Figure 2.7 Streptavidin agarose affinity assay revealed the interaction between As3+ and FANCL protein in HEK293T cells. The interaction was diminished after pretreatment with 10 μM NaAsO2 or PAPAO, but not Zn2+.

Figure 2.8 a) The Western blot result revealed that As3+ exposure elicited reduced ubiquitination of FANCD2 in the lysate of HeLa cells after As3+ exposure upon ICL induction by MMC. b) Quantitative data of relative levels of FANCD2 ubiquitination after MMC treatment. The data represent the mean and standard deviation of results obtained from three biological replicates.

Figure 2.9 a) As3+ exposure diminished the ubiquitination level of FANCD2 and perturbed its chromatin localization. "CF" and "SF" designate the chromatin and soluble fractions, respectively. b) Quantitative data of total FANCD2 level in chromatin fractions. The levels of FANCD2 were represented as the ratio of FANCD2/histone H3 in chromatin fractions, and the relative level of FANCD2 in the control group was normalized to unity.

Figure 2.10 a) Levels of FANCD2-ub were diminished upon arsenite treatment in a dose dependent manner. b) The relative levels of FANCD2 ubiquitination were calculated as the ratios of FANCD2-ub over unmodified FANCD2 in chromatin fractions, and the ratio for the control group was normalized into unity. *P < 0.05; **P < 0.01; ***P < 0.001. The P values were calculated using two-tailed, unpaired Student's t test.

Figure 2.11 MS results for FANCD2 K561 ubiquitination from the forward and reverse SILAC labeling samples. In the forward sample, cells cultured in light SILAC medium were treated with 5 μM NaAsO2 for 24 h and mixed with an equal amount of lysate from untreated cells cultured in heavy SILAC medium. In the reverse sample, lysate of cells cultured in heavy medium and treated with 5 μM NaAsO2 was mixed with an equal amount of lysate of untreated cells cultured in light medium. The spectrum shows the [M + 2H]2+ ions for FANCD2 K(ub)QLSSTVFK (light, m/z 576.3217) and K(ub)*QLSSTVFK* (heavy, m/z 584.3246) peptides.

Figure 2.12 Relative levels of ubiquitination of K561 in FANCD2 with or without arsenite treatment. The data represent the mean and standard deviation of results obtained from three independent experiments. The level of FANCD2 ubiquitination in the control group was normalized into 1.0. ***P < 0.001, and the P values were calculated using a two-tailed, unpaired Student's t test.

Figure 2.13 MS/ MS results for K(ub)QLSSTVFK (light) and K(ub)*QLSSTVFK* (heavy) peptides.

Figure 2.14 Cells were treated with TMP ± NaAsO2 (5 or 20 μM) and targeted

with a 365 nm laser in a defined ROI in the cell nuclei to photoactivate the 4,5′,8-trimethylpsoralen and introduce ICLs. The cells were subsequently fixed and stained for γH2AX and FANCD2 to quantify the recruitment of FANCD2 to laser-localized ICLs as a function of time. Representative images showing γH2AX (damage marker) and the colocalizing FANCD2 stripe for each condition at the different time intervals following ICL induction.

Figure 2.15 Quantification results for the data shown in A. The intensity of FANCD2 in the stripe and the nuclear background was quantified in at least 30 cells per time point per condition analyzed, where the images were acquired under identical exposure conditions. Three independent experiments were performed and showed equivalent results. Means were compared using a Rank-sums test (*P < 0.05; **P < 0.01; ***P < 0.001).

Figure 2.16 Clonogenic survival assay showing diminished resistance toward ICL agents upon As3+ exposure. (A) HEK293T cells were plated in six- well plates and treated with increasing doses of MMC to induce ICLs and exposed to As3+. After being cultured for 10 days, the cells exposed to As3+ displayed diminished resistance to MMC as reflected by lower survival rates relative to the control group. (B) HEK293T cells were treated with increasing doses of TMP and irradiated with 365 nm light to photoactivate the 4,5′,8-trimethylpsoralen to introduce ICLs. Compared to the control group, the cells exposed to As3+ manifested increased sensitivity to TMP + UVA. **P < 0.01; ***P < 0.001. The P values refer to the comparisons between the groups treated with ICL agents alone and those treated with ICL agents together with As3+, and the values were calculated using a two- tailed, unpaired Student’s t test.

Figure 3.1 Workflow of di-Glycine immunoprecipitation and identification of ubiquitinated peptides by LC-MS/MS

Figure 3.2 Regulation of ubiquitination by arsenite

Figure 3.3 KEGG pathway analysis of downregulated ubiquitinated proteins

Figure 3.4 a) Ubiquitination of proteins involved in cholesterol synthesis were inhibited upon arsenite treatment. b) Sequence structure of HMGCR Lys248 ubiquitinated peptide

Figure 3.5 a) Full scan of HMGCR-K248-ub. B) Ratio of HMGCR-K248-ub with arsenite treatment.

Figure 3.6 MS/MS spectrums for both light (up) and heavy (down) HMGCR-K248-ub peptides

Figure 3.7 a) knockdown efficiencies for shRNA species targeting gp78, TRC8, MARCH6 and HRD1. b) The ubiquitination levels of HMGCR upon shRNA knockdown of the four E3 ubiquitin ligases involved in HMGCR

ratios obtained from 30 individual cells. The P values were calculated using unpaired two-tailed student's t-test (**, P< 0.005;***, P< 0.001). Shown in the inset is the structure of ReAsH-EDT2.

Figure 4.7 Fluorescence microscopy results revealed the co-localization between ReAsH-EDT2 and ectopically expressed GFP-Rbx1. The co-localization was significantly diminished in cells pretreated with 10 μM NaAsO2 or PAPAO, but not Zn2+.

Figure 4.8 Quantitative analysis of the frequencies of co-localization between ReAsH-EDT2 and Rbx1. The data represent the mean and standard deviation of results obtained from images of 30 different cells. The P values were calculated using two-tailed, unpaired Student's t test (*, P< 0.05; ***, P< 0.001). Shown the insert is the structure of p-aminophenyl arsenoxide (PAPAO).

Figure 4.9 a) Arsenite exposure stabilized Nrf2 protein in cells. HEK293T cells were transfected with FLAG-Nrf2 treated with increasing concentrations of As3+. After MG132 treatment, the levels of Nrf2 and β-actin were detected by using anti-Nrf2 and anti-β-actin primary antibody. b) Relative protein levels of Nrf2 in cells exposed to arsenite. The data represent the means and standard deviations of each group acquired from 3 biological replicates. The P values were calculated using unpaired two-tailed student's t-test (*, P< 0.05).

Figure 4.10 HEK293T cells were either transfected with control, non-targeting siRNA (lane 1 and 6) or siRbx1 (lane 2-5 and 7-10), complemented with wild-type Rbx1 (lanes 3 and 8), Rbx1-H80C (lanes 4 and 9), or Rbx1-C83H (lanes 5 and 10), and transfected with FLAG-Nrf2 and ubiquitin-HA, followed by treatment with 5 μM As3+ (lanes 6-10) and 5 μM MG132 (lanes 1-10). Anti-FLAG M2 beads were used to immunoprecipitate the FLAG-Nrf2 protein, and the ubiquitination of Nrf2 was detected by Western blot using anti-HA antibody.

Chapter 1. General Overview

1.1 Arsenic toxicity

Arsenic, an environmental toxicant that threatens public health, is widely present in ground water, air, soil and food derived from natural and anthropogenic sources. The major concern of human arsenic toxicity arises from drinking arsenic-contaminated water (1-3). In many severely contaminated areas, the arsenic concentration in drinking water largely excesses the maximum permissible limit set by the World Health Organization (50 μg/L). The permissible content of arsenic in drinking water in the United States had been lowered from 50 parts per billion (ppb) to 10 ppb in 2001. However, in many geographic areas such as the Millard County, the arsenic content ranges from 14 ppb to 166 ppb. Long-term ingestion of arsenic from water and food leads to high risk in developing diseases. The most common and severe result of arsenic toxicity is its potential role of inducing cancers, as well as cardiovascular diseases (4-10).

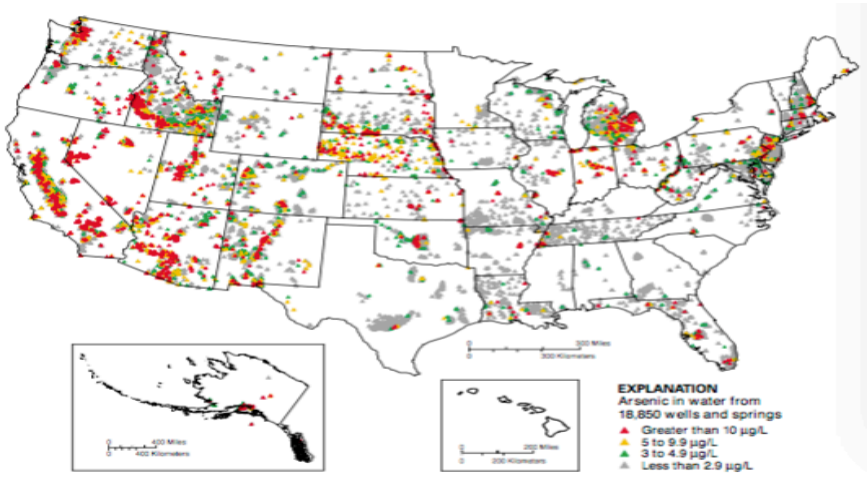

Figure 1.1 Map of common levels of Arsenic in the water supply (11)

1.1.1 Arsenic properties

Arsenic is a metalloid with chemical and physical properties that is intermediate between a metal and a non-metal with an average atomic mass of 74.92 Da. It has four oxidation states, -3, 0, +3 and +5, among which the +5 charged arsenate, As(V), and +3 charged arsenite, As(III), are the predominant oxidation states under oxygenated and reducing conditions, respectively (12). There are inorganic arsenic compounds and organic compounds in nature. The most common inorganic trivalent arsenic compounds include sodium arsenite, arsenic trioxide and arsenic trichloride (13), while the most common inorganic pentavalent arsenic compounds include calcium arsenate, arsenic acid and arsenic pentoxide (14). Common organic arsenic compounds include arsenobetaine, dimethylarsinic acid, methylarsonic acid, and arsanilic acid (15). Arsenic in its inorganic form is highly toxic (16).

Chemical name	CAS Reg. No.	Synonyms	Formula
Arsanilic acid	98-50-0	Arsonic acid, (4-aminophenyl)-	$C_6H_8AsNO_3$
Arsenic[a]	7440-38-2	Metallic arsenic	As
Arsenic(V) pentoxide[b]	1303-28-2	Arsenic oxide [As_2O_5]	As_2O_5
Arsenic(III) sulfide	1303-33-9	Arsenic sulfide [As_2S_3]	As_2S_3
Arsenic(III) trichloride	7784-34-1	Arsenic chloride [$AsCl_3$]	$AsCl_3$
Arsenic(III) trioxide[a,c]	1327-53-3	Arsenic oxide [As_2O_3]	As_2O_3
Arsenobetaine	64436-13-1	Arsonium, (carboxymethyl) trimethyl-, hydroxide, inner salt; 2-(trimethylarsonio)acetate	$C_5H_{11}AsO_2$
Arsine	7784-42-1	Arsenic hydride	AsH_3
Calcium arsenate	7778-44-1	Arsenic acid [H_3AsO_4] calcium salt (2:3)	$(AsO_4)_2.3Ca$
Dimethylarsinic acid	75-60-5	Cacodylic acid	$C_2H_7AsO_2$
Lead arsenate	7784-40-9	Arsenic acid [H_3AsO_4], lead (2+) salt (1:1)	$HAsO_4.Pb$
Methanearsonic acid, disodium salt	144-21-8	Arsonic acid, methyl-, disodium salt	$CH_3AsO_3.2Na$
Methanearsonic acid, monosodium salt	2163-80-6	Arsonic acid, methyl-, monosodium salt	$CH_4AsO_3.Na$
Potassium arsenate[d]	7784-41-0	Arsenic acid [H_3AsO_4], monopotassium salt	$H_2AsO_4.K$
Potassium arsenite	13464-35-2	Arsenous acid, potassium salt	$AsO_2.K$
Sodium arsenate[e]	7631-89-2	Arsenic acid, [H_3AsO_4], monosodium salt	$H_2AsO_4.Na$
Sodium arsenite	7784-46-5	Arsenous acid, sodium salt	$AsO_2.Na$
Sodium cacodylate	124-65-2	Arsinic acid, dimethyl-, sodium salt	$C_2H_6AsO_2.Na$

Figure 1.2 Common arsenic compounds (17)

1.1.2 Acute and chronic toxicity of arsenic

Acute exposure of excessive amount of arsenic could lead to severe consequences. In most cases, acute arsenic poisoning is related to accidental uptake of pesticides or insecticides, or prepense suicide in rare cases. It was reported that in most cases, the acute toxicity of inorganic arsenic is much greater than that of organic arsenic compounds, while the toxicity of As(III) is greater than that of As(V).The lethal dose of inorganic trivalent arsenic for adult humans ranges from 1 mg/kg to 3 mg/kg. The clinical features of severe acute arsenic toxicity includes, but not limited to gastrointenstinal discomfort, nausea, vomiting, diarrhea, colicky abdominal pain, bloody urine, shock, anuria, coma, convulsions and death (18-24).

Chronic exposure to arsenic affects multiple systems in the human body and causes many diseases, with the hallmarks of skin lesions and malignancy. The clinical features of chronic arsenic exposure vary among individuals from different geographic areas and population groups (25-29).

System	Effect
Skin	Skin lesions
Cardiovascular	Blackfoot disease
Nervous	Peripheral neuropathy, encephalopathy
Hepatic	Hepatomegaly, cirrhosis, altered heme metabolism
Hematological	Bone marrow depression
Endocrine	Diabetes
Renal	Proximal tubule degeneration, papillary and cortical necrosis

Figure 1.3 Clinical features of chronic arsenic exposure in humans (30)

1.1.3 Arsenic carcinogenicity

Inorganic arsenic has been identified as a carcinogen by the International Agency for Research on Cancer (IARC) in 1980 and the US Environmental Protection Agency (EPA) in 1988. Humans exposed to arsenic have a high risk of developing various cancers through inhalation or ingestion of arsenic species (31). Lung tumors are primarily observed in people after inhalation of arsenic (32-34), whereas skin lesions are the first signal of oral exposure to arsenic (35). Arsenic-induced tumor can also be found in many organs including bladder, kidney, prostate and liver (13,36-38). A large number of animal experiments also demonstrated the correlation between arsenic exposure and cancer development (39-42). The mechanisms underlying arsenic carcinogenicity are complicated. Scientists have proposed several distinct mechanisms to account for its carcinogenicity, including altered cell proliferation, impaired DNA repair, aberrant DNA methylation and elevated oxidative stress (43-47).

1.1.4 Arsenic metabolism

In human body, cells are equipped with a system for the detoxication of arsenic species through a series of hepatic methylation processes. Inorganic arsenic is methylated to monomethylarsonic acid (MMA) and dimethylarsinic acid (DMA) that are less toxic, among which the dimethylarsinic acid is the predominant metabolite during the process that is rapidly excreted out of the body. The final product in this methylation process is the trimethylarsine oxide (TMAO) that is detected with a very low amount in urine (48-51).

1.1.5 Potential action mechanisms of arsenic toxicity

Arsenate has similar structure and properties as phosphate, which enable it to substitute phosphate in many biological reactions (52). Arsenate can replace phosphate in the anion exchange transport system in human red blood cells, as well as the sodium pump. In addition, arsenate can form glucose-6-arsenate and gluconate-6-arsenate by reacting with glucose and gluconate, respectively, which inhibits the function of hexokinase (53,54). Arsenate can also inhibit ATP synthesis by competing with phosphate in the reaction (55,56).

The mechanisms of trivalent arsenic toxicity are different from that of the arsenate. Arsenite has been found to inactivate more than 200 enzymes that are involved in many crucial cellular processes such as DNA repair and cellular respiration, due to its high affinity towards thiols in cysteine residues, especially those that are in close proximity (57,58). Cysteine residues in some proteins assume important roles in their activation and function. The interaction between arsenite and critical thiol groups of proteins may deactivate proteins that are involved in crucial biological events. In this vein, it was reported that arsenite inhibits pyruvate dehydrogenase (PHD) by binding to the cofactor lipoic acid moiety, leading to decreased ATP production (59,60). In addition, MMA was found to be a potential inhibitor for GSH reductase, resulting in cellular redox status alteration and cytotoxicity (61).

1.1.6 Application of arsenic

Arsenic and arsenic compounds have been widely used in many areas for centuries. Inorganic arsenic has been used to treat leukemia (62), chronic bronchial asthema and psoriasis (63), while organic arsenic is used as an antibiotic to treat protozoal disease (64). Due to their toxic effects, arsenic compounds have also been used as pesticides and insecticides in the agricultural industry, as well as biochemical weapons during wars. In addition, arsenic compounds are also used as wood preservatives, and in glass making, mining and semiconductor industries (65).

1.2 Ubiquitin code

As one of the most ubiquitous and important post-translational modifications of proteins in mammalian species, protein ubiquitination plays major roles in regulating almost all cellular processes such as signaling transduction, protein-protein interaction and protein degradation (66). The ubiquitination process is catalyzed by three enzymes, including ubiquitin-activating enzymes (E1s), ubiquitin-conjugating enzymes (E2s) and ubiquitin ligase enzymes (E3s). In the first step, ubiquitin is activated and binds to C-terminus of an E1 enzyme with the use of ATP, followed by the conjugation of the activated ubiquitin to an E2 enzyme. Next, E2 interacts with an E3 ubiquitin ligase that binds to a substrate protein, and transfers the ubiquitin to the lysine residues in the substrates. All the enzymes are then dissociated form the substrate protein to complete the ubiquitination process. These steps can be repeated to form polyubiquitinated chains (67).

1.2.1 Properties of ubiquitin

Ubiquitin, a highly conserved protein, is composed of 76 amino acids that can be recognized by the ubiquitin-binding domains of proteins (68-70). The most crucial parts of a ubiquitin molecule are its N terminus and the seven lysine residues in its amino acid sequence (K6, K11, K27, K29, K33, K48 and K63), which can be attached by other ubiquitin molecules to form various polyubiquitination chains (71).

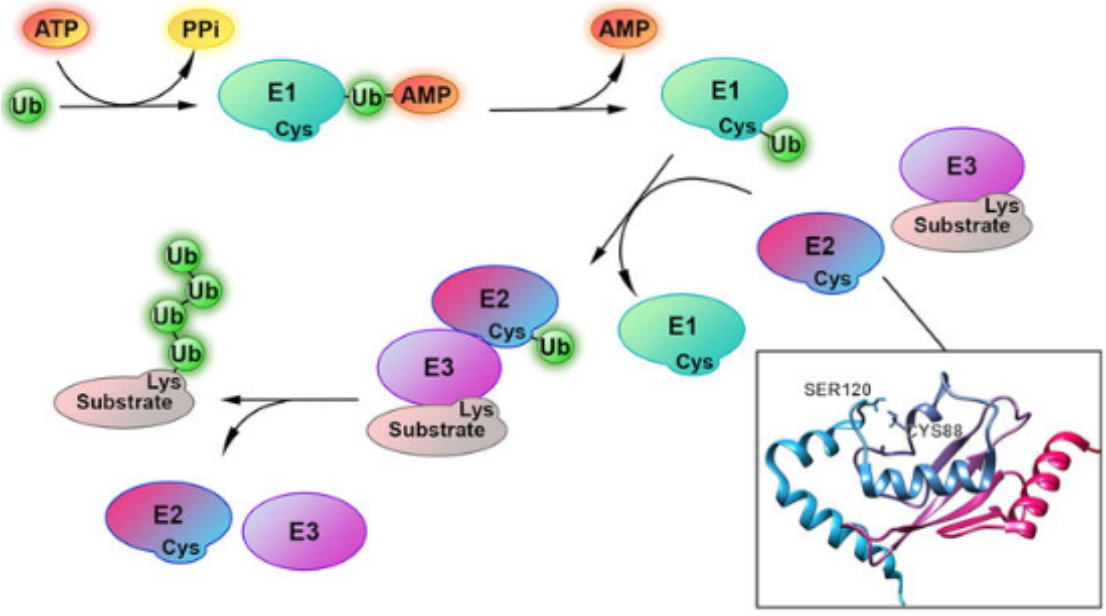

Figure 1.4 The process of ubiquitination (72)

1.2.2 Diversity of protein ubiquitination

Owing to diverse lysine residues in proteins, proteins can be either ubiquitinated on a single lysine residue or on multiple lysine residues, resulting in monoubiquitination and multiubiquitination, respectively (73,74). Moreover, proteins can also be polyubiquitinated by homotypically attaching a

number of ubiquitin molecules on the same lysine residue sequentially (74). In addition, when the attachments of additional ubiquitin to the lysine residues of the previous ubiquitin molecule at different positions, it leads to the formation of branched polyubiquitination chains (75). Ubiquitination can also occur on cysteine, threonine and serine residues in some cases, which make protein ubiquitination more diverse (76-78).

The diversity of protein ubiquitination is of great significance for protein functions. Different ubiquitination chains display variant structures that can be recognized by different ubiquitin binding domains in a specific manner, leading to different fates of proteins through different pathways. Monoubiquitination was reported to be important for regulation of histone functions, modulation of DNA repair, receptor endocytosis and gene expression (79-81). The polyubiquitination chains through K63 is thought to be involved in the regulation of kinase activity, signal transduction and DNA damage response (82,83). The K48- and K11-linked polyubiquitination, on the other hand, mainly guides proteins for proteasome-mediated degradation (84,85). The monoubiquitination of histone H2A is mediated by the branched ubiquitination chains on RING1B E3 ubiquitin ligase through ubiquitinating lysine residues at position 6, 27 and 48 (86). In a word, the structural diversity of ubiquitination chains serves as important signal for distinct functions of proteins. The generation of various types of ubiquitination chains arises from the distinct combination of E2 and E3 enzymes used in the ubiquitination processes. Up to date, there are more than 30 E2s and 1000 E3s discovered in mammalian system. Nevertheless, the mechanism of the distinct selection of E2s and E3s

for different types of ubiquitination remains largely elusive (87).

1.2.3 Ubiquitin chain formation specificity

The main specificity of a typical ubiquitination process is largely dependent on the selection of E3 ubiquitin ligases, since each E3 ubiquitin ligase targets its own substrates for ubiquitination. E3 ubiquitin ligases catalyze the transfer of an ubiquitin molecule to the substrate proteins. According to the way through which ubiquitin is transferred, the E3 ubiquitin ligases are generally clarified into two classes: E3 ubiquitin ligases with homologous to E6-AP carboxy-terminus (HECT) domain and E3 ubiquitin ligases with Really Interesting New Genes (RING) finger domain, which are called HECT E3s and RING finger E3s in short (87).

HECT E3s are a large group of E3 ubiquitin ligases with two major functional domains. The N-terminal domain of HECT E3s attracts E2s, and the C-terminal domain of HECT E3s is a catalytic domain containing an active site cysteine. The E2s transfer ubiquitin to HECT E3s by charging the catalytical cysteine in this domain with active ubiquitin to form a thioester linkage, which is attacked by acceptor lysine residues to take over ubiquitin (88). Rather than selection of specific E2s, the ubiquitination linkage specificity mainly depends on specific HECT E3s (89). For example, The E6-associated protein (E6-AP) specifically directs Lys48 ubiquitination. Lack of E6-AP causes an inherited neurologic disorder, Angelman' syndrome (90). Another example is yeast RSP5 or human Nedd4. They specifically assemble Lys63 linkage. Lack of Nedd4 results in Liddle' syndrome (91).

The RING finger E3s guides ubiquitination through a different mechanism. The RING finger E3s contains a RING finger with 40-60 amino acids harboring 2 zinc-binding motifs. The zinc-binding motifs contain core cysteine and histidine residues that can coordinate with zinc ions, which stabilize protein structure and maintain protein function. RING finger E3s can either function individually or form complexes with other cofactors to act as E3 ubiquitin ligase complexes, of which both act as scaffolds that bring the E2 and substrates into close proximity to promote the conjugation of ubiquitin to substrates (92). The linkage specificity for RING finger E3s is not determined by RING finger E3s, but E2s, supported by the fact that many RING finger ubiquitin ligases can form various types of ubiquitination chains combined with different E2s (93). For instance, the RING finger E3s BRCA1-BARD1 and MuRF can enable the synthesis of Lys63-linked ubiquitination chain with Ube2N-Uev1A E2, while facilitate the synthesis of Lys48-linked ubiquitination chain with the help of Ube2K E2 enzyme (94,95). Another example is the CHIP E3, which directs the Lys63-linked ubiquitination with Ube2N-Uev1A while showing no specificity with Ube2D (95). In addition, some E2s themselves display distinct preferences towards types of ubiquitination. For example, Ube2R and Ube2G2 specifically assemble Lys48-linked ubiquitination, and Ube2S a Lys11-specific E2 (95).

1.2.4 Major E3 ubiquitin ligase categories

There are individual E3 ubiquitin ligases and E3 ubiquitin ligase complexes composed of the E3 and other cofactors. The oncoprotein Mdm2 is a

monomeric RING finger E3 that acts as a regulator for p53 and guides its proteasome-mediated degradation by monoubiquitinating p53 (96). Other monomeric RING finger E3s include muscle RING finger-1 (MuRF-1), E3a and c-Cbl. MuRF-1 and E3a are important for the processes of muscle atrophy, and c-Cbl ubiquitinates several cell surface receptors (97,98).

The anaphase-promoting complex (APC/C) is the largest and most complex E3 that is composed of 11-13 highly conserved subunits. It plays a key role in marking target cell cycle proteins for the 26S-proteasome-mediated degradation, including securin and S/M cyclins (99,100).

The largest groups of E3 ubiquitin complexes are the Cullin-RING ubiquitin ligases. Cullins act as scaffolds to bind to RING finger E3 ligases and bring the E2 and substrate proteins into close proximity. There are eight cullin genes in the human genome that form part of a multi-subunit ubiquitin complex. The typical RING component binding to the Cullins is Rbx1/Roc1 that can ubiquitinate different substrates with the aid of different adaptor proteins (101,102).

1.2.5 Ubiquitination response to arsenic toxicity

Ubiquitination response to arsenic toxicity is complicated and not conclusive. In some studies, it was reported that arsenic exposure could activate the ubiquitin-proteasome system by activating specific E3 ubiquitin ligases. In this vein, arsenic trioxide has been found to increase the level of Parkin protein in mitochondria in mice, which is the E3 ubiquitin ligase for the ubiquitination of the voltage-dependent anion channel 1 (VDAC1). The activation of Parkin by

arsenic trioxide led to the polyubiquitination of VDAC1 and its proteasome-mediated degradation, contributing to cellular and mitochondria homeostasis (103). In addition, arsenic trioxide was reported to enhance the expression of Pirh2 E3 ubiquitin ligase to activate proteasome-dependent degradation of p53 protein (104). Moreover, arsenic could stabilize RNF4 and E3 ubiquitin ligases to promote the ubiquitination and proteasome-mediated degradation of PML (105,106).

It was also found that arsenic could stabilize proteins by disrupting the function of their upstream E3 ubiquitin ligases. In this vein, our previous work showed that arsenite targets the RING finger domain of RNF20/40 E3 ubiquitin ligase by binding to the thiol groups of core cysteine residues (44). This interaction disrupts the binding of zinc ions to the RING finger motif, which impairs the E3 ligase activity of RNF20/40. As a result, the ubiquitination of histone H2B was perturbed since H2B is the substrate of RNF20/40 E3 ubiquitin ligase, which suppresses the DNA double strand break repair pathway (44).

1.3 Technologies to study proteomics

The rapid development of biological and biochemical techniques allows us to study biology in a more advanced and profound way. For example, the development of shotgun sequencing technologies laid a solid foundation for the sequencing of the whole human genome (107). The discovery of CRISPR/Cas9 system gave rise to a powerful tool that enables gene editing that is faster, cheaper, more accurate and more efficient (108).

The large-scale analysis of proteins was first named as “proteomics” by Peter James in 1997, including studies of protein function, protein-protein interaction, protein modifications, localization, etc. (109). Proteomics is the next step to study biological system following genomics and transcriptomics. However, the study of proteomics is more complex than genomics and transcriptomics because proteome varies from cell to cell and among different time points due to alternative splicing of mRNA, post-translational modifications on proteins and some other factors (110,111). Multiple technologies have been developed for the study of proteomics. In general, people either detect targeted proteins by immunoassays using specific antibodies, or utilize mass spectrometry for large-scale detection of proteins (112,113).

1.3.1 Immunoassays for protein detection

Antibodies are the most commonly used tools for biologists to detect targeted proteins by immunoassays nowadays. Western blot is the most widely used technique to detect specific proteins in tissues, cells or in vitro. It normally combines with gel electrophoresis, which separate proteins according to their molecular weights. Briefly, the denatured proteins are subjected to a gel electrophoresis and transferred to a stationary membrane. The membrane carrying all the proteins is then incubated with antibodies that detect specific proteins. A secondary antibody is needed to bind to the primary antibody, which is subsequently detected by various methods including radioactivity, immunofluorescence, staining, etc. (114). The enzyme-linked immunosorbent

assay (ELISA) is another technique that uses antibodies and color change to detect specific proteins. Normally antigens are attached to a solid surface and incubated with specific primary antibodies. These antibodies are linked to an enzyme that can catalyze the chemical reaction of substrates added in the final step to produce a color change that can be observed (115).

1.3.2 Mass-spectrometry-based characterization of proteome

Mass spectrometry is a powerful tool to quantitatively and qualitatively analyze properties of chemical and biological species. It has been applied to study proteomics for decades in a profound way. For absolute and relative quantification of proteins, mass spectrometry is normally combined with other techniques such as stable isotope labeling by amino acids in cell culture (SILAC), isobaric tag for relative and absolute quantification (iTRAQ), Tandem Mass Tag (TMT) labeling, and absolute quantification of proteins (AQUA) (116-118). Mass spectrometry is also coupled with affinity immunoprecipitation to study protein-protein interaction and protein complexes (119). By doing this, the protein-protein interaction networks can be established as called “interactome” that is important for revealing the roles of proteins in different signaling pathways (120).

Another application of mass spectrometry is to identify protein post-translational modifications (PTMs) (110). After translation, proteins can undergo various types of modifications that are important for protein function and cell signaling, including methylation, phosphorylation, acetylation, oxidation, ubiquitination and so on. PTMs can either occur by modifying the

existing functional groups or attaching new functional groups to proteins such as ubiquitin and methyl groups, and these modifications change protein structures and properties that are normally difficult to be identified by immunoassays (121). Mass spectrometry overcomes those shortcomings and allows for the identification of PTMs by providing the specific site information, chemical structures and relative or absolute amount of these modifications in an efficient way.

1.3.3 Mass spectrometry instrumentation and methodology

In this dissertation, I utilized mass spectrometry coupled with nano liquid chromatography (nano-LC-MS) to identify and quantify arsenite-induced alteration of protein ubiquitination in the whole proteome. Before injected into LC-MS, the SILAC samples were digested and immunoprecipitated with an antibody that specifically enrich di-glycine containing peptides. The enriched samples were then injected into LC-MS/MS analysis and searched using Maxquant software for peptide mapping. The instrument I used for this study is the Thermo Q Exactive-Plus Hybrid Quandrupole-Orbitrap^{TM} Mass Spectrometer.

The Q Exactive-Plus MS used electrospray ionization (ESI) to ionize proteins or digested peptides. ESI is a type of soft ionization method that produces ions using an electrospray. The electrospray is applied with a high voltage, which disperses and charges the droplets containing analytes of interests. The ESI-MS is compatible to liquid-based separation tools such as liquid chromatography (122).

There are several ion fragmentation methods that are widely used for mass spectrometry analysis of analytes. Collision-induced dissociation (CID) is the most frequently used fragmentation method for proteomics study. The precursor ions undergo collisions with neutral gas molecules, which break the amide bonds in the peptide backbone, producing b and y ions that can be detected by mass analyzer. The CID fragmentation method has a bias towards small, low charged peptides and is not suitable for the analysis of intact proteins or labile post-translational modifications such as phosphorylation. The higher-energy collision dissociation (HCD) is a beam-type CID fragmentation method. The feature of HCD is that it uses higher activation energy and shorter activation time. HCD fragmentation method has no low mass cut-off limitation and provides higher mass accuracy. Other fragmentation methods include electron-capture dissociation (ECD) and electron-transfer dissociation (ETD). ECD generates radical cations for protonated proteins or peptides, while ETD transfers electrons to protonated proteins or peptides. Both ECD and ETD cleave the N-Cα bonds along the peptide backbone and generate c and z ions that can be detected by the mass analyzer. ECD and ETD are complementary to CID and HCD. Combination of ECD/ETD and CID/HCD provides more peptide information by generating more fragmented ions (123-127). The Q-Exactive Plus MS uses HCD as fragmentation methods for peptides identification.

Another core component of a mass spectrometer is the mass analyzer. In general, there are four types of mass analyzers used for the study of proteomics (quadrupole, ion trap, time-of-flight and Fourier transform ion

cyclotron resonance). Each of them has its advantages and limitations. For example, the quadrupole mass analyzer has good reproducibility but limited resolution, and the ion trap mass analyzer has high sensitivity but poor dynamic range. On the other hand, time-of-flight (TOF) mass analyzer has a faster scan rate but lower resolution compared to the ion cyclotron resonance (ICR) mass analyzer, while the ICR mass analyzer has the highest resolution but limited dynamic range. Therefore, hybrid mass spectrometers are developed to make good for deficiency to get a better performance in terms of mass accuracy, resolving power, dynamic range, scan rate and so on. The Q-Exactive Plus hybrid mass spectrometer combines the quadrupole and Orbitrap mass analyzers (128-132).

1.4 Scope of the dissertation

This dissertation focused on arsenite-induced alteration of ubiquitin-modified proteome in cultured mammalian cells. By employing LC-MS-based quantification of ubiquitinated peptides, I was able to find three interesting protein targets, of which their ubiquitination is perturbed upon arsenite treatment, as discussed in chapters 2 to 4 individually. I also studied the function of ubiquitination of these proteins and discovered new roles of arsenite in affecting their function by inhibiting their ubiquitination.

Chapter 2. Arsenite Binds to the RING Finger Domain of FANCL E3 Ubiquitin Ligase and Inhibits DNA Interstrand Cross-link Repair

Introduction

Arsenic is a naturally occurring metalloid that is ubiquitously present in the environment throughout the world. Prolonged exposure to arsenic through drinking and cooking using contaminated groundwater poses significant threats to public health. In this vein, human exposure to arsenic compounds is known to be associated with a variety of cancers including those of the skin, bladder, kidney, liver and lung, as well as other human diseases encompassing neurological disorders, cardiovascular diseases and diabetes (133).

Several mechanisms have been proposed to account for the carcinogenic effects of arsenic species, including perturbation of growth factor signaling, induction of oxidative stress, inhibition of DNA repair, alterations of DNA and histone methylation, and binding to vicinal thiols in proteins (134,135). In this respect, *in-vitro* studies with model synthetic peptides revealed that As(III) binds much more strongly to Cys3His (C3H)- or Cys4 (C4)-type zinc fingers than those of the Cys2His2 (C2H2)-type (136).

Emerging recent studies have demonstrated that As(III) may compromise DNA repair by binding directly to DNA repair proteins, or through modulating histone epigenetic marks that are crucial in DNA repair. As(III) could bind to the zinc finger motifs of xeroderma pigmentosum complementation group A (XPA) (137,138) and poly(ADP-ribose) polymerase 1 (PARP1) (139), thereby inhibiting nucleotide excision repair (NER) and base excision repair (BER) (137-139), respectively. Our recent study showed that As(III) could bind to the

RING finger motifs of RNF20/RNF40 histone E3 ubiquitin ligase, which leads to diminished ubiquitination of histone H2B at lysine 120 (140). Consistent with the notion that this ubiquitination is important for decompacting the 30 nm chromatin fiber and for establishing a biochemically accessible chromatin environment required for DNA double strand break (DSB) repair (141), we observed that As(III) exposure could result in compromised repair of DNA DSBs via the homologous recombination and non-homologous end-joining pathways (140). Along this line, As(III) was also observed to bind to the C3H-type zinc fingers in ten-eleven translocation (Tet) family of enzymes, which perturbs DNA epigenetic marks through inhibition of Tet-mediated oxidation of 5-methylcytosine to 5-hydroxymethylcytosine (142). On the other hand, arsenic trioxide has been successfully employed in the clinical remission of acute promyelocytic leukemia (APL), especially for those patients carrying the *PML-RARα* fusion oncogene (143). In this vein, the fusion with PML led to the constitutive activation of the RARα transcription factor, and As(III) was found to bind to the RING-finger domain of PML, resulting in the oligomerization and proteasomal degradation of PML-RARα fusion protein (143,144). Thus, As(III) induces the clinical remission of APL and perturbs DNA DSB repair on the basis of the same chemical rationale, i.e., through targeting zinc finger proteins, though the cellular protein targets differ under these two scenarios.

Not much is known about whether As(III) also interferes with the repair of DNA interstrand cross-link lesions (ICLs). In this respect, DNA ICLs may arise from endogenous metabolism or from exposure to chemotherapeutic agents such as mitomycin C (MMC) (145). Owing to the covalent linkage of two strands of

DNA and the ensuing blockage of crucial cellular processes including DNA replication and transcription, the ICLs are extremely cytotoxic (145). Thus, multiple repair pathways have been evolved to repair ICLs, which encompass the NER, homologous recombination (HR), and Fanconi anemia (FA) pathways (145). So far 19 genes involved in the FA pathway have been identified (146,147). Specifically, the anchor complex of the FA pathway, comprised of FANCM, FAAP24, MHF1 and MHF2, is activated by recognition of the ICL sites, which leads to the recruitment of the FA core complex that consists of FANCA, FANCB, FANCC, FANCE, FANCF, FANCG, FANCL, FAAP20, and FAAP100 (146,147). Within the core complex, FANCL harbors a PHD/RING finger domain and is an E3 ubiquitin ligase, which monoubiquitinates FANCI and FANCD2. These monoubiquitination events are thought to be crucial for the recruitment of nucleases and downstream repair factors in the NER and HR pathways to remove DNA ICL lesions (146,147).

On the grounds of the previous findings that As(III) was capable of binding to the zinc finger domain of proteins, we reasoned that As(III) may also interact with the RING finger domain of FANCL, thereby blocking its E3 ubiquitin ligase activity and perturbing the repair of DNA ICLs. In the present study, we demonstrated the interaction between As(III) and FANCL *in vitro* and in cultured human cells by using streptavidin agarose affinity assay, mass spectrometry (MS) and fluorescent microscopy measurements. We also showed that arsenite exposure could compromise MMC-induced monoubiquitination of FANCD2, and reduce the recruitment of FANCD2 to chromatin and DNA damage sites in cultured human cells. Additionally, we

found that arsenite exposure rendered cells sensitive toward ICL-inducing agents. Together, our study established a novel mechanism underlying the carcinogenic effects of arsenite.

Experimental Section

Cell Culture

All cell culture experiments were conducted at 37°C in a humidified atmosphere containing 5% CO_2. HEK293T human embryonic kidney epithelial cells (ATCC, Manassas, VA) and HeLa cells were cultured in Dulbecco's Modified Eagle Medium (DMEM, ATCC) supplemented with 10% fetal bovine serum (FBS, Invitrogen, Waltham, MA) containing 100 U/mL penicillin and streptomycin.

For stable isotope labeling by amino acids in cell culture (SILAC) experiments, the complete light or heavy media were prepared by adding light and heavy lysine ([$^{13}C_6$,$^{15}N_2$]-L-lysine) and arginine ([$^{13}C_6$]-L-arginine) into RPMI 1640 medium without L-lysine or L-arginine. The light and heavy SILAC medium also contained 10% dialyzed FBS and 100 U/mL penicillin and streptomycin. The GM00637 cells were cultured in heavy medium for at least 10 days to ensure complete stable isotope labeling prior to further experiments.

Plasmid Construction

The expression plasmids of GFP-FANCL harboring C312,315A or C364,367A mutations were obtained from the plasmid for expressing the wild-type GFP-FANCL provided by Dr. Grover C. Bagby from Oregon Health and Science University (148) by using GeneArt Site-directed Mutagenesis Kit (Thermo Fisher Scientific, Waltham, MA), following the vendor's recommended procedures.

In-vitro Arsenite Binding Assay

The RING finger peptide derived from the PHD domain of FANCL (with amino acid sequences DCGICYAYQL DGTIPDQVCD NSQCGQPFHQ ICLYEWLRGL LTSRQSFNII FGECPYCSK) was obtained from New England Peptide, Inc. (Gardner, MA) and purified by HPLC. The peptide was dissolved in 20 mM Tris-HCl (pH 6.8) containing 1 mM dithiothreitol. Aliquots of 100 μM peptide were incubated with 200 μM $NaAsO_2$ on ice for 1 hr and subsequently diluted by 100 fold. The resultant solution was mixed with an equal volume of 2,5-dihydroxybenzoic acid matrix solution followed by spotting onto a sample plate (136). The sample was then analyzed by matrix-assisted laser desorption/ionization-time of flight (MALDI-TOF) MS on a Voyager DE STR instrument in the linear, positive-ion mode (Applied Biosystems, Foster City, CA).

Streptavidin Agarose Affinity Assay and Western Blot

The streptavidin agarose affinity assay was performed with the use of a biotin-As probe as described previously (149,150). Briefly, HEK293T cells were transfected with GFP-FANCL plasmid for 24 hr followed by treatment with 5 μM biotin-As probe (149,150) in Opti-MEM medium (Invitrogen, Carlsbad, CA) for 2 hr. The cells were subsequently lysed in CelLytic M lysis buffer supplemented with a protease inhibitor cocktail (Sigma-Aldrich, St. Louis, MO), and incubated with streptavidin agarose beads at 4°C for 3 hr. Streptavidin agarose beads were then washed for 6 times with 1× PBS containing 0.5% NP-40 and resuspended in SDS-PAGE loading buffer.

After SDS-PAGE separation, the proteins on the gel were transferred to a nitrocellulose membrane using a buffer containing 10 mM $NaHCO_3$, 3 mM Na_2CO_3, and 20% methanol. The membrane was subsequently blocked with 5% non-fat milk in PBS-T at room temperature for 2 hr and incubated with anti-GFP primary antibody (1:10000 dilution, Sigma-Aldrich) at 4°C overnight. After washing with PBS-T for 6 times, the membrane was incubated with anti-rabbit secondary antibody at room temperature for 1 hr, and subsequently washed with PBS-T for 6 times. The secondary antibody was detected using ECL Advanced Western Blotting Detection Kit (GE Healthcare, Chicago, IL) and visualized with Hyblot CL autoradiography film (Denville Scientific, Inc., Metuchen, NJ). Similar experiments were carried out by transfecting HEK293T cells with FANCL-C312,315A and C364,367A mutants, or by pre-treating cells with 10 μM Zn^{2+}, $NaAsO_2$ or PAPAO for 1 hr prior to treatment with the biotin-As probe.

Fluorescence Microscopy

HEK293T cells were seeded on cover glasses in 24-well plates at a density of ~ 1 × 10^5 cells per well and transfected with 1 μg plasmid encoding GFP-FANCL, GFP-FANCL-C312,315A, or GFP-FANCL-C364,367A for 24 hr. The cells were then incubated with Opti-MEM containing 5 μM ReAsH-EDT_2 (Invitrogen) at 37°C for 2 hr, washed for 3 times with BAL buffer, fixed with 4% paraformaldehyde, stained with DAPI, and imaged using a Leica TCS SP2 confocal microscope (Leica Microsystems, Buffalo Grove, IL). Similar experiments were carried out by pre-treating cells with 10 μM Zn^{2+}, $NaAsO_2$ or PAPAO for 1 hr prior to transfection with GFP-FANCL plasmid and treatment with ReAsH-EDT_2.

Isolation of Chromatin-associated Proteins

Chromatin-associated proteins were isolated following previously described procedures (151). Briefly, cells were first lysed by incubating, for 30 min on ice, in a cytoplasmic lysis buffer, which contained 10 mM Tris-HCl (pH 8.0), 0.34 M sucrose, 3 mM $CaCl_2$, 2 mM $MgCl_2$, 0.1 mM EDTA, 1 mM DTT and 0.5% NP-40. The intact nuclei were isolated by centrifugation at 5000 rpm for 2 min and lysed with nuclear lysis buffer, which contained 20 mM HEPES (pH 7.9), 1.5 mM $MgCl_2$, 1 mM EDTA, 150 mM KCl, 0.1% NP-40, 1 mM DTT, 10% glycerol, as well as protease and phosphatase inhibitors. The chromatin-enriched fraction was isolated by centrifugation at 14000 rpm for 30 min, resuspended in a buffer containing 20 mM HEPES (pH 7.9), 1.5 mM $MgCl_2$,

150 mM KCl, 10% glycerol, protease and phosphatase inhibitors, and 0.15 unit/μL benzonase (Sigma-Aldrich, St. Louis, MO). After incubating on ice for 1 hr, the chromatin-associated proteins were obtained by collecting supernatant after centrifugation (152).

Ubiquitin Remnant Peptide Immunoprecipitation and LC-MS/MS Analysis

GM00637 cells cultured in RPMI 1640 medium containing heavy or light lysine and arginine were treated with or without 5 μM sodium arsenite for 24 hr, followed by treatment with 5 μM MG132 for 1 hr. The cells were then harvested and lysed in a lysis buffer with 8 M urea and mixed at a 1:1 ratio, and digested with trypsin overnight at an enzyme/substrate ratio of 1:50 (by mass). The resulting peptides were desalted on a Sep-Pak C18 column (Waters), followed by immunoprecipitation of peptides carrying the K-ε-GG ubiquitin remnant using the PTMScan® Ubiquitin Remnant Motif (K-ε-GG) Kit (Cell Signaling). The enriched ubiquitinated peptides were eluted with 0.15% trifluoroacetic acid and injected for LC-MS/MS analysis on a Q Exactive Plus quadrupole-Orbitrap Mass Spectrometer (Thermo).

Recruitment of FANCD2 to DNA Damage Sites Induced by 4,5′,8-Trimethylpsoralen (TMP)

HeLa cells were plated in 35 mm glass-bottom culture dish. On the next day, the cells were incubated for 15 min in media containing 6 μM TMP with or without $NaAsO_2$ (5 or 20 μM), prior to laser treatment to photoactivate the

TMP and generate laser-localized ICLs. Localized irradiation was performed using a Nikon Eclipse TE2000 confocal microscope (Nikon Instruments Inc., Melville, NY) equipped with an SRS NL100 nitrogen laser-pumped dye laser (Photonics Instruments, St. Charles, IL) that fires 5 ns pulses with a repetition rate of 10 Hz at 365 nm, at a power of 0.7 nW, which was measured at the back aperture of the 60× objective. The laser was directed to a specified rectangular region of interest (ROI) within the nucleus of a cell visualized with a Plan Fluor 60×/NA1.25 oil objective. The laser beam was oriented by galvanometer-driven beam displacers and fired randomly throughout the ROI until the entire region was exposed. Throughout the experiment, the cells were maintained at 37°C, 5% CO_2 and 80% humidity using an environmental chamber. For each plate, cells in successive fields along a cross on the glass (made with a diamond pen) were targeted during the course of 20 min. The plate was immediately fixed in freshly prepared 4% formaldehyde in PBS at room temperature for 10 min, followed by immunostaining for γH2AX (05-636, Millipore) and FANCD2 (NB100-182, Novus). Image processing and subsequent quantification of FANCD2 intensity in the ICL stripe minus the nuclear background were performed in Volocity (PerkinElmer, Waltham, MA).

Clonogenic Survival Assay

HEK293T cells were seeded in 6-well plates at densities of 100-400 cells per well. After incubation with 5 μM $NaAsO_2$ for 24 hr, the cells were exposed to various doses of MMC (0-72 ng/μL) or TMP (0-75 ng/μL) + 100 J/m^2 UVA in DMEM medium, and cultured for 10 days. The colonies were then fixed with

6% glutaraldehyde and stained with 0.5% crystal violet. Colonies with more than 50 cells were counted under a microscope (153).

Results

As(III) Binds to the RING-finger Domain of FANCL Protein in vitro and in Cells

To test our hypothesis that As(III) exposure may compromise DNA interstrand cross-link repair via the FA pathway, we first examined the interaction between As(III) and the PHD-finger-containing protein FANCL. To this end, we performed an *in vitro* binding assay to examine whether As(III) can interact directly with the RING finger domain of FANCL protein with the use of a synthetic RING finger peptide derived from human FANCL protein (see Experimental Section). MALDI-TOF MS data revealed the mass increases of 72 and 144 Da upon incubation of the synthetic peptide with As(III). These mass increases reflect the binding of one and two As(III) to the peptide along with the releases of three and six protons, respectively, from cysteine residues at the RING finger domain (Figure 2.1) (136,140). This result supports that As(III) can bind directly to the RING-finger domain of FANCL protein *in vitro*.

We next asked whether this interaction also occurs in cells. Toward this end, we incubated HEK293T cells with a synthetic biotin-As probe followed by streptavidin agarose affinity pull-down assay to assess the interaction

between As(III) and FANCL. Western blot analysis showed that incubation of HEK293T cells with the biotin-As probe facilitates the pull-down of ectopically expressed FANCL protein, indicating that As(III) is indeed able to bind to FANCL in cells (Figure 2.2a). Mutations of two critical cysteine residues in the RING-finger domain to alanines led to marked diminution in this interaction, suggesting that the interaction between FANCL and As(III) necessitates the intact RING-finger domain of FANCL (Figure 2.2b). To further substantiate this finding, we performed fluorescence microscopy experiments using an As(III)-containing dye, ReAsH-EDT_2, which displays red fluorescence after its arsenic moieties bind to four cysteine residues in proteins (154). Indeed, fluorescence microscopy results revealed that the GFP-tagged FANCL, but not the FANCL mutants, co-localizes with ReAsH-EDT_2 (Figure 2.3-2.4), again supporting the binding between As(III) and the RING-finger domain of FANCL in cells. However, pretreatment of cells with $NaAsO_2$ or PAPAO, but not Zn^{2+}, led to significant reductions in the co-localization between ReAsH-EDT_2 and FANCL (Figure 2.5-2.6), supporting the competitive binding of As(III) to cysteine residues in the RING finger motif of FANCL.

Arsenite Binding to FANCL Perturbs the Ubiquitination and Chromatin Localization of FANCD2

Having demonstrated the interaction between As(III) and FANCL, we next investigated the effect of this binding on the function of FANCL. To this end, we treated HEK293T and HeLa cells with MMC to induce ICLs in cells and subsequently incubated the cells with As(III). Western blot results illustrated

that the level of monoubiquitination of FANCD2 was significantly elevated after MMC treatment; however, the MMC-stimulated ubiquitination of FANCD2 was dramatically reduced after incubation with arsenite (Figure 2.7). Considering that FANCL is the major E3 ligase involved in the monoubiquitination of FANCD2 (155), the above results supported that the binding of arsenite to the RING finger motif of FANCL diminishes its E3 ubiquitin ligase activity. In addition, chromatin fractionation assay results showed that the ubiquitinated FANCD2 was primarily localized in the chromatin fraction (Figure 2.8), which agrees with the notion that the recruitment of ubiquitinated FANCD2 to chromatin is an important step in DNA ICL repair (156). Moreover, treatment of cells with increasing concentrations of arsenite led to a dose-dependent decrease in the localization of FANCD2 to chromatin (Figure 2.9). These results support that arsenite binding to the RING finger motif of FANCL perturbs its E3 ligase activity, thereby resulting in diminished ubiquitination and chromatin localization of FANCD2.

To further confirm the diminished ubiquitination of FANCD2 after arsenite treatment, we conducted a quantitative proteomic experiment to assess the level of this ubiquitination with the use of SILAC labeling, immunoprecipitation of tryptic peptides containing the ubiquitin remnant (i.e. diglycine-modified lysine), and LC-MS/MS analysis (Figure 2.10). We were able to detect the $[M+2H]^{2+}$ ions for both the light (*m/z* 576.3217 for the monoisotopic peak) and heavy (*m/z* 584.3246 for the monoisotopic peak) forms of the FANCD2 peptide harboring the ubiquitin remnant at Lys561 (Figure 2.10-2.12). The LC-MS data revealed that the level of FANCD2 ubiquitination at Lys561 was

decreased by more than 2 fold after arsenite treatment (Figure 2.10-2.12).

Arsenite Exposure Led to Compromised Recruitment of FANCD2 to DNA Damage Sites and Sensitized Cells toward DNA ICL Agents

We next utilized immunofluorescence microscopy to examine the effect of arsenite treatment on the recruitment of FANCD2 to DNA damage sites upon ICL induction. In this vein, HeLa cells were exposed to TMP and UVA light (TMP+UVA) (157) to induce ICLs and subsequently stained with γH_2AX (158) and FANCD2 antibodies to reveal the co-localization of damage sites and FANCD2 protein in the presence or absence of arsenite treatment. Compared to the control group, the recruitment of FANCD2 to ICL sites was substantially reduced upon arsenite treatment (Figure 2.13). Moreover, recruitment of FANCD2 to DNA damage sites decreases with the dose of arsenite used (Figure 2.13-2.14). This finding, in conjunction with the results obtained from the chromatin fractionation assay, led us to conclude that, upon ICL induction by MMC or TMP+UVA, arsenite inhibits the recruitment of FANCD2 to ICL sites, which may compromise the repair of ICLs via the FA pathway.

To further substantiate the above findings, we performed a clonogenic survival assay to assess whether arsenite exposure sensitizes cultured human cells toward DNA interstrand cross-linking agents. To this end, we treated the cells with increasing concentrations of arsenite prior to exposure to MMC or TMP+UVA. After culturing the cells for 10 days, we quantified the survival rates of cell colonies. Our results showed that the number of surviving colonies reduced with the dose of arsenite, suggesting that arsenite conferred

elevated sensitivities of cells toward the cytotoxic effects of DNA interstrand cross-linking agents (Figure 2.15).

Discussion

Arsenic is a widespread environmental carcinogen (159), and binding to vicinal thiols in proteins is thought to be one of the major mechanisms underlying the cytotoxic and carcinogenic effects of arsenic species (135). Zinc fingers are small structural motifs in proteins characterized by the coordination of one or more zinc ions with their Zn^{2+}-binding regions. They assist to stabilize the folded structures of proteins and maintain their functions (160). It was observed previously that As(III) displayed stronger binding affinity towards C3H- and C4-types of zinc fingers (136). Arsenite was found to bind to C4-type zinc finger in XPA (137,138) and C3H-type zinc finger in PARP-1 (139), which impair their functions in DNA repair. RING finger is a specific type of Zn^{2+}-binding domain that contains a C3HC4 amino acid motif and can coordinate two zinc ions (161). RING finger is present in many E3 ubiquitin ligases including, among others, APC/C, MDM2, BRCA1, and the above-mentioned RNF20/40 (162). Replacement of Zn^{2+} ions with As(III) in the RING finger domain of PML was found to lead to the proteasomal degradation of PML-RARα fusion protein (144). Arsenite binding to the RING finger domains of RNF20-RNF40 E3 ubiquitin ligase inhibits the ubiquitination of lysine 120 in histone H2B and produces a chromatin environment that is

not biochemically accessible for DNA double-strand break repair (140).

The Fanconi anemia syndrome is a genetic disease manifested with progressive bone marrow failure, developmental abnormalities and increased cancer susceptibility (163). FA arises from germ-line mutation in one of the 19 FA genes discovered to date, resulting in compromised repair of DNA ICLs as well as stalling of DNA replication and transcription machineries (145-147). Central to the FA-mediated DNA repair pathway is the genotoxic stress-induced monoubiquitination of Lys561 in FANCD2 by FANCL in complex with E2 ligases UBE2T or UBE2W (164), which promote the initiation of downstream nucleolytic incisions by recruiting MTMR15/FAN1 to DNA damage sites (165). Monoubiquitination of FANCD2 is required for its binding to chromatin, its interactions with BRCA1 (164) and MTM15/FAN1 (166), DNA repair and normal cell cycle progression. FANCD2 is deubiquitinated by USP1 once DNA repair is complete (167).

As a component of the FA core complex that ubiquitinates FANCD2 and FANCI, the E3 ubiquitin ligase FANCL, harboring a C4HC3 RING finger motif (168), plays an important role in the FA pathway for the repair of ICLs. Our present study demonstrated that arsenite binds to the RING finger domain of FANCL both *in vitro* and in cultured human cells. In keeping with the fact that the coordination of Zn^{2+} ions with the RING finger motif of FANCL is essential for its structural integrity, protein interaction and E3 ligase activity (168), we found that the occupancy of As(III) at the Zn^{2+}-binding sites of FANCL led to a diminished ubiquitination and compromised localization of FANCD2 to chromatin and DNA damage sites. The impaired ubiquitination of FANCD2

triggered by arsenite exposure perturbs the FA pathway-mediated repair of DNA ICL lesions. Consistent with this notion, we observed that cells exposed to arsenite exhibited diminished resistance to agents that can induce DNA ICL lesions. Together, we uncovered, for the first time, that arsenite is able to bind to the RING finger domain of FANCL and this binding leads to diminished DNA ICL repair. This novel discovery provides a better understanding of the mechanism underlying the carcinogenic effect of arsenite.

Figures

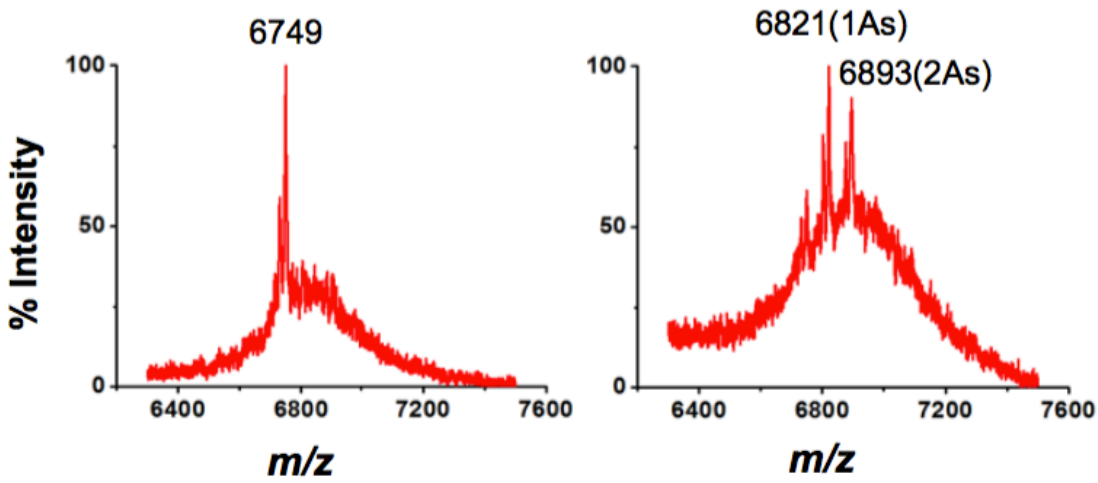

Figure 2.1 MALDI-TOF mass spectrum showing the interaction between As^{3+} and the RING-finger peptide of FANCL. The peptide was capable of binding up to two As^{3+}.

a)

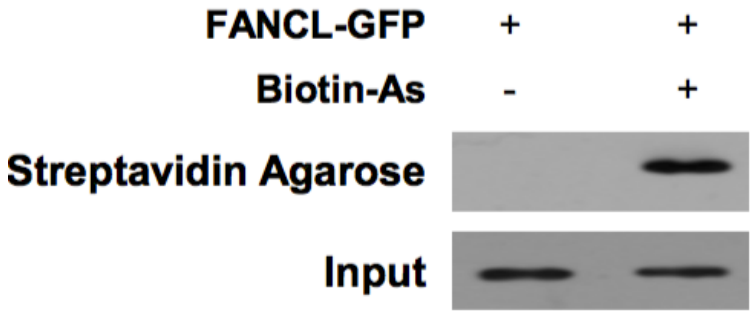

b)

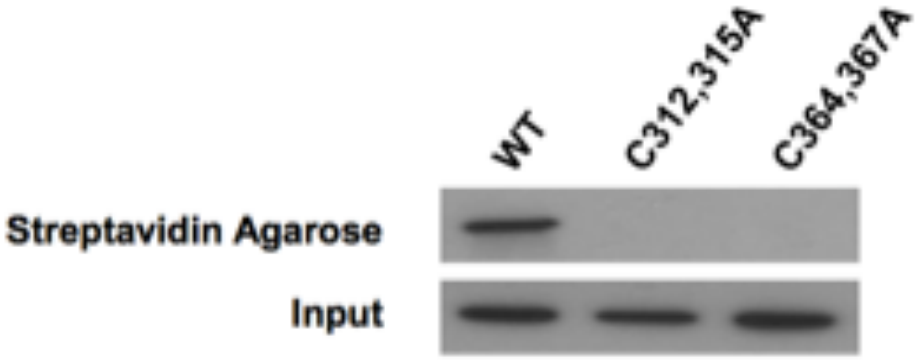

Figure 2.2 a) Streptavidin agarose affinity assay revealed the interaction between As^{3+} and FANCL protein in HEK293T cells. Biotin-As probe was used to assess the binding between As^{3+} and ectopically expressed GFP-FANCL protein. b) Streptavidin agarose affinity assay revealed the abolished interaction between As^{3+} and FANCL protein mutants in HEK293T cells, where the RING-finger cysteine residues 312 and 315 or 364 and 367 were mutated into alanines.

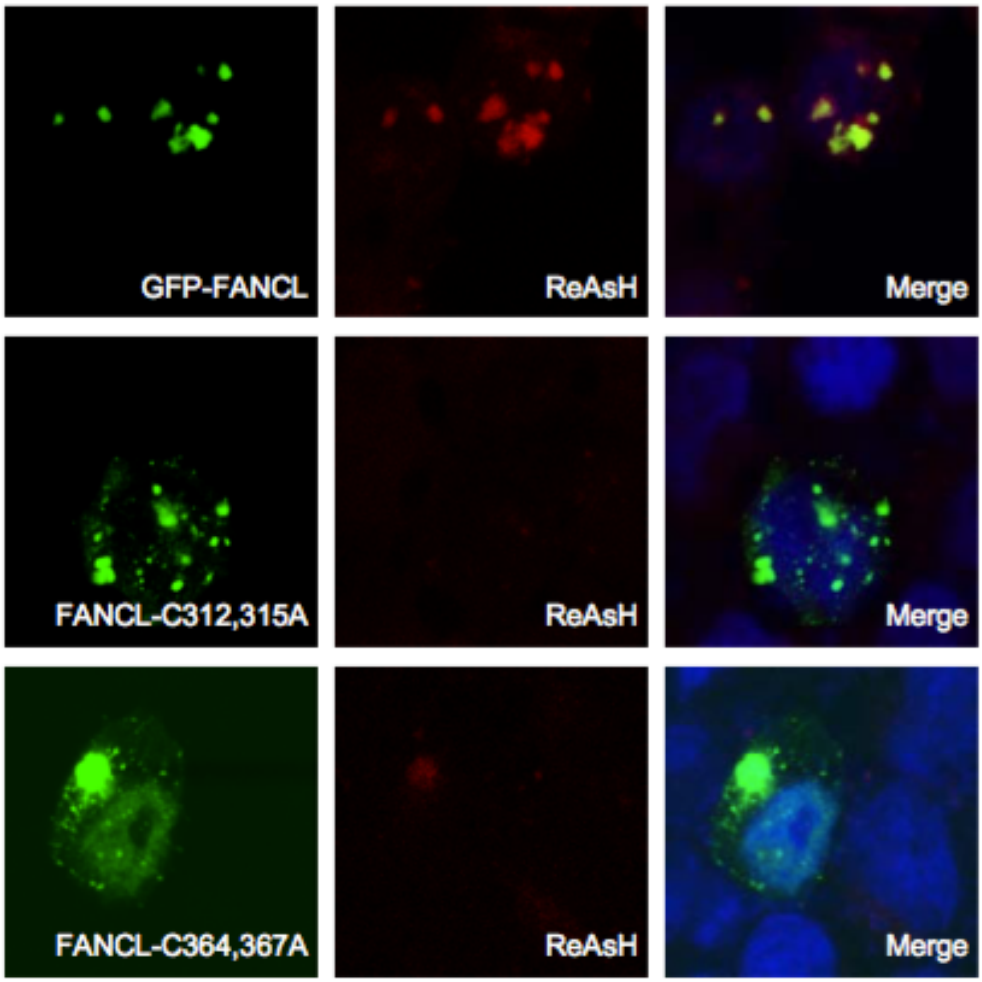

Figure 2.3 Fluorescence microscopy results revealed the colocalization of As^{3+}-bearing ReAsH-EDT_2 and GFP-FANCL in HEK293T cells, and mutations of cysteines to alanines in the RING-finger domain diminished the colocalization.

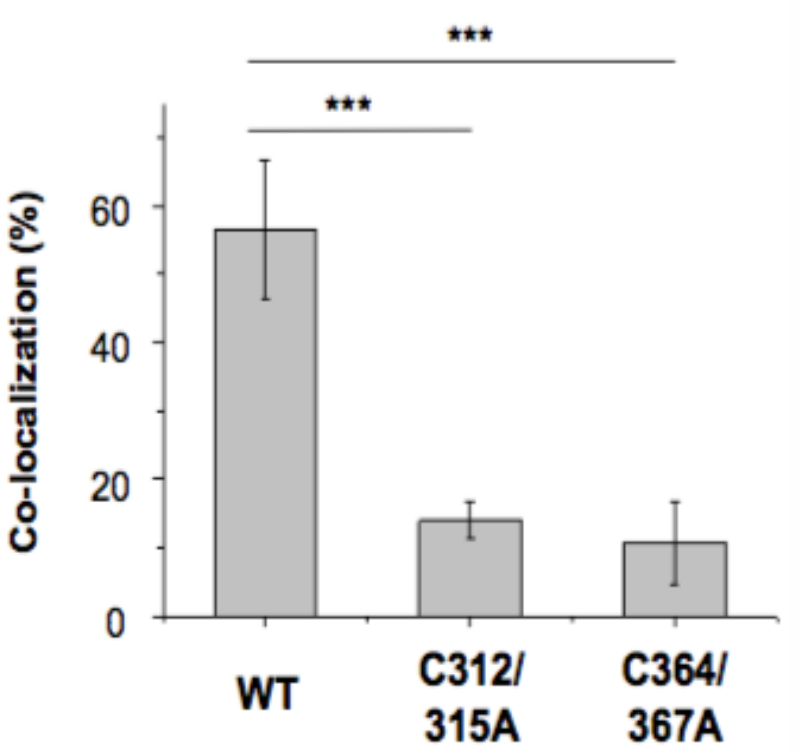

Figure 2.4 Quantitative analysis of the extents of colocalization between ReAsH-EDT$_2$ and FANCL or its mutants. The signal intensities of fluorescence emission in each channel were determined by using ImageJ. The colocalization ratios were calculated as the signal intensity of ReAsH-EDT$_2$ divided by the signal intensity of GFP. The data represent the mean and standard deviation of results obtained from images of 30 different cells. ***P < 0.001. The P values were calculated using two-tailed, unpaired Student's t test.

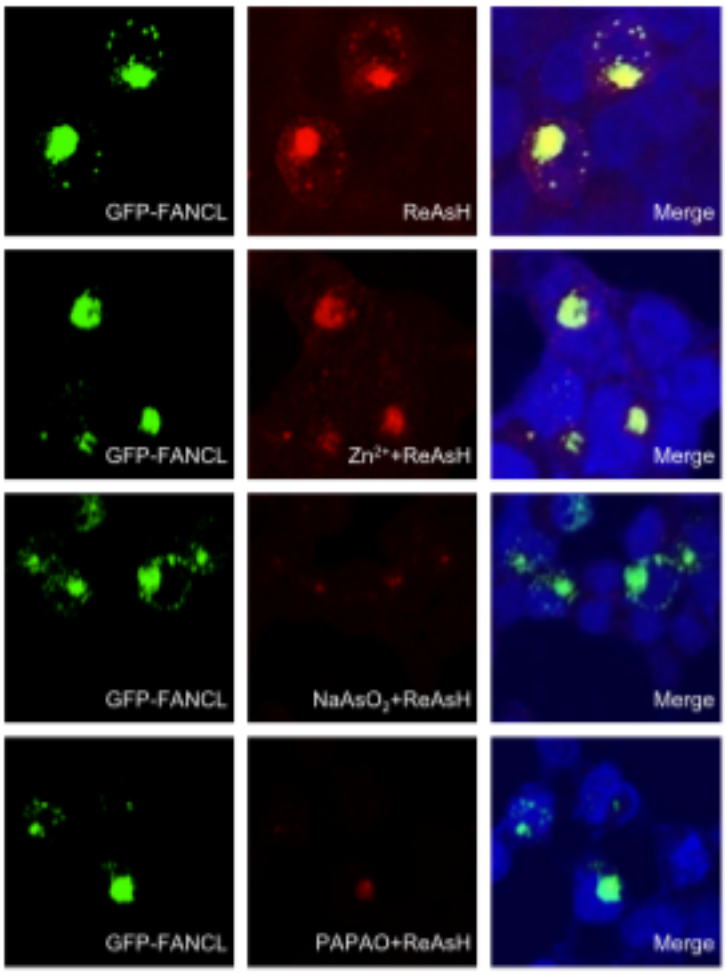

Figure 2.5 Fluorescence microscopy showing the colocalization between As^{3+}-bearing ReAsH-EDT_2 and GFP-FANCL in HEK293T cells. The colocalization was abolished in cells pretreated with 10 μM $NaAsO_2$ or PAPAO, but not Zn^{2+}, prior to staining with ReAsH-EDT_2.

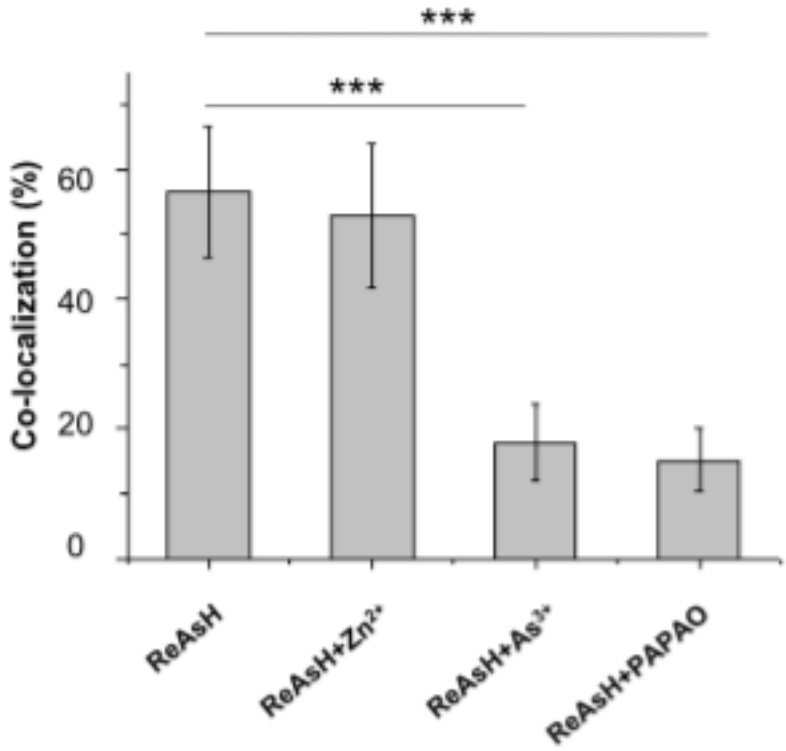

Figure 2.6 Quantitative analysis of the frequencies of colocalization between ReAsH-EDT$_2$ and FANCL. The data represent the mean and standard deviation of results obtained from images of 30 different cells. ***P < 0.001. The P values were calculated using two-tailed, unpaired Student's t test.

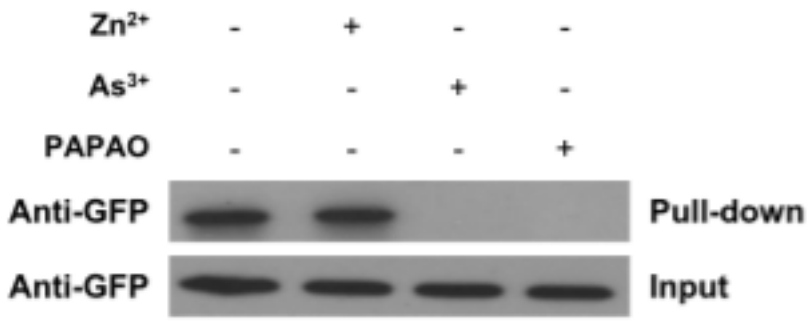

Figure 2.7 Streptavidin agarose affinity assay revealed the interaction between As^{3+} and FANCL protein in HEK293T cells. The interaction was diminished after pretreatment with 10 μM $NaAsO_2$ or PAPAO, but not Zn^{2+}.

a)

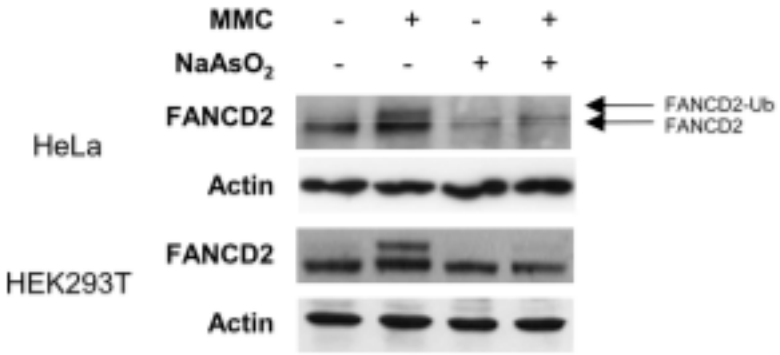

b)

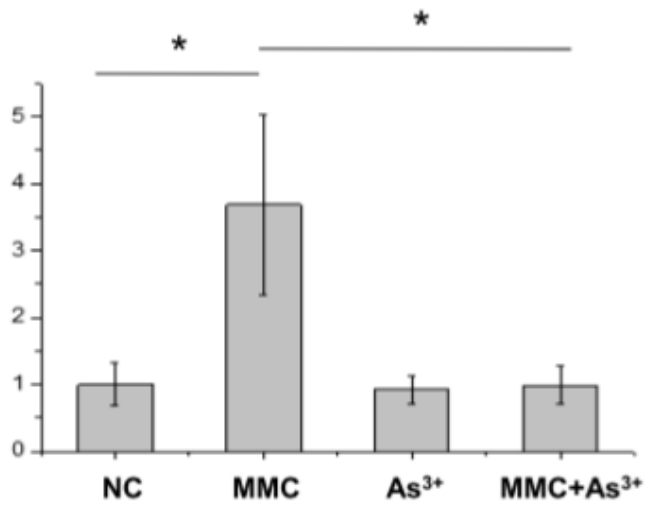

Figure 2.8 a) The Western blot result revealed that As^{3+} exposure elicited reduced ubiquitination of FANCD2 in the lysate of HeLa cells after As^{3+} exposure upon ICL induction by MMC. b) Quantitative data of relative levels of FANCD2 ubiquitination after MMC treatment. The data represent the mean and standard deviation of results obtained from three biological replicates.

a)

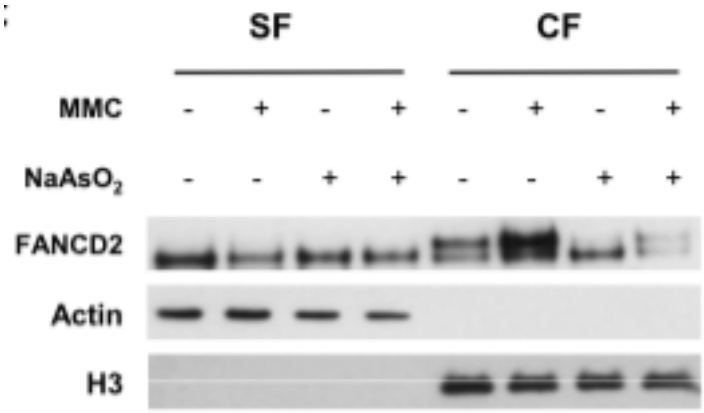

b)

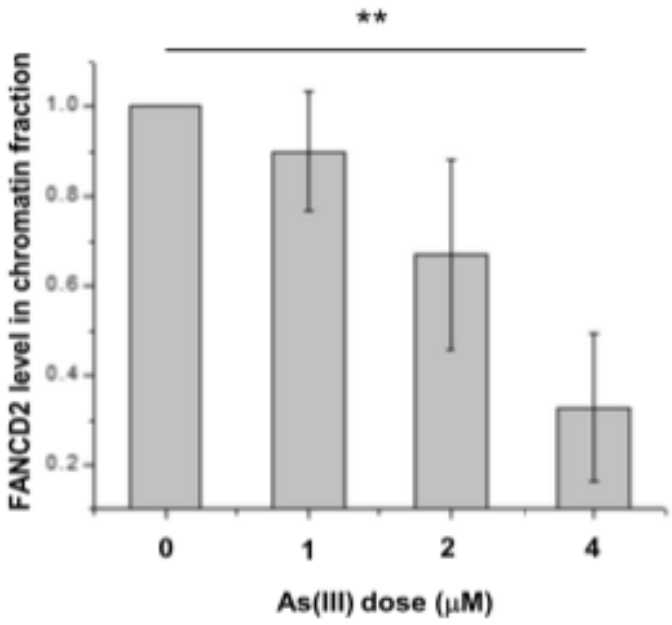

Figure 2.9 a) As^{3+} exposure diminished the ubiquitination level of FANCD2 and perturbed its chromatin localization. "CF" and "SF" designate the chromatin and soluble fractions, respectively. b) Quantitative data of total FANCD2 level in chromatin fractions. The levels of FANCD2 were represented as the ratio of FANCD2/histone H3 in chromatin fractions, and the relative level of FANCD2 in the control group was normalized to unity.

a)

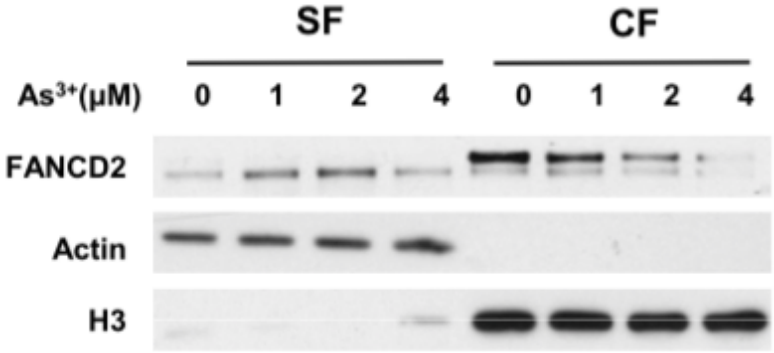

b)

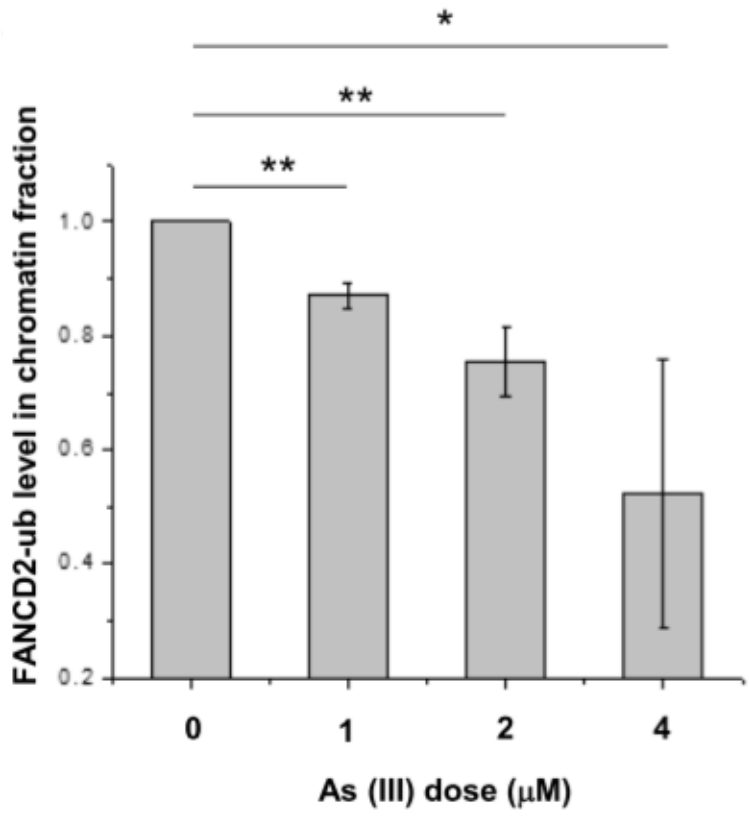

Figure 2.10 a) Levels of FANCD2-ub were diminished upon arsenite treatment in a dose dependent manner. b) The relative levels of FANCD2 ubiquitination were calculated as the ratios of FANCD2-ub over unmodified FANCD2 in chromatin fractions, and the ratio for the control group was normalized into unity. *P < 0.05; **P < 0.01; ***P < 0.001. The P values were calculated using two-tailed, unpaired Student's t test.

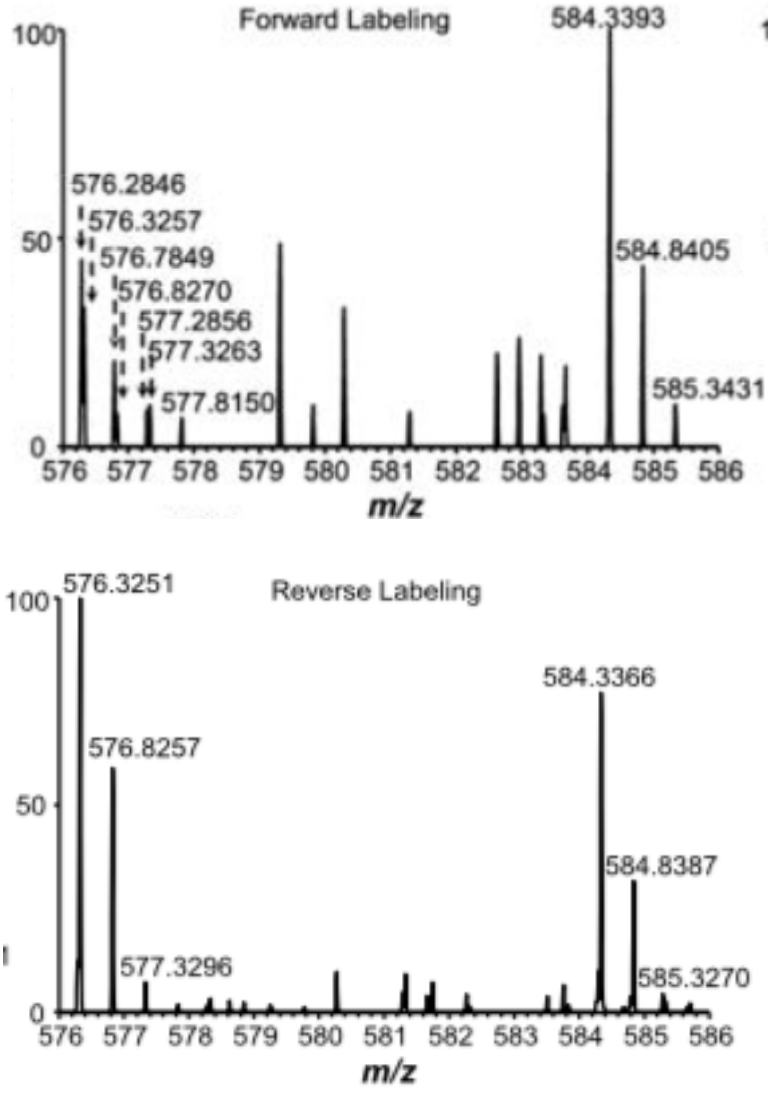

Figure 2.11 MS results for FANCD2 K561 ubiquitination from the forward and reverse SILAC labeling samples. In the forward sample, cells cultured in light SILAC medium were treated with 5 μM $NaAsO_2$ for 24 h and mixed with an equal amount of lysate from untreated cells cultured in heavy SILAC medium. In the reverse sample, lysate of cells cultured in heavy medium and treated with 5 μM $NaAsO_2$ was mixed with an equal amount of lysate of untreated cells cultured in light medium. The spectrum shows the $[M + 2H]^{2+}$ ions for FANCD2 K(ub)QLSSTVFK (light, m/z 576.3217) and K(ub)*QLSSTVFK* (heavy, m/z 584.3246) peptides.

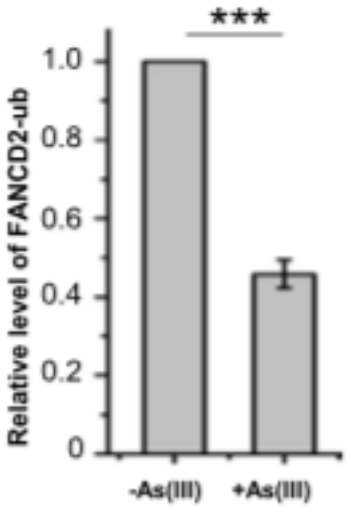

Figure 2.12 Relative levels of ubiquitination of K561 in FANCD2 with or without arsenite treatment. The data represent the mean and standard deviation of results obtained from three independent experiments. The level of FANCD2 ubiquitination in the control group was normalized into 1.0. ***P < 0.001, and the P values were calculated using a two-tailed, unpaired Student's t test.

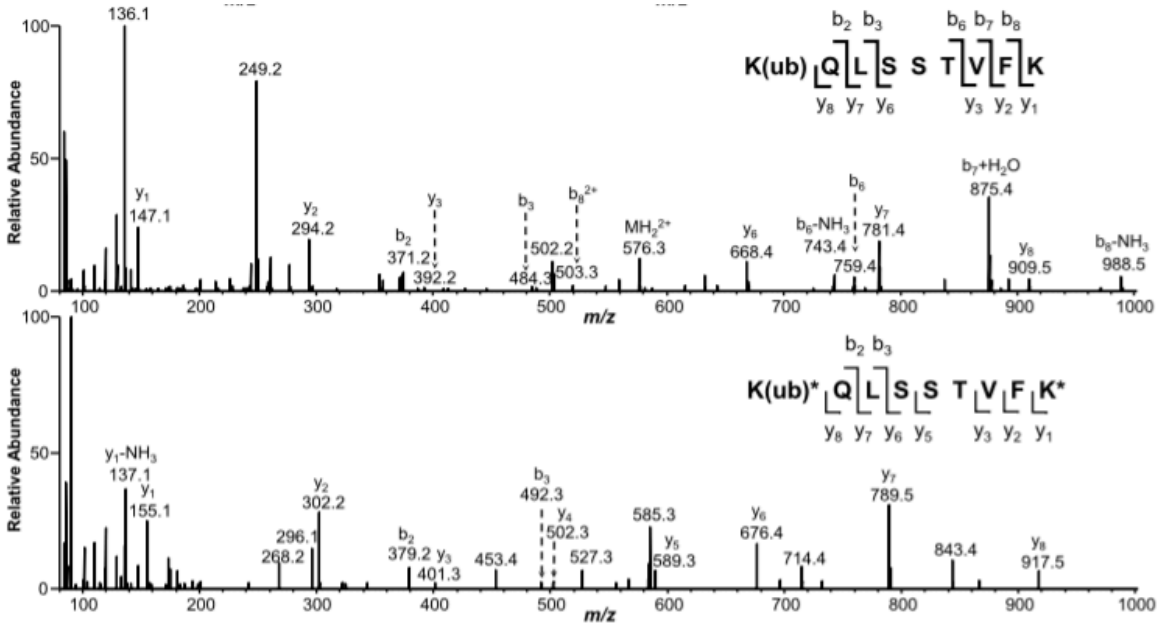

Figure 2.13 MS/ MS results for K(ub)QLSSTVFK (light) and K(ub)*QLSSTVFK* (heavy) peptides.

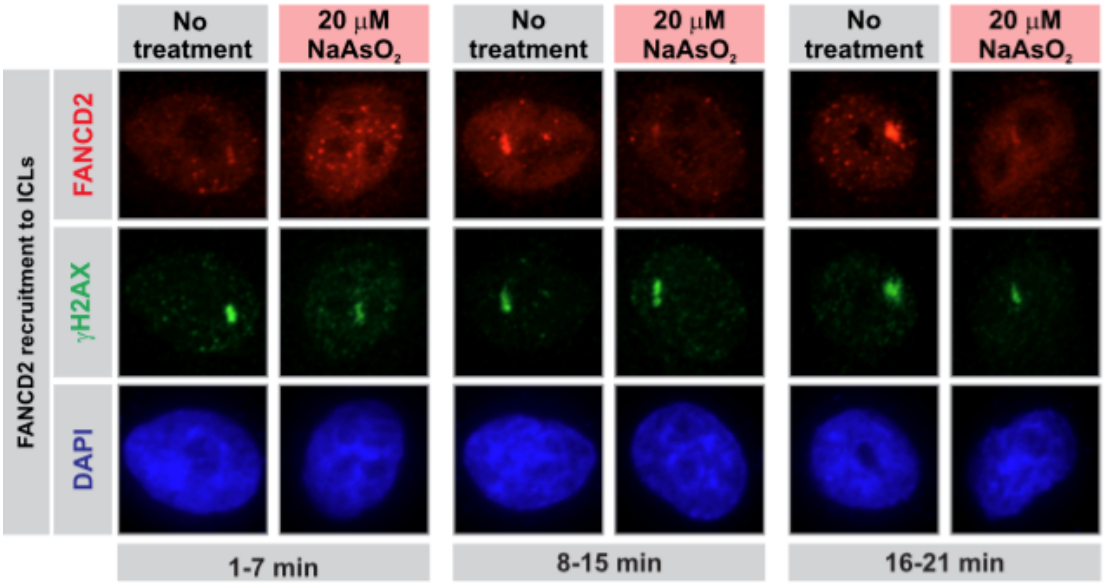

Figure 2.14 Cells were treated with TMP ± $NaAsO_2$ (5 or 20 μM) and targeted with a 365 nm laser in a defined ROI in the cell nuclei to photoactivate the 4,5′,8-trimethylpsoralen and introduce ICLs. The cells were subsequently fixed and stained for γH2AX and FANCD2 to quantify the recruitment of FANCD2 to laser-localized ICLs as a function of time. Representative images showing γH2AX (damage marker) and the colocalizing FANCD2 stripe for each condition at the different time intervals following ICL induction.

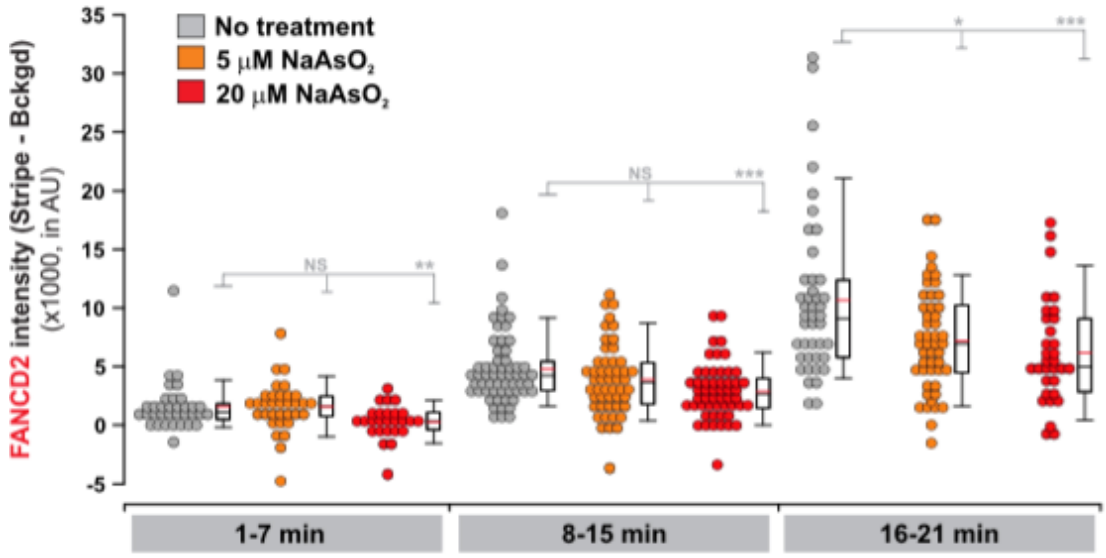

Figure 2.15 Quantification results for the data shown in A. The intensity of FANCD2 in the stripe and the nuclear background was quantified in at least 30 cells per time point per condition analyzed, where the images were acquired under identical exposure conditions. Three independent experiments were performed and showed equivalent results. Means were compared using a Rank-sums test (*P < 0.05; **P < 0.01; ***P < 0.001).

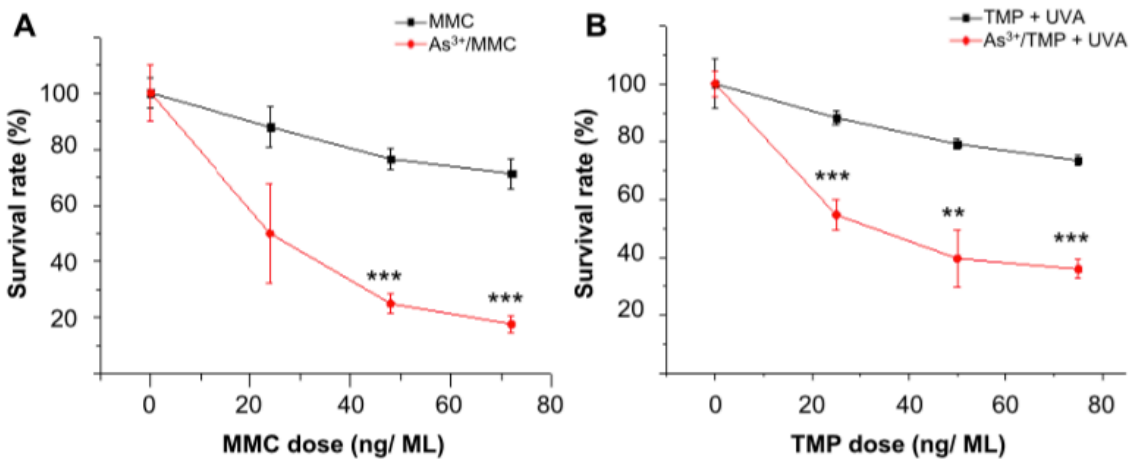

Figure 2.16 Clonogenic survival assay showing diminished resistance toward ICL agents upon As^{3+} exposure. (A) HEK293T cells were plated in six- well plates and treated with increasing doses of MMC to induce ICLs and exposed to As^{3+}. After being cultured for 10 days, the cells exposed to As^{3+} displayed diminished resistance to MMC as reflected by lower survival rates relative to the control group. (B) HEK293T cells were treated with increasing doses of TMP and irradiated with 365 nm light to photoactivate the 4,5′,8-trimethylpsoralen to introduce ICLs. Compared to the control group, the cells exposed to As^{3+} manifested increased sensitivity to TMP + UVA. **P < 0.01; ***P < 0.001. The P values refer to the comparisons between the groups treated with ICL agents alone and those treated with ICL agents together with As^{3+}, and the values were calculated using a two- tailed, unpaired Student's t test.

Chapter 3. A Quantitative Study of Ubiquitin Proteome Identifies TRC8 as a New Target of Arsenite to Inhibit HMGCR ubiquitination

Introduction

Being a metalloid, arsenic is ubiquitously present many places around the world, especially in soil and ground water (169). It's originally derived from the earth crust, which contains arsenic in the range of 1 mg/kg to 490 mg/kg, with a mean of 2 mg/kg (170). Arsenic species were brought to the surface through volcano eruption, which makes the surroundings an arsenic-rich area (171). Arsenic often coordinates with sulfide to form sulfide minerals like pyrite (172). In water, inorganic arsenic is dominant over a few organic arsenic species, which is the main concern of arsenic for human health (173). The mechanism of arsenic toxicity has caught the attention of researchers for decades because arsenic exposure leads to severe human diseases including cancers and cardiovascular diseases (174-178). Recent studies have revealed that As(III) is able to interact with the side-chain sulfhydryl groups in vicinal cysteine residues of RING-finger containing E3 ubiquitin ligase proteins, which inhibits protein ubiquitination (44,57,179-182).

Protein ubiquitination is one of the most important post-translational modifications (PTM) that play significant roles in regulating protein-protein interactions, signal transduction and protein degradation, etc. (183-186). The ubiquitination process starts by the conjugation of a ubiquitin to a substrate Lys residue, with the aid of ubiquitin-activating enzymes (E1), ubiquitin conjugating enzymes (E2) and ubiquitin ligases (E3). The 76-amino acid protein ubiquitin can be ubiquitinated on the N-terminus or one of its seven Lys residues, creating diverse polyubiquitination chains that encompass complex topologies (187). Over the past several decades, researchers have

been using mass spectrometry combined with other biological techniques to identify protein ubiquitination sites. In most cases, researchers ectopically overexpressed affinity-tagged ubiquitin and enriched ubiquitinated proteins by immunoprecipitation (188,189). However, identification of ubiquitinated proteins by these methods were found to be challenging because of the ubiquitin chain types arising from diverse ubiquitination process and the low stoichiometry of ubiquitinated proteins. The disadvantages of these methods also came from sample complexity, in which both ubiquitinated and nonubiquitinated peptides are present in the sample after enzymatic digestion (190). This may lead to a poor coverage of ubiquitinated peptides if they are overwhelmed by nonubiquitinated peptides, especially for those ubiquitinated peptides with low abundances. Along this line, quantitative analysis of ubiquitinated proteome by LC-MS/MS coupled with these methods permits the identification of ubiquitinated proteins in a large scale, whereas it loses the information of specific ubiquitination sites.

A technique to specifically enrich only ubiquitinated peptides of substrate proteins is required for the quantitative identification of ubiquitination sites in the whole proteome. In this vein, substantial progress has been made from the development of antibodies that specifically recognize the di-Glycine remnant generated on lysine resides of trypsin-digested ubiquitinated peptides (191-194). In a ubiquitination process, the C-terminal glycine residue of ubiquitin protein is attached to the lysine residue of a substrate protein. Digestion of ubiquitinated proteins by trypsin cleaves lysine and arginine residues of the proteins, leaving the two C-terminal glycine residues attached

to the ε-amino group of the ubiquitinated lysine residues, producing K-ε-GG containing peptides that can be prevented from being cleaved by trypsin and recognized and immunoprecipitated by the di-Glycine remnant antibodies, which enables the global identification of ubiquitination sites in the whole proteome (195).

Since our previous work has already demonstrated that arsenite can suppress ubiquitination of several proteins by targeting to their E3 ligases, here we expanded our study toward the analysis of alterations in ubiquitinated proteome induced by arsenite exposure. By analyzing whole-cell protein lysate derived from arsenite-treated cells using LC-MS/MS coupled with SILAC labeling (116) and di-Glycine remnant antibody immunoprecipitation, we were able to detect ~1000 ubiquitination sites, among which we found that the ubiquitination level of HMGCR at Lys248 was decreased by four-fold upon arsenite treatment, which led us to explore the role of arsenite in stabilizing HMGCR since HMGCR is a rate-limiting enzyme in cholesterol biosynthesis (196). We also demonstrated that arsenite targets the TRC8 E3 ubiquitin Ligase to inhibit HMGCR ubiquitination.

Experimental Procedures

Plasmid construction

To construct the pCDNA3.0-HMGCR-FLAG plasmid, the total RNA of HEK293T were extracted from HEK293T cells using the E.Z.N.A.® Total RNA Kit I (Omega, Norcross, GA), and used as a template to construct the cDNA library by reverse-transcription. Two primers were designed to amplify the coding sequence of human HMGCR from HEK293T cDNA library by PCR. The coding sequence of HMGCR was subsequently ligated into the *BamHI/Xbal* sites of pCDNA3.0 vector. The construct was confirmed by sequencing (Retrogen Inc, San Diego, CA).

Similar procedure was performed to insert the coding sequence of TRC8 into *AgeI/XhoI* sites of pEGFP-C3 vector to construct pEGFP-C3-TRC8 plasmid.

HMGCR primers:

forward (5'-AAAGGATCCGGCTGTCTTCTTGGTGCAAG-3')

reverse (5'-AAATCTAGAATGTTGCTAAGACTTTTTCGAATGCA-3')

TRC8 primers:

forward (5'-AAAACCGGTATGGCGGCCGTGGGGCCCCC-3')

reverse (5'-CCGCTCGAGGTCAGTATCATCATTAAATTCTTCA-3')

The designed primers for the construct PLKO-shTRC8 were annealed, phosphorylated, and ligated to the dephosphorylated *EcorI/AgeI* sites of PLKO vector. The ligation product was transformed into *Escherichia coli* cells for amplification. The plasmid was extracted and its identity was validated by Sanger sequencing.

shTRC8 primers:

forward (5'-CCGGCCTTTC TGTTAGCTGCA ACTTCTCGAG AAGTTGCAGC TACAGAAAGG TTTTT-3')

reverse (5'-AATTCAAAAA CCTTTCTGTT AGCTGCAACT TCTCGAGAAG TTGCAGCTAA CAGAAAG-3')

The HA-ub plasmid was purchased from Addgene.

Cell culture and transfection

HEK293T human embryonic kidney epithelial cells and GM00637 cells were maintained in a humidified atmosphere containing 5% CO_2 at 37°C, and cultured in Dulbecco's Modified Eagle Medium (DMEM, ATCC, Manassas, VA) containing 10% fetal bovine serum (FBS, Invitrogen, Waltham, MA) and 100 U/mL penicillin and streptomycin. Typically, 1 μg plasmid or 100 pmol siRNA was transfected into cells with 5 μL of Lipofectamine 2000 (Thermo Fisher, Waltham, MA).

SILAC Labeling and As(III) exposure of cells

GM00637 cells were cultured in either light or heavy RPMI 1640 medium. In heavy medium, the cells were labeled with isotopic $^{13}C_6$ $^{15}N_2$ L-lysine (K8) and $^{13}C_6$ L-arginine (R6). A labeling efficiency of >95% was confirmed by LC-MS/MS analysis. Cells were then mock treated in light medium and treated with 5 μM As(III) in heavy medium or vise verse for 24 hr, followed by 5 μM MG132 treatment for 1 hr. The light and heavy cells were harvested and the

whole cell lysate were mixed at 1:1 ratio, as quantified by Bradford assay. Ten mg tryptic digested mixture of lysates was subjected to the pull-down of di-Glycine peptides.

Ubiquitin Remnant Peptide Immunoprecipitation

A mixture of 10 mg of the light and heavy lysate was first reduced with DTT and alkylated by iodoacetamide, followed by trypsin digestion at an enzyme/substrate mass ratio of 1:50 overnight. The tryptic peptides were subjected to a Sep-Pak C18 column (Waters) for sample desalting and purification following the published protocol (197). The eluted peptides after desalting were subsequently incubated with the commercial antibody from the PTMScan Ubiquitin Remnant Motif (K-ε-GG) Kit (Cell Signaling) that specifically recognizes di-Glycine-containing peptides. The immunoprecipitated di-Glycine-containing peptides were eluted with 0.15% trifluoroacetic acid, desalted with ZipTip (EMD Millipore), and subsequently subjected to LC-MS/MS analysis.

LC-MS/MS Analysis of ubiquitinated Peptides and Peptide Mapping to the Database

The samples were injected into a Thermo Q Exactive Plus Hybrid Quadrupole-Orbitrap Mass Spectrometer coupled with nano-LC for a data-dependent scan analysis with a top 20 method using a 181-min gradient with a flow rate of 230 nl/min. Water and acetonitrile with 0.1% TFA were used as solvent A and

solvent B, respectively. The gradient we used was listed below:

0 min – 0% B, 5 min – 9% B, 155 min – 39% B, 156 min – 88% B, 166 min – 95% B, and 181min - 95% B.

The full-MS scans were obtained in the Orbitrap mass analyzer within the m/z range from 200-1200 with a resolution 35000 at m/z 200. Twenty most abundant ions were fragmented in the HCD collision cell, and the full tandem mass spectra were acquired in the Orbitrap mass analyzer with a resolution 17500 at m/z 200. The maximum injection time for the full-MS scans and the tandem mass spectra were 100 ms and 75 ms, respectively.

After LC-MS/MS analysis, the raw data files were subjected to Maxquant software for peptide mapping searching against FASTA human whole proteome database with a false discovery rate 0.01. Trypsin digestion was chosen and GlyGly on Lys was set as a variable modification, while cysteine carbamidomethylation was set as a fixed modification.

Evaluation of HMGCR Expression Level and Ubiquitination Level by Western Blot

To monitor HMGCR expression level, HEK293T cells were exposed to increasing concentrations of As(III) for 24 hr. The treated cells were harvested, lysed and subsequently subjected to SDS-PAGE analysis. The separated proteins were transferred to a nitrocellulose membrane and probed for HMGCR and β-actin with the use of anti-HMGCR and anti-actin primary antibodies, respectively.

In parallel, cells were also co-transfected with 1 μg FLAG-HMGCR and 500 ng HA-ubiquitin plasmids for 24 hr and subsequently treated with 5 μM As(III) for 24 hr day, followed by 5 μM MG132 treatment for 2 hr. An amount of 80 μg whole cell lysate was incubated with 30 μL anti-FLAG M2 magnetic beads overnight. The binding protein was eluted with 1x SDS loading buffer at 95 °C for 5 min after washing the beads with 1xPBS three times. The eluted proteins were subjected to SDS-PAGE separation and probed for HA using anti-HA primary antibody to detect the ubiquitination of HMGCR.

Fluorescence Microscopy

HEK293T cells (1×10^5) were seeded on cover glasses and transfected with the pEGFP-C3-TRC8 plasmid (0.5 μg each). After 24 hr, the transfected cells were incubated with 5 μM ReAsH-EDT_2 (Invitrogen, Waltham, MA) in Opti-MEM medium at 37°C for 1 hr, and subsequently washed with BAL buffer for 3 times, fixed with 4% paraformaldehyde for 20 min, and stained with 4',6-diamidino-2-phenylindole (DAPI). The sample slides were subjected to a Leica TCS SP5 confocal microscope (Leica Microsystems, Buffalo Grove, IL) for imaging in the wavelength range of 425-450 nm, 500-550 nm and 580-650 nm for DAPI, GFP and ReAsH, respectively. Competition experiments were performed in a similar procedure with pretreatments with 10 μM $ZnCl_2$, $NaAsO_2$ or PAPAO, respectively.

Results

Identification of ubiquitinated peptides by LC-MS/MS

To begin with, we were interested to investigate how arsenite affects ubiquitination levels in the whole proteome. To this end, we developed a workflow that can assess quantitatively the ubiquitin remnant peptide by immunoprecipitation and LC-MS/MS analysis of the SILAC-labeled GM00637 cells. Briefly, we treated SILAC GM00637 cells with arsenite and immunoprecipitated di-Glycine-containing peptides with an antibody that specifically recognizes di-Glycine after trypsin digestion and purification of samples with Sep-Pak C18 column. The samples were desalted and subjected to LC-MS/MS analysis in the data-dependent acquisition mode, and the raw data were searched against the FASTA human whole proteome database using Maxquant (Figure 3.1). As shown in the results, we were able to quantify 1458 site-specific ubiquitinated peptides from 352 proteins and 6638 non-ubiquitinated peptides from ~2000 proteins, among which 277 of the ubiquitinated peptides in 197 proteins were downregulated upon arsenite treatment and 306 of the ubiquitinated peptides in 167 proteins were upregulated upon arsenite treatment, suggesting a role of arsenite in modulating the ubiquitinated proteome and potentially affecting protein function (Figure 3.2) （cut off ratio 1.5). Since we are typically interested in arsenite-mediated inhibition of ubiquitination, we conducted a KEGG pathway analysis and functional category analysis for all the 197 proteins in which the downregulated ubiquitinated peptides were identified. Both the KEGG

pathway and functional category analyses revealed a role of arsenite in decreasing ubiquitination of proteins involved in cholesterol biosynthesis pathway. In this vein, we identified eight cholesterol-synthesis-related proteins including HMGCR, which is the rate-limiting enzyme that is crucial for cholesterol biosynthesis (198) (Figure 3.3-4.4a).

Arsenite exposure led to diminished ubiquitination and proteasome-mediated degradation of HMGCR

We were also able to identify the HMGCR Lys248 ubiquitinated peptide using LC-MS/MS analysis (Figure 3.4b). The relative abundance of this di-Glycine-containing peptide was found to be decreased by ~73.4% upon arsenite exposure (Fig 4.5b). We detected both the light and heavy ubiquitinated peptide of HMGCR Lys248 as shown in the MS (Fig 4.5a-4.6). This indicated that arsenite exposure significantly downregulates ubiquitination of HMGCR at Lys248, which is thought to be important for the proteasome-mediated degradation of HMGCR (199). In addition, we monitored the total ubiquitination level of HMGCR by immunoprecipitation coupled with Western blot. In this vein, cells were transfected with plasmids for the ectopic overexpression of FLAG-HMGCR and HA-tagged ubiquitin, followed by treatment with arsenite at different doses. The cells were subsequently treated with MG132 to inhibit the degradation of proteins by the 26S proteasome, and the FLAG-HMGCR was pulled down by incubation of anti-FLAG M2 magnetic beads. The Western blot results showed that the levels of

HMGCR ubiquitination level were diminished upon arsenite treatment in a dose dependent manner (Fig 4.8a). Taken together, we found that arsenite exposure led to diminished ubiquitination of HMGCR.

It is well established that HMGCR ubiquitination is responsible for its degradation (200). To explore if arsenite-mediated inhibition of HMGCR ubiquitination accounts for the stabilization of HMGCR, we measured the basal levels of HMGCR protein in HEK293T cells exposed with increasing doses of arsenite (Figure 3.9). The Western blot results showed that exposure with elevated doses of arsenite resulted in heightened level of HMGCR in cells, indicating that the diminished ubiquitination of HMGCR by arsenite correlates with the stabilization of HMGCR.

TRC8 is a major E3 ubiquitin ligase that ubiquitinates HMGCR in HEK293T cells

Having demonstrated that arsenite negatively regulates the ubiquitination of HMGCR in cells, we next examined the underlying mechanism. To this end, we first assessed which E3 ubiquitin ligase is responsible for HMGCR ubiquitination in HEK293T cells, since there are several E3 ubiquitin ligases that were reported to ubiquitinate HMGCR, including gp78, TRC8, MARCH6 and HRD1 (201-204). Toward this end, we first confirmed the role of the four E3 ubiquitin ligases in HMGCR ubiquitination in HEK293T cells by knocking down their expression levels using constructed shRNAs, and monitored the ensuing ubiquitination level of HMGCR. Since ubiquitination serves as a signal for the proteasome-mediated degradation of HMGCR, the level of

HMGCR ubiquitination is tightly regulated and limited under basal conditions. In order to observe an obvious ubiquitination of HMGCR, we ectopically expressed FLAG-tagged HMGCR and HA-tagged ubiquitin in HEK293T cells, and subsequently treated the transfected cells with a proteasome inhibitor, MG132, to stabilize ubiquitinated HMGCR. We probed for HA to monitor HMGCR ubiquitination by Western blot after immunoprecipitating FALG-HMGCR using anti-FLAG M2 magnetic beads. The results showed that the expression levels of all the E3 ligases were downregulated by approximately 75%, as confirmed by RT-PCR (Fig 4.7a). However, we only observed a significant decrease of HMGCR ubiquitination after knocking down TRC8, demonstrating that TRC8 is the major E3 ubiquitin ligase for HMGCR ubiquitination in HEK293T cells (Fig 4.7b).

Arsenite binds to TRC8 to inhibit the ubiquitination of HMGCR

Since the E3 ubiquitin ligase TRC8 contains a RING finger domain (205), we next investigated if arsenite perturbs HMGCR ubiquitination by interacting with TRC8. Therefore, we performed a fluorescence microscopy-based assay with the use of ReAsH-EDT_2, which contains two As^{3+} and displays red fluorescence when cysteine residues in proteins bind to its arsenic moieties (206,207). Along this line, we ectopically expressed GFP-tagged TRC8 in HEK293T cells and subsequently incubated the cells with ReAsH-EDT_2. We observed an obvious co-localization between the GFP-TRC8 and the ReAsH, suggesting an interaction between TRC8 and As^{3+} in cells (Figure 3.10).

We next asked if the interaction between arsenite and TRC8 is responsible for

the inhibition of HMGCR ubiquitination and degradation. To this end, we monitored the levels of HMGCR ubiquitination in TRC8-knockdown HEK293T cells by Western blot. The results showed that arsenite could diminish the ubiquitination of HMGCR in HEK293T cells, whereas this diminution was compromised in cells transfected with shTRC8, demonstrating the critical role of TRC8 in arsenite-mediated perturbation of HMGCR ubiquitination and degradation (Fig 4.8b). Hence, our results showed, for the first time, that arsenite targets TRC8 to inhibit HMGCR ubiquitination and degradation, which may contribute to the upregulation of cholesterol synthesis.

Discussion

The use of LC-MS coupled with the di-Gly immunoprecipitation has been recently established as a robust workflow to study ubiquitin-modified proteome and to identify ubiquitination sites in the global proteome (208). Scientists have been using the K-ε-GG antibody for multiple experiments that include studies of cullin-RING ubiquitin ligase substrates, and the effects of proteasome inhibitor on the landscape of ubiquitination (209,210). This workflow helps to establish ubiquitination networks in core signaling pathways, and the identification of specific ubiquitination sites allows for studying the roles of ubiquitination in a site-specific manner. Researchers have also combined other techniques to further optimize the workflow to expand the number of identified ubiquitinated peptides and reduce noise,

including fractionation of digested peptides by using basic pH reverse-phase chromatography and crosslinking of the K-ε-GG antibody to agarose beads before immunoprecipitating peptides (116,192,211).

The enrichment of di-Gly containing peptides by K-ε-GG antibody helps to reduce the interference of non-ubiquitinated peptides that are produced from the same protein after trypsin digestion, which allows for the identification of ubiquitinated peptides of low abundance. In this study, we applied this workflow to investigate arsenite-mediated alteration of ubiquitin-modified proteome, and were able to identify ~1450 ubiquitinated peptides in GM00637 cells. Consistent with the fact that Lys248 is the dominant site for HMGCR ubiquitination, we were able to detect the ubiquitinated Lys-2480-containing peptide of HMGCR by LC-MS/MS. On the other hand, we also performed off-line SDS-PAGE or affinity pull down to purify and enrich HMGCR protein before LC-MS/MS analysis. However, we failed to detect HMGCR Lys248 ubiquitination using either method, suggesting a low abundance of this ubiquitinated peptide, which is not surprising viewing that this ubiquitination event leads to HMGCR degradation (data not shown). In addition, we observed a diminished level of ubiquitination of Lys248 in HMGCR upon arsenite treatment, indicating that arsenite may influence the cholesterol synthesis pathway by affecting HMGCR ubiquitination. Along this line, we observed decreased total ubiquitination levels of HMGCR, as well as increased basal HMGCR levels upon arsenite treatment in a dose-dependent manner in HEK293T cells by Western blot, suggesting that the arsenite-induced suppression of HMGCR ubiquitination stabilizes HMGCR protein.

Cholesterol is one of the essential components of cell membranes and it helps maintain the membrane integrity and fluidity that enables animal cells to alter shape rapidly in response to condition change (212). It's also a precursor for the biosynthesis of many important molecules such as vitamin D, bile acid and sterol hormones (213-215). Cholesterol is synthesized through the mevalonate pathway, in which the conversion of HMG-CoA to mevalonate by HMGCR is the rate-limiting step (216). Therefore, the level of HMGCR in cells tightly correlates with the biosynthesis of cholesterol and nonsterol isoprenoids. Cells modulate cholesterol biosynthesis through a feedback mechanism, of which the level of the rate-limiting enzyme, HMGCR, is negatively regulated by sterol. That is to say, sterol facilitates the ubiquitination of HMGCR and its subsequent degradation by proteasome, thus forming a negative feedback loop that maintains cholesterol homeostasis (217,218). Several E3 ubiquitin ligases have been proposed to account for the ubiquitination of HMGCR in a cell type specific manner, including gp78, TRC8, MARCH6 and HRD1. In our study, we knocked down each E3 ubiquitin ligase individually in HEK293T cells and found that only the knockdown of TRC8 compromised ubiquitination of HMGCR, suggesting TRC8 is the major specific E3 ubiquitin ligase in ubiquitinating HMGCR in HEK293T cells.

In our previous work, arsenite was found to interact with the RING finger domain of several E3 ubiquitin ligases to inhibit the ubiquitination of their substrate proteins (12,13). In keeping with our previous finding, we also observed an interaction between arsenite and TRC8 E3 ubiquitin ligase, as demonstrated by a fluorescence-microscopy-based assay with the use of the

ReAsH-EDT_2. This led us to consider if arsenite reduces HMGCR ubiquitination through binding to TRC8, since we already demonstrated the major role of TRC8 in ubiquitinating HMGCR in HEK293T cells. Indeed, the arsenite-induced perturbation of HMGCR ubiquitination was completely abolished after knocking down TRC8 in HEK293T cells, supporting our hypothesis that arsenite targets TRC8 to inhibit HMGCR ubiquitination and degradation.

In summary, by using LC-MS coupled with SILAC labeling and di-Gly peptide immunoprecipitation, we quantitatively assessed the alteration of ubiquitin-modified proteome induced upon arsenite exposure in mammalian cells, and identified TRC8 as a new target for arsenite binding to inhibit HMGCR ubiquitination and degradation in HEK293T cells.

Figures

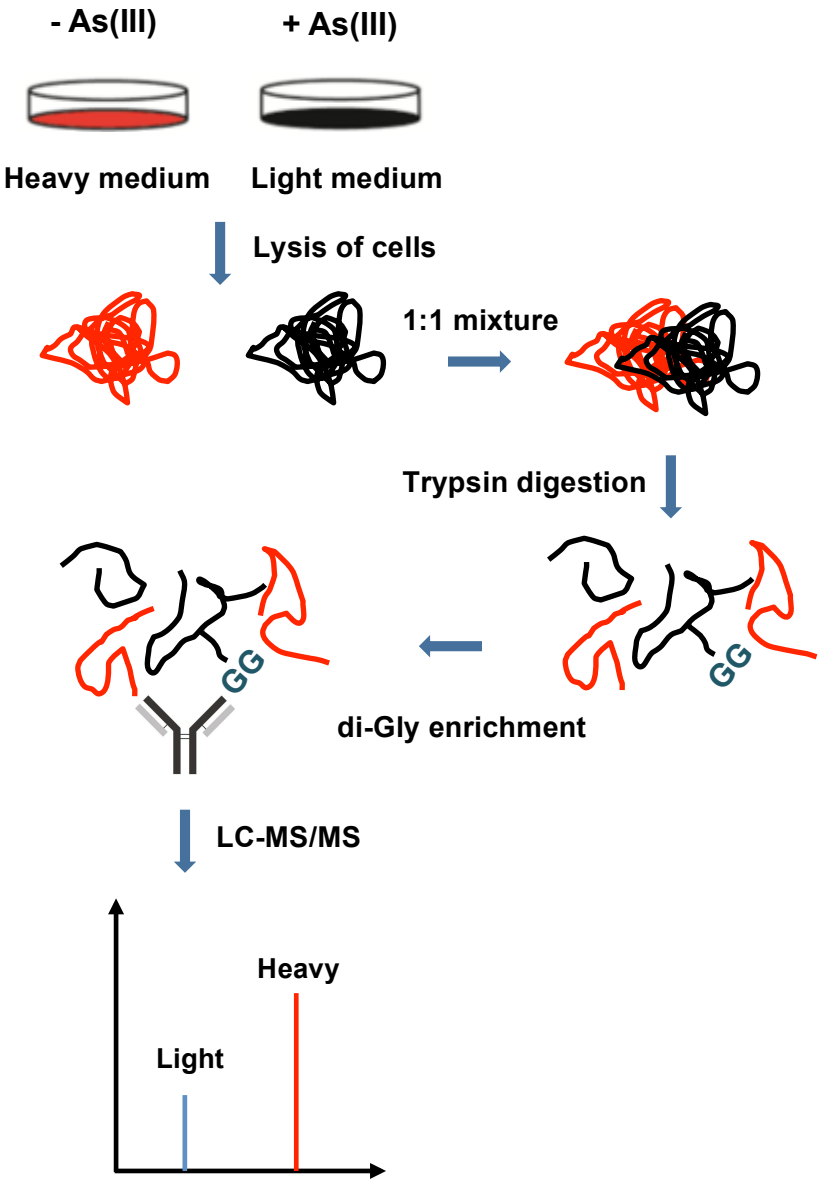

Figure 3.1 Workflow of di-Glycine immunoprecipitation and identification of ubiquitinated peptides by LC-MS/MS

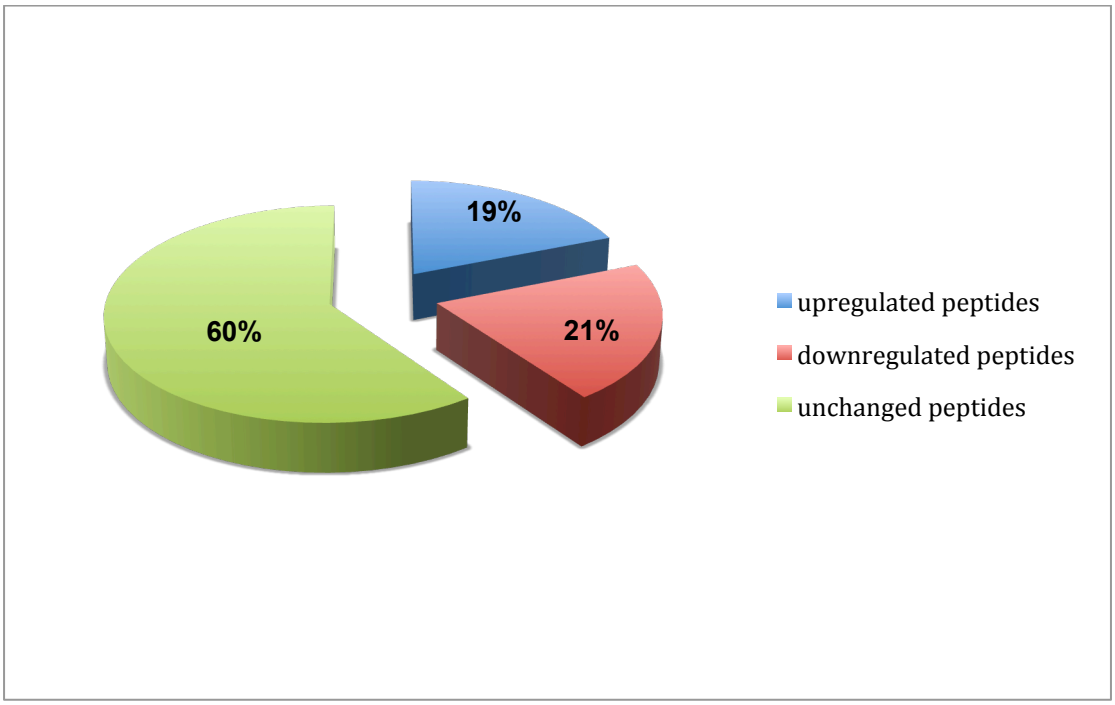

Figure 3.2 Regulation of ubiquitination by arsenite

Sublist	Category	Term	RT	Genes	Count	%	P-Value	Benjamini
	KEGG_PATHWAY	Ribosome	RT		14	4.4	2.3E-6	2.6E-4
	KEGG_PATHWAY	Arrhythmogenic right ventricular cardiomyopathy (ARVC)	RT		11	3.4	1.1E-4	6.1E-3
	KEGG_PATHWAY	Steroid biosynthesis	RT		6	1.9	1.3E-4	4.8E-3
	KEGG_PATHWAY	Dilated cardiomyopathy	RT		11	3.4	5.3E-4	1.5E-2
	KEGG_PATHWAY	Systemic lupus erythematosus	RT		11	3.4	9.6E-4	2.1E-2
	KEGG_PATHWAY	Leukocyte transendothelial migration	RT		12	3.8	1.1E-3	2.0E-2
	KEGG_PATHWAY	ECM-receptor interaction	RT		10	3.1	1.1E-3	1.8E-2
	KEGG_PATHWAY	Hypertrophic cardiomyopathy (HCM)	RT		10	3.1	1.2E-3	1.7E-2
	KEGG_PATHWAY	Focal adhesion	RT		16	5.0	1.4E-3	1.8E-2
	KEGG_PATHWAY	Tight junction	RT		12	3.8	2.9E-3	3.3E-2
	KEGG_PATHWAY	Proteasome	RT		7	2.2	3.2E-3	3.2E-2
	KEGG_PATHWAY	Neurotrophin signaling pathway	RT		11	3.4	5.1E-3	4.7E-2
	KEGG_PATHWAY	Viral myocarditis	RT		8	2.5	6.3E-3	5.4E-2
	KEGG_PATHWAY	Pathogenic Escherichia coli infection	RT		7	2.2	8.3E-3	6.5E-2
	KEGG_PATHWAY	Endocytosis	RT		12	3.8	2.8E-2	1.9E-1
	KEGG_PATHWAY	Adherens junction	RT		7	2.2	3.3E-2	2.1E-1
	KEGG_PATHWAY	Regulation of actin cytoskeleton	RT		13	4.1	3.6E-2	2.2E-1
	KEGG_PATHWAY	Cell adhesion molecules (CAMs)	RT		9	2.8	5.4E-2	2.9E-1
	KEGG_PATHWAY	Vibrio cholerae infection	RT		5	1.6	9.7E-2	4.5E-1

Figure 3.3 KEGG pathway analysis of downregulated ubiquitinated proteins

a)

IPI_ID	GENE NAME	Related Genes	Species
IPI00016703	24-dehydrocholesterol reductase	RG	Homo sapiens
IPI00922451	3-hydroxy-3-methylglutaryl-Coenzyme A reductase	RG	Homo sapiens
IPI00294501	7-dehydrocholesterol reductase	RG	Homo sapiens
IPI00926839	cytochrome P450, family 51, subfamily A, polypeptide 1	RG	Homo sapiens
IPI00914971	farnesyl diphosphate synthase (farnesyl pyrophosphate synthetase, dimethylallyltranstransferase, geranyltranstransferase)	RG	Homo sapiens
IPI00909973, IPI00020944	farnesyl-diphosphate farnesyltransferase 1	RG	Homo sapiens
IPI00923487	lanosterol synthase (2,3-oxidosqualene-lanosterol cyclase)	RG	Homo sapiens
IPI00556210	sterol-C4-methyl oxidase-like	RG	Homo sapiens

b)

HMGCR-K248-ub

light m/z 632.6534 $[M+3H]^{3+}$
heavy m/z 637.3334 $[M+3H]^{3+}$

Figure 3.4 a) Ubiquitination of proteins involved in cholesterol synthesis were inhibited upon arsenite treatment. b) Sequence structure of HMGCR Lys248 ubiquitinated peptide

a)

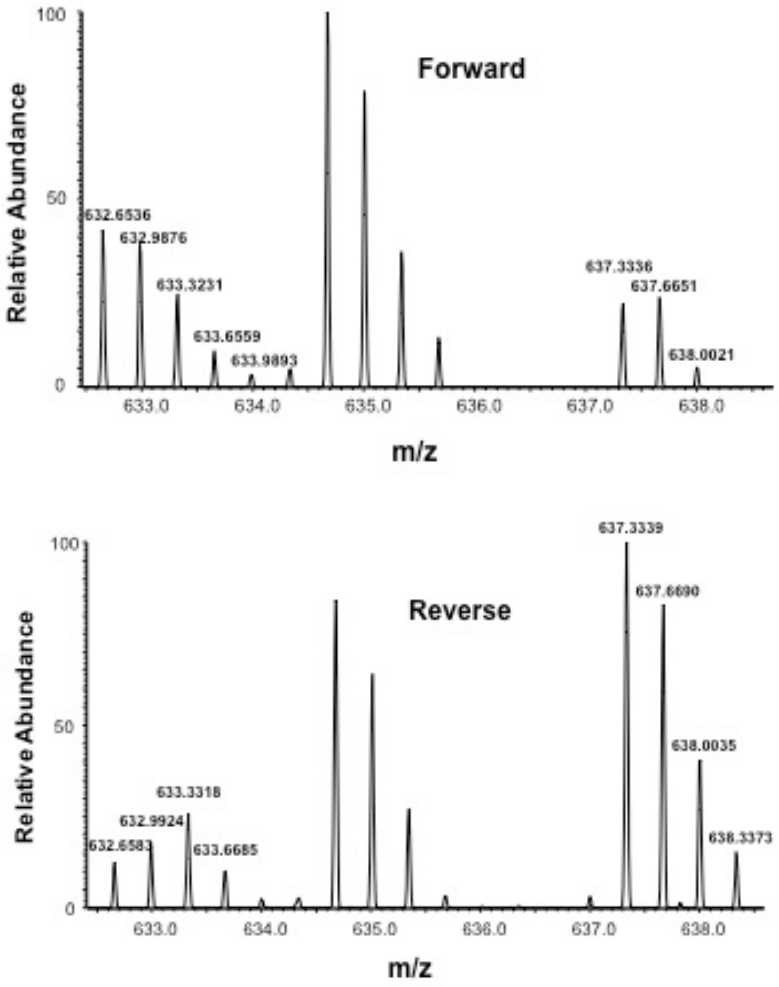

b)

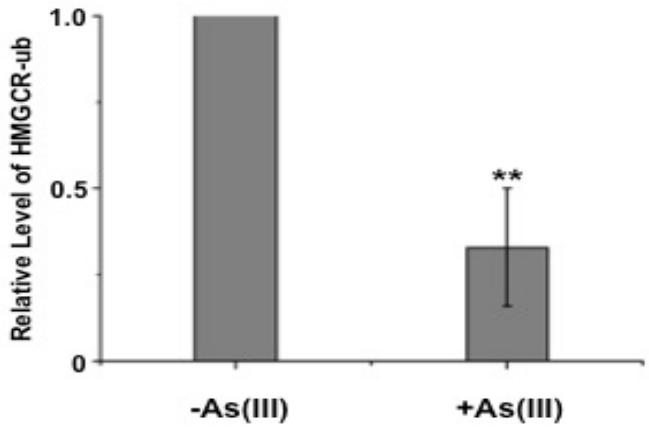

Figure 3.5 a) Full scan ESI-MS of HMGCR peptide containing di-Gly remnant on K248. B) Ratio of HMGCR-K248-ub with arsenite treatment.

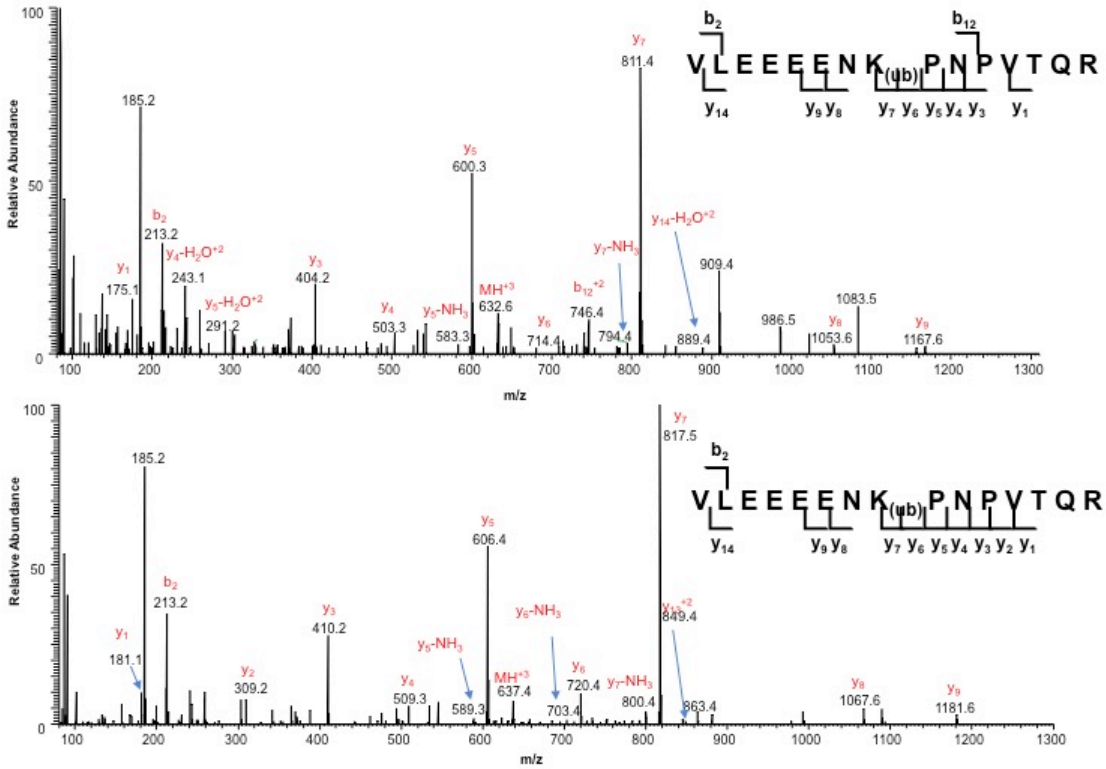

Figure 3.6 MS/MS for the $[M+3H]^{3+}$ ions of light (top) and heavy (bottom) di-Gly-modified K248-containing peptide from HMGCR.

a)

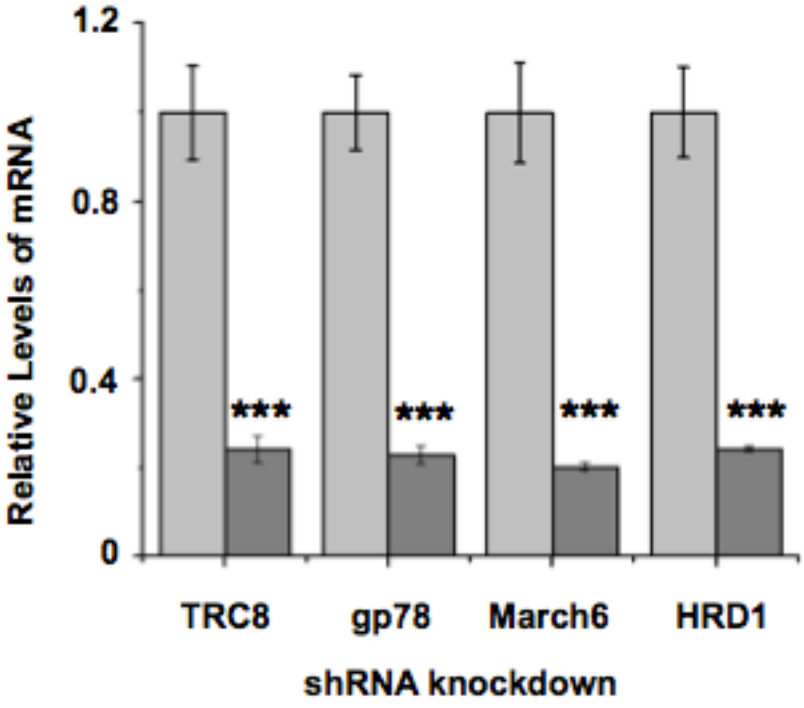

b)

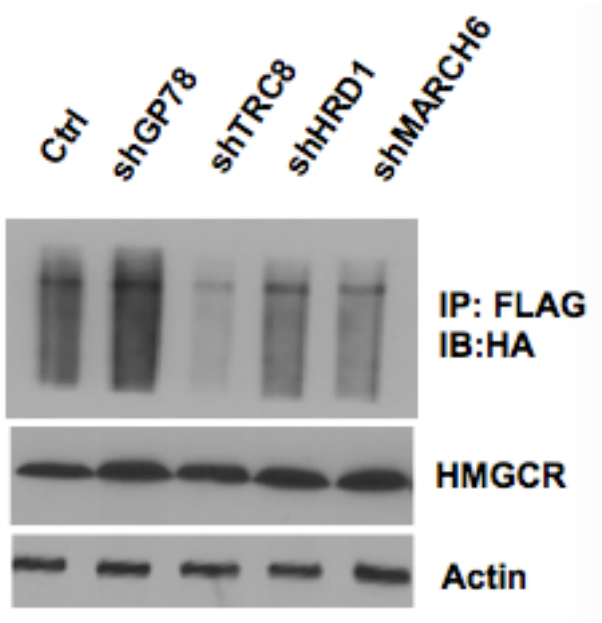

Figure 3.7 a) knockdown efficiencies for shRNA species targeting gp78, TRC8, MARCH6 and HRD1. b) The ubiquitination levels of HMGCR upon shRNA individual knockdowns of the four E3 ubiquitin ligases involved in HMGCR ubiquitination.

a)

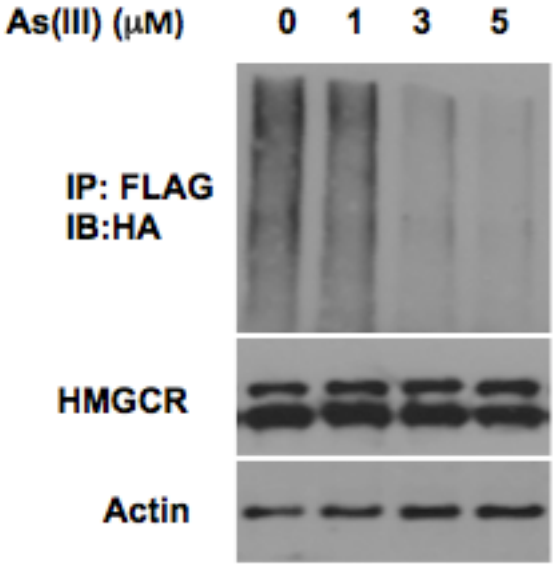

b)

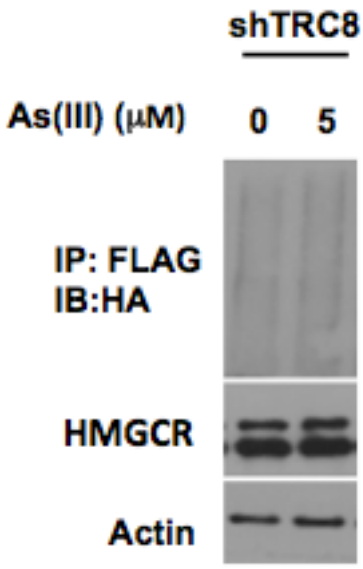

Figure 3.8 a) The levels of ubiquitination of HMGCR with or without arsenite treatment. b) HMGCR ubiquitination level upon arsenite treatment after TRC8 knockdown.

a)

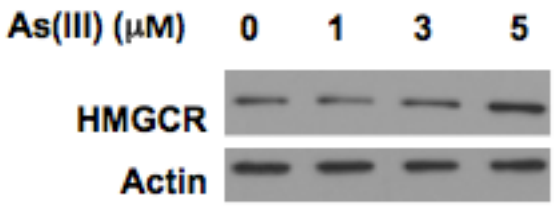

b)

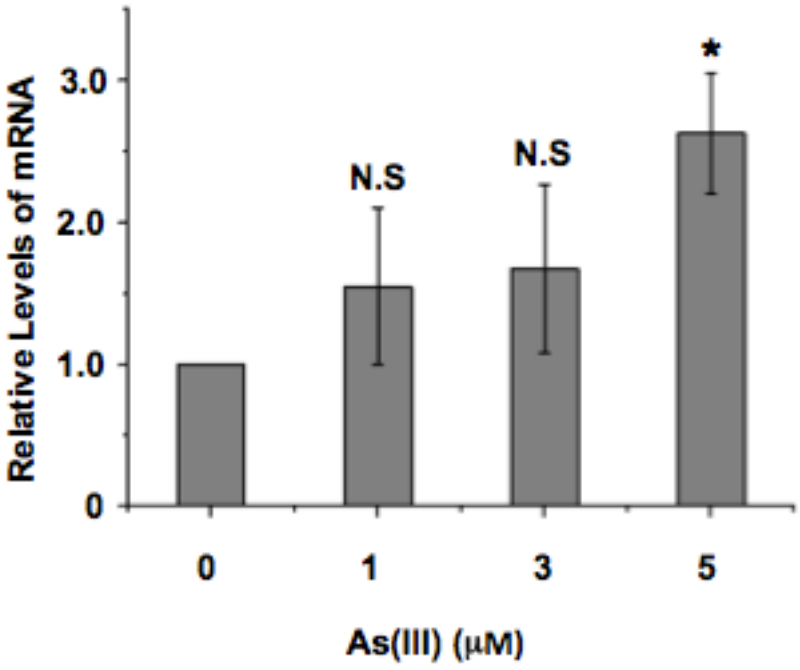

Figure 3.9 a) arsenite stabilizes HMGCR protein level in HEK293T cells. b) Quantitative analysis of HMGCR level upon arsenite treatment with different concentrations of As(III).

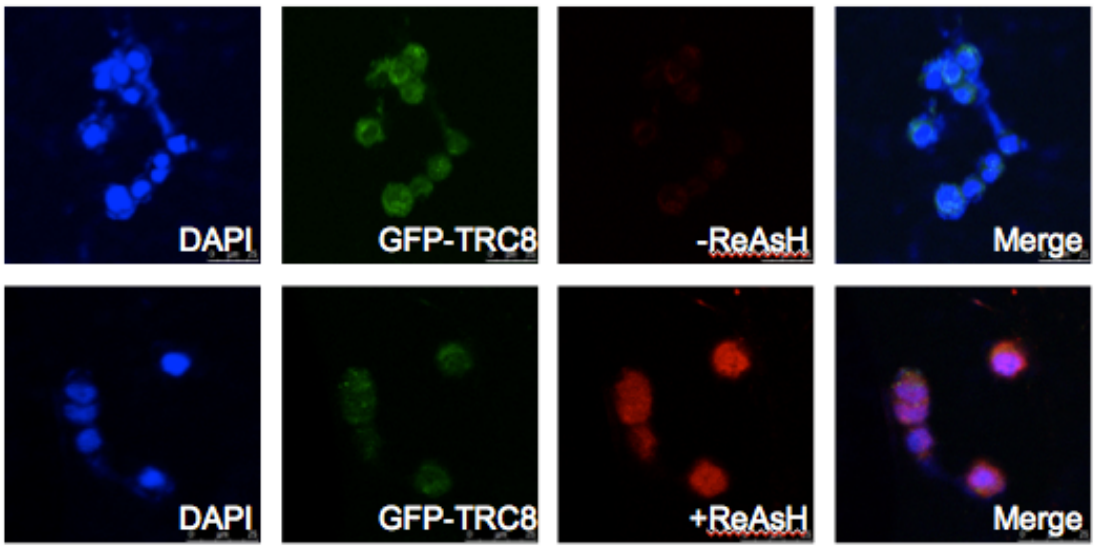

Figure 3.10 ReAsH staining shows a co-localization between TRC8 and As^{3+}-containing ReAsH.

Chapter 4. Arsenite Targets the RING Finger Domain of Rbx1 E3 Ubiquitin Ligase to Inhibit Proteasome-mediated Degradation of Nrf2

Introduction

Arsenic is one of the most ubiquitous toxic substances in the environment, and more than 150 million people in > 70 countries are chronically exposed to excessive amounts of arsenic speciesin drinking water, leading to high incidences of skin, lung, kidney, liver, and bladder cancers as well as neurological disorders, cardiovascular diseases and diabetes(219,220). Numerous studies have been conducted to explore the molecular mechanisms underlying the toxic and carcinogenic effects of arsenic species, where DNA hypomethylation, perturbation of signal transduction, repression of DNA repair, alteration of gene expression, and induction of oxidative stress are thought to be important(221,222).

Previous studies have shown that arsenite could bind to side chain sulfhydryl groups in vicinal cysteine residues in the zinc finger domains of proteins, which may contribute to arsenic toxicity and carcinogenicity(135). In this aspect, arsenite was found to bind to the Cys3His (C3H)- or Cys4 (C4)-type zinc fingers much more strongly than those of the Cys2His2 (C2H2)-type(136). Since most RING finger domains harbor a C3H- and a C4-type zinc finger(87,162,223), our recently published work demonstrated the interactions between arsenite and the RING finger domains of proteins, including several E3 ligases such as FANCL and RNF20-RNF40, and these interactions ultimately led to inhibition of repair of DNA interstrand crosslink lesions and double strand breaks, respectively(140,224). Our previous work also elucidated the interaction between arsenite and the RING finger domains of

Tip60 histone acetyltransferase and ten-eleven translocation (Tet) family proteins, which perturbs histone and DNA epigenetic marks(179,225).

Oxidative stress has also been proposed to contribute to arsenic toxicity(226). Under normal physiological conditions, reactive oxygen species (ROS), such as hydrogen peroxide, hydroxyl radical, and superoxide anion, are regulated, which serve as signaling molecules to modulate multiple biological processes including inflammation, cell division, autophagy and stress response(227-231). Nonetheless, ROS are excessively produced in cells exposed to arsenite, which results in oxidative stress that impairs cellular functions and induces cell cycle arrest, apoptosis, and even cancer development(232-234).

Activation of the Nrf2-Keap1 pathway is the main cellular defense mechanism to protect cells from oxidative stress(235). Under unstressed conditions, Nrf2 is negatively regulated by Keap1, which functions as an adaptor of Nrf2 to facilitate its ubiquitination and degradation by Cul3-Rbx1 E3 ubiquitin ligase and the 26S proteasome, respectively(236). However, under stress conditions, Nrf2 is stabilized due to the deactivation of Keap1, which activates transcription of downstream antioxidant genes such as *NQO1* and *HO-1*(237). Keap1 is a highly susceptible target for thiol-reactive chemical species because it contains a large number of cysteine residues(238). Indeed, cysteine residues at positions 151, 257, 288 and 297 were previously identified as the sites for attack by electrophilic species and thought to be crucial for Keap1's function(239).

Since arsenite is known to induce oxidative stress, previous studies have demonstrated that the Nrf2-Keap1 pathway can also be activated by

arsenite(240). However, arsenite-induced activation of Nrf2 has been shown to be independent of cysteine residues in Keap1, suggesting a distinct mechanism contributing to the arsenite-induced activation of the Nrf2-Keap1 pathway(241). It remains insufficiently understood about the exact mechanism underlying this pathway, though it was found to be p62-dependent(242).

On the grounds of the previous findings that arsenite could bind to the RING finger domain of proteins, we hypothesized that arsenite is capable of binding to the RING finger domain of Rbx1, the E3 ubiquitin ligase component of the Cul3-Rbx1 complex, which may inhibit Nrf2 ubiquitination and activate antioxidant response through stabilizing Nrf2 protein in cells.

Experimental Procedures

Plasmid Construction and Site-directed Mutagenesis

Primers 5'-AAACTCGAGGCGGCAGCGATGGATGTGGATA-3' and 5'-AAAGATCCCTAGTGCCCATACTTTTGGAATTCCC-3' were designed to construct pEGFP-C3-Rbx1 plasmid. Total RNA was extracted from HEK293T cells using the E.Z.N.A.® Total RNA Kit I (Omega, Norcross, GA) and reverse-transcribed into a cDNA library, which served as a template to clone the coding sequence of Rbx1 into the *Bam*HI/*Xho*I sites of pEGFP-C3 vector by PCR.

The pCDNA3.1-Nrf2-FLAG and HA-ubiquitin plasmids were purchased from Addgene, and the pCDNA3.1-Rbx1-HA plasmid was kindly provided by Dr. Pengbo Zhou at Weill Cornell Medical College. Primers 5'-GTAAC CATGC TTTTT GCTTC CACTG-3', 5'-GTGGA AGCAA AAAGC ATGGT TACAG-3' or 5'-GCTTT TCACT TCCAC CACAT CTCTC-3', 5'-GCGAG AGATG TGGTG GAAGT GAAAA-3' were designed and used to construct plasmids of Rbx1-HA and Rbx1-GFP harboring H80C or C83H mutations, respectively, by employing GeneArt Site-directed Mutagenesis Kit (Thermo Fisher Scientific, Waltham, MA).

Cell Culture and Transfections

HEK293T human embryonic kidney epithelial cells were maintained in a humidified atmosphere containing 5% CO_2 at 37°C, and cultured in Dulbecco's Modified Eagle Medium (DMEM, ATCC, Manassas, VA) containing

10% fetal bovine serum (FBS, Invitrogen, Waltham, MA) and 100 U/mL penicillin and streptomycin. Typically, 1 μg plasmid or 100 pmol siRNA was transfected into cells with 5 μL of Lipofectamine 2000 (Thermo Fisher, Waltham, MA).

In Vitro Arsenite Binding Assay

The procedures for monitoring the interaction between the RING finger peptide of Rbx1 and As(III) were previously described(179). Briefly, the RING-finger peptide derived from Rbx1 (VDNCAICRNAFHFHCISR) was synthesized by Genemed Synthesis Inc. (San Antonio, TX), dissolved in 50% acetonitrile and used for the *in-vitro* binding assays. Aliquots of 100 μM peptide were mixed with 200 μM $NaAsO_2$, 100 μM dithiothreitol (DTT) and incubated on ice for 1 hr. The solution was subsequently mixed with an equal volume of 2,5-dihydroxybenzoic acid matrix solution and spotted onto a sample plate. The samples were analyzed on a MALDI TOF/TOF^{TM} 5800 system in the positive-ion, reflection mode. Competition experiments were conducted by incubating the peptide with $NaAsO_2$ and $ZnCl_2$ at varying molar ratios. The peptide was also titrated with increasing amount of $NaAsO_2$ and subjected to UV absorption measurements on a Varian Cary 50 UV-visible spectrophotometer (Palo Alto, CA). The UV absorbance was monitored in the wavelength range of 230-400 nm.

Streptavidin Agarose Affinity Assay and Western Blot

HEK293T cells were seeded in 6-well plates at a density of 1 × 10^6 cells per well and transfected with wild-type or mutant pCDNA3.1-Rbx1-HA plasmids for 24 hr. The cells were then mock-treated or treated with 5 μM $ZnCl_2$, $NaAsO_2$ or PAPAO for 1 hr, and subsequently incubated with 5μM biotin-As probe for 1 hr, as described previously(140). The cells were then harvested and lysed in CelLytic M lysis buffer containing 1% protease inhibitor cocktail (Sigma-Aldrich, St. Louis, MO). Streptavidin agarose beads (Thermo Fisher, Waltham, MA) were incubated with the whole cell lysate at 4°C overnight, washed with 1 × PBS for three times, re-suspended in SDS-PAGE loading buffer, and subjected to SDS-PAGE analysis.

After SDS-PAGE separation, proteins were transferred to a nitrocellulose membrane at 40 V for 2 hr in a buffer containing 10 mM $NaHCO_3$, 3 mM Na_2CO_3, and 20% methanol. The membrane was then pretreated with phosphate buffered saline with Tween-20 (PBS-T) containing 5% non-fat milk at room temperature for 1 hr and incubated with anti-HA primary antibody (Abcam, Cambridge, MA) at 4°C overnight. The membrane was subsequently incubated with anti-rabbit secondary antibody at room temperature for 1hr, and thoroughly washed with PBS-T. The protein bands were detected by ECL Advanced Western Blotting Detection Kit (GE Healthcare, Chicago, IL) and visualized with Hyblot CL autoradiography film (Denville Scientific, Inc., Metuchen, NJ). The membranes were also probed for input Rbx1 and β-actin using anti-HA and anti-actin antibodies (Abcam, Cambridge, MA) to confirm equal protein loading.

Fluorescence Microscopy

Wild-type and mutant pEGFP-C3-Rbx1 plasmids (0.5 μg each) were transfected individually into 1 × 10^5 HEK293T cells seeded on cover glasses. After 24 hr, the transfected cells were mock treated or treated with 10 μM $ZnCl_2$, $NaAsO_2$ or PAPAO, and then incubated with 5 μM ReAsH-EDT_2 (Invitrogen, Waltham, MA) in Opti-MEM medium at 37°C for 1 hr, washed with BAL buffer for 3 times, fixed with 4% paraformaldehyde for 20 min, and stained with 4',6-diamidino-2-phenylindole (DAPI). The sample slides were subjected to a Leica TCS SP5 confocal microscope (Leica Microsystems, Buffalo Grove, IL) for imaging in the wavelength range of 425-450 nm, 500-550 nm and 580-650 nm for DAPI, GFP and ReAsH, respectively.

Nrf2 Ubiquitination Assay

HEK293T cells were seeded in 6-well plates at a density of 2 × 10^5 cells per well. A 100 pmol of siRbx1 targeting the 3'-UTR of Rbx1 mRNA (5'-GACUUUCCCUGCUGUUACCUAAdTdT-3') was transfected into each well to knock down endogenous Rbx1 protein. After 24 hr, 1 μg siRNA-resistant plasmid encoding wild-type or mutant Rbx1-HA, 1 μg Nrf2-FLAG and 0.5 μg ubiquitin-HA plasmids together with Lipofectamine 2000 were added into each well. After one day, the cells were treated with 5 μM $NaAsO_2$ for 24 hr, and subsequently incubated with 10 μM MG132 for 2 hr. The resulting whole cell lysate was incubated with anti-FLAG M2 magnetic beads (Sigma, St. Louis,

MO) at 4°C overnight, and the beads were then resuspended in SDS-PAGE loading buffer. After SDS-PAGE separation, Western blot analysis was performed to detect Nrf2 ubiquitination using anti-HA antibody. The input Nrf2 and β-actin were detected using anit-Nrf2 (Santa Cruz Biotechnology, Dallas, Texas) and anti-Actin antibody.

Results

Arsenite binds to the RING finger domain of Rbx1 *in vitro*

To explore if Rbx1 plays a role in arsenite-induced Nrf2 activation, we first assessed the interaction between arsenite and the RING finger domain of Rbx1. To this end, we performed a matrix-assisted-laser-desorption/ionization-time-of-fly (MALDI-TOF MS)-based *in-vitro* binding assay with the use of a synthetic peptide derived from the RING finger domain of human Rbx1 protein, which contains a $Cys_3HisCys_2HisAsp$ (C3HC2HD)-type zinc finger(243) (Figure 4.1a). The $[M+H]^+$ ion of the apopeptide was detected at *m/z* 2106 in MALDI-MS, while a mass increase of 72 Da was found upon incubation of the synthetic peptide with As^{3+} at a molar ratio of 1:2 (Fig 3.2). This mass increase reflects the coordination of one As^{3+} with the peptide along with the releases of three protons from the sulfhydryl groups of cysteine residues in the RING finger domain(136).We also added increasing concentrations of Zn^{2+} to the As^{3+}-peptide mixture, and found that, even in the presence of excessive amount of Zn^{2+} relative to As^{3+}, we could still observe

the interaction between As^{3+} and the synthetic peptide in MALDI-MS, while the corresponding peptide-Zn^{2+} complex was not detectable, suggesting that As^{3+} binds to the peptide much more strongly than Zn^{2+} (Figure 4.2).

The alteration in charge-transfer electronic transitions of the peptide forged by coordination of As^{3+} with the sulfhydryl group of cysteine residues in the RING finger domain can be monitored by UV absorptionin the wavelength range of 230-400 nm(244). As expected, a heightened absorbance of the peptide was detected upon titrating the peptide with increasing amounts of As^{3+} from 0 to 2eq, indicating a gradual increase in binding of As^{3+} to the RING finger peptide (Figure 4.1b). Together, the above results demonstrated that As^{3+} could bind to the RING finger domain of Rbx1 *in vitro*.

Arsenite interacts with Rbx1 in cells

Having demonstrated the interaction between As^{3+} and Rbx1 *in vitro*, we next performed a streptavidin agarose affinity pull-down assay to examine if this interaction could also be observed in mammalian cells. Toward this end, we ectopically expressed HA-tagged Rbx1 protein in HEK293T cells and incubated the transfected cells with a synthetic biotin-As probe(245) (Figure 4.3a). We subsequently precipitated biotin-As-binding proteins with streptavidin beads(246) and probed for HA-Rbx1 by using Western blot. The results showed that biotin-As probe could facilitate the pull-down of HA-Rbx1 from HEK293T cells with the use of streptavidin beads, manifesting that arsenite could indeed bind to Rbx1 in cells (Figure 4.3b). Next we asked if As^{3+} could compete with Zn^{2+} to bind to Rbx1 protein. In this vein, we

pretreated cells with Zn^{2+}, As^{3+}or *p*-aminophenyl arsenoxide (PAPAO) before we incubated cells with the biotin-As probe. Our results showed that the interaction between biotin-As and Rbx1 was substantially compromised upon pretreatment with As^{3+} or PAPAO, though a slight suppression was also detected with Zn^{2+} pretreatment, demonstrating a stronger binding of Rbx1 toward As^{3+} than Zn^{2+} (Figure 4.4a-3.4b).

Arsenite interacts with the RING finger domain of Rbx1 in cells

To further illustrate the interaction between arsenite and the RING finger domain of Rbx1, we employed a fluorescence-microscopy-based assay with the use of the ReAsH-EDT_2 dye, which contains two As^{3+} and displays red fluorescence when cysteine residues in proteins bind to its arsenic moieties(154) (Figure 4.5a). We observed substantial co-localization of the ectopically expressed Rbx1 and ReAsH, suggesting the interaction between As^{3+} and Rbx1 protein (Figure 4.5b).

To test if cysteine residues in the RING finger domain of Rbx1 are crucial for this interaction, we also expressed mutant Rbx1 proteins, i.e. Rbx1-H80C and Rbx1-C83H, in HEK293T cells and measured their co-localization with ReAsH. Our results revealed that, relative to wild-type GFP-Rbx1, GFP-Rbx1-H80C exhibited a slightly elevated co-localization with ReAsH, whereas this co-localization was nearly abolished for GFP-Rbx1-C83H (Figure 4.5-3.6). Together, our results revealed that arsenite could co-localize with ectopically expressed Rbx1 in mammalian cells, and the co-localization requires the cysteine residues in the RING finger domain of RBX1. In addition, we

pretreated transfected cells with Zn^{2+}, As^{3+} or PAPAO prior to incubating cells with the ReAsH-EDT_2 dye. As expected, we observed a reduced co-localization between GFP-Rbx1 and ReAsH upon pretreatment with As^{3+} or PAPAO, but not Zn^{2+}, supporting the competitive binding of As^{3+} to cysteine residues in the RING finger motif of Rbx1 (Figure 4.7-3.8).

Interaction between arsenite and Rbx1 is required for arsenite-induced stabilization of Nrf2

Exposure of cells to arsenite has been known to activate the Nrf2-induced antioxidant pathway, though the detailed mechanism remains incompletely understood(240). Having demonstrated the interaction between arsenite and Rbx1 both *in vitro* and in cells, we next asked if this interaction could affect the activation of Nrf2. We first exposed HEK293T cells with increasing concentrations of As^{3+} from 0μM to 5 μM. Not surprisingly, the levels of endogenous Nrf2 were increased, in a dose-dependent manner, with arsenite exposure, indicating that arsenite could stabilize Nrf2 protein in cells (Figure 4.9).

It is well established that Nrf2 is ubiquitinated by Keap1-Cul3-Rbx1 E3 ligase complex(247). When endogenous Rbx1 was depleted using siRNA, the ubiquitination level of Nrf2 was dramatically decreased (Figure 4.10, lane 1-2). Nevertheless, if we complemented cells with siRNA-resistant constructs for the expression of wild-type or mutant Rbx1 proteins after knocking down endogenous Rbx1, the ubiquitination of Nrf2 was rescued to a similar level as to the control (Figure 4.10, lanes 1and 3-5). These results indicated that Rbx1 is essential for Nrf2 ubiquitination.

Previous studies have revealed that arsenite could perturb ubiquitination of proteins by targeting E3 ubiquitin ligases(140). As expected, we observed a significant reduction of Nrf2 ubiquitination in cells upon arsenite treatment (Figure 4.10, lanes 1 and 6). This result suggested that arsenite stabilized Nrf2 protein through inhibiting its ubiquitination and proteasomal degradation.

To further demonstrate that the binding of arsenite with the RING finger domain of Rbx1 accounts for the perturbation of Nrf2 ubiquitination, we complemented HEK293T cells with plasmids for the ectopic expression of wild-type or mutant Rbx1 proteins, followed by arsenite treatment. The results showed that Nrf2 ubiquitination was only rescued in cells reconstituted with Rbx1-C83H (Figure 4.10, lane 8-10). This finding is in keeping with the fact that arsenite could not target Rbx1-C83H as strongly as wild-type Rbx1 or Rbx1-H80C, as shown from the aforementioned fluorescence microscopy experiments. Thus, the above results support that the binding of arsenite to the RING finger domain of Rbx1 is crucial for Nrf2 ubiquitination. However, arsenite could still suppress Nrf2 ubiquitination even in the presence of Rbx1-C83H (Figure 4.10, lane 5 and 10), though the suppression was not as pronounced as in the presence of wild-type Rbx1 or Rbx1-H80C (Figure 4.10, lane 8-10). The latter might be attributed to the presence of other mechanisms contributing to arsenite-induced perturbation of Nrf2 ubiquitination(241,242,248).

Taken together, our finding suggested that arsenite targets the RING finger domain of Rbx1 E3 ubiquitin ligase, which is responsible for stabilizing Nrf2 protein by inhibiting its ubiquitination and proteasome-mediated degradation.

Discussion

A global genome-wide analysis of Nrf2 targets has identified a number of antioxidant-element-containing genes such as heme oxygenase-1 (*HO-1*), glutathione S-transferase (*GST*), and NAD(P)H-quinone oxidoreductase (*NQO1*), revealing the major role of Nrf2 to activate antioxidant response and for the detoxification of harmful substances(249). Along this line, Nrf2-knockout mice displayed higher sensitivity towards a wide range of oxidative stress inducers, including, but not limited to, *tert*-butylhydroquinone (*t*BHQ), sulforaphane (SF) and arsenite(250-254). The activity of Nrf2 is suppressed under basal conditions. The Cul3-Rbx1 guides the polyubiquitination and rapid degradation of Nrf2 by proteasomes with the aid of Keap1, which acts as a substrate adaptor to localize Nrf2 to the Cul3-Rbx1 E3 ligase, leading to a low constitutive level of Nrf2 protein with a turnover rate of ~20 min under normal conditions(255,256). Hence, the constant assembly/disassembly cycle of Keap1 to Cul3-Rbx1 E3 ligase is required for Keap1-mediated Nrf2 ubiquitination and degradation, whereas both enhanced and diminished associations of Keap1 with Cul3-Rbx1 E3 ligase could lead to Nrf2 stabilization(257). Nrf2 inducers such as *t*BHQ and SF were found to activate Nrf2 by negatively modulating the interaction between Keap1 and Cul3(258,259). Several distinct reactive cysteine residues in Keap1 serve as sensors for inducers to modify and impede Nrf2 ubiquitination. In this vein, C273 and C288 were shown to be crucial for suppression of Nrf2 under basal conditions, whereas C151 was required for activation of Nrf2 by inducers like

tBHQ and SF(239). It was also found that different inducers might target different cysteine residues. For example, C288 is a sensor for alkenals, whereas C226/C613 serve as a sensor for Zn^{2+}(260). The preferences of disparate cysteine residues for different inducers suggest the presence of "cysteine codes" for Nrf2 activation by various chemicals.

The "cysteine codes" of Keap1 are not always sufficient for understanding the activation of Nrf2 since some inducers require additional protein factors. For instance, unlike *t*BHQ and SF, arsenite was found to activate Nrf2 by enhancing the interaction between Keap1 and Cul3 in a Keap1 C151-independent manner(241), promoting us to explore distinct mechanisms of arsenite-induced activation of Nrf2. Since the interaction between arsenite and vicinal thiols in proteins has been proposed to account for the carcinogenic and cytotoxic effects of arsenic species(135), cysteine residues in Nrf2, which is an evolutionarily conserved protein, have been found to be arsenite sensors to facilitate Nrf2 activation. Studies in mouse cells have revealed an interaction between arsenite and wild-type Nrf2, whereas this interaction was compromised in Nrf2 C311/C316, C235, C414 and C506 mutants. Moreover, arsenite activated wild-type Nrf2 but not Nrf2 C191A, C235A, C311A/C316A, C414A, or C506A mutants in mouse cells(248). Another protein factor that is important for arsenite-induced activation of Nrf2 is p62, which is a selective substrate adaptor for the degradation of specific proteins through autophagy(261). Arsenite deregulates autophagy and causes an overexpression of p62, which directly binds to Keap1 to block Keap1-mediated Nrf2 ubiquitination. Interestingly, this p62-dependent pathway is only

responsible for arsenite-induced activation of Nrf2, but not for the activation of Nrf2 by tBHQ or SF(242). The Bcl-XL-interacting protein PGAM5 and p53-regulated p21 were also identified as disruptors for the binding of Keap1 with Nrf2 to activate Nrf2(262,263).

Rbx1 is a major player in the activation of Nrf2 antioxidant pathway since it serves as the E3 ubiquitin ligase that ubiquitinates Nrf2. Based on the fact that it contains a cysteine-rich RING finger domain, it prompted us to investigate if cysteine residues in Rbx1 could also serve as sensors for arsenite-induced activation of Nrf2. In this study, we demonstrated the interaction between arsenite and the RING finger domain peptide of Rbx1 by MALDI-TOF MS analysis. We also revealed, for the first time, the competitive binding of arsenite to wild-type Rbx1 in human cells by streptavidin agarose affinity pull down assay and ReAsH-EDT_2 fluorescent microscopy assay, whereas Rbx1-C83H mutant failed to co-localize with As^{3+}-containing ReAsH, indicating the critical role of the cysteine residue in the RING finger domain for arsenite binding to Rbx1. Furthermore, we demonstrated the significance of this interaction in arsenite-mediated impairment of Nrf2 ubiquitination, where the Rbx1-C83H mutant compromised the arsenite-induced activation of Nrf2. To summarize, our novel finding provides a distinct mechanism underlying activation of antioxidant Nrf2 pathway by arsenite.

Figures

a)

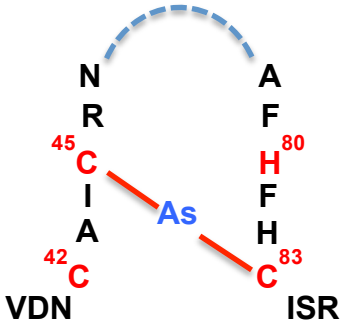

b)

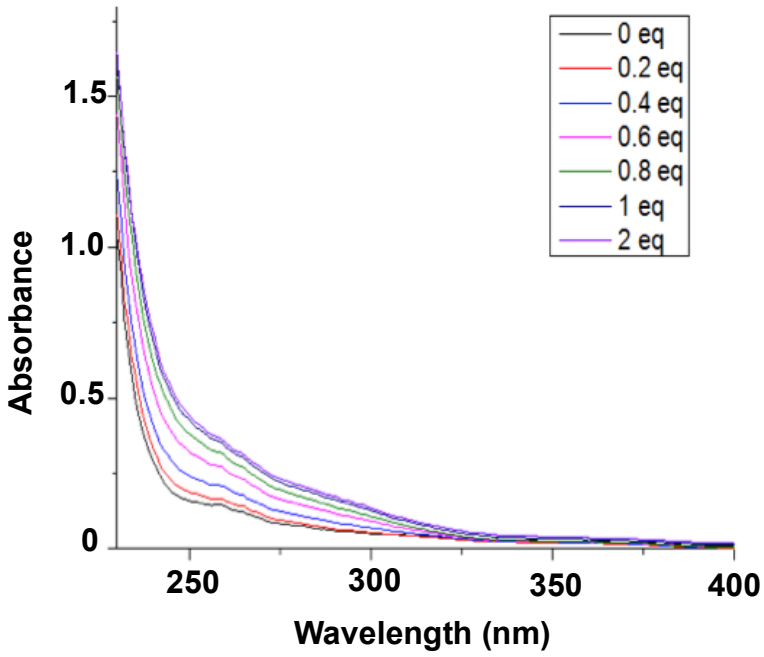

Figure 4.1 a) The interaction between As3+ and a peptide derived from the RING finger domain of RBX1 (a.a 39-47 and 78-84). b) UV absorption spectrum of the RING finger peptide of Rbx1. The synthetic peptide was sequentially titrated with increasing concentrations of NaAsO2, and its UV absorbance was monitored in the wavelength range of 230-400 nm.

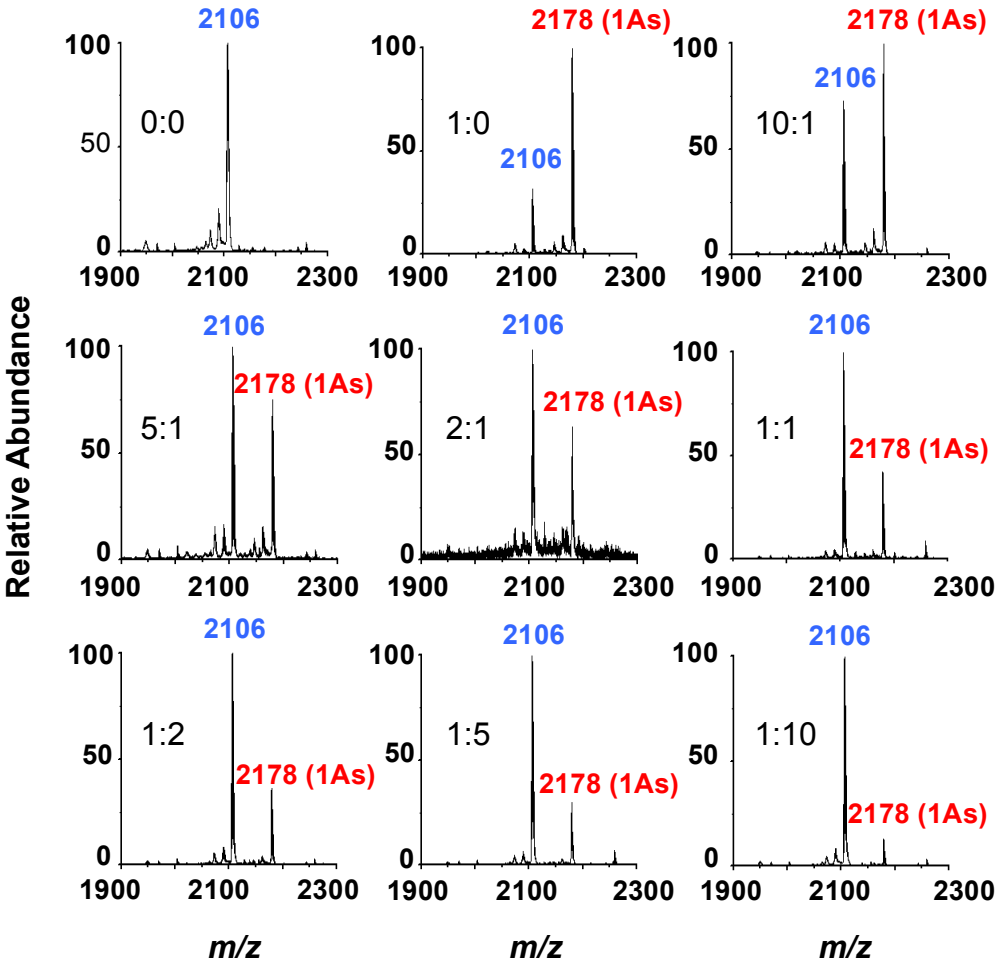

Figure 4.2 MALDI-TOF mass spectrum showing the interaction between Arsenite and the RING-finger peptide of Rbx1. The synthetic peptide was incubated with different molar ratios of As^{3+}/Zn^{2+} as indicated in each spectrum. The results showed that the apopeptide could bind to one As^{3+}.

a)

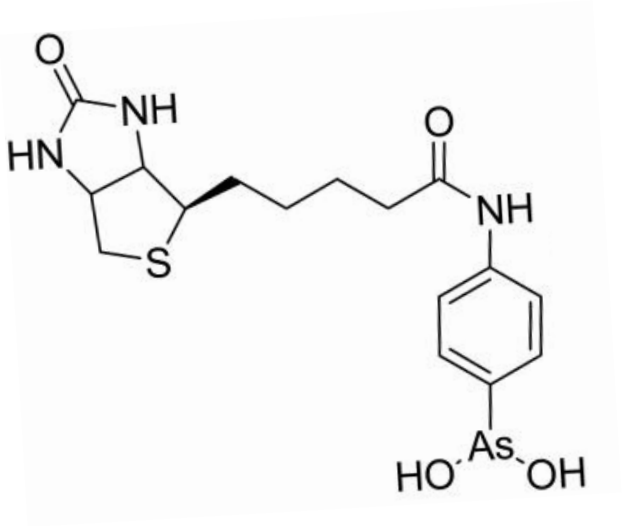

b)

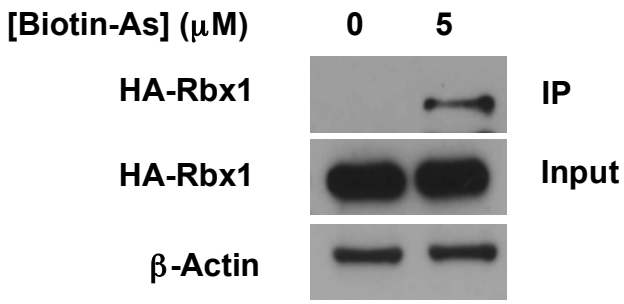

Figure 4.3 a) The chemical structure of the biotin-As probe. b) Streptavidin agarose affinity pull-down assay indicating the interaction between As^{3+} and Rbx1 in cells. Biotin-As probe was used to pull down ectopically expressed HA-Rbx1 in HEK293T cells. The HA-Rbx1 signal was detected using anti-HA antibody, and the input HA-Rbx1 and actin were also detected as below.

a)

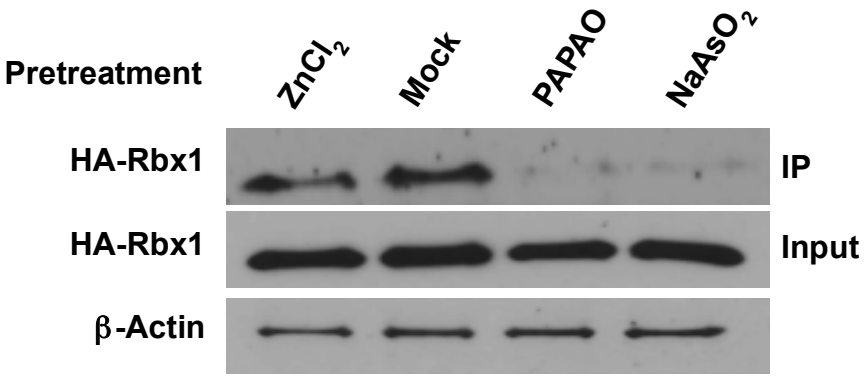

b)

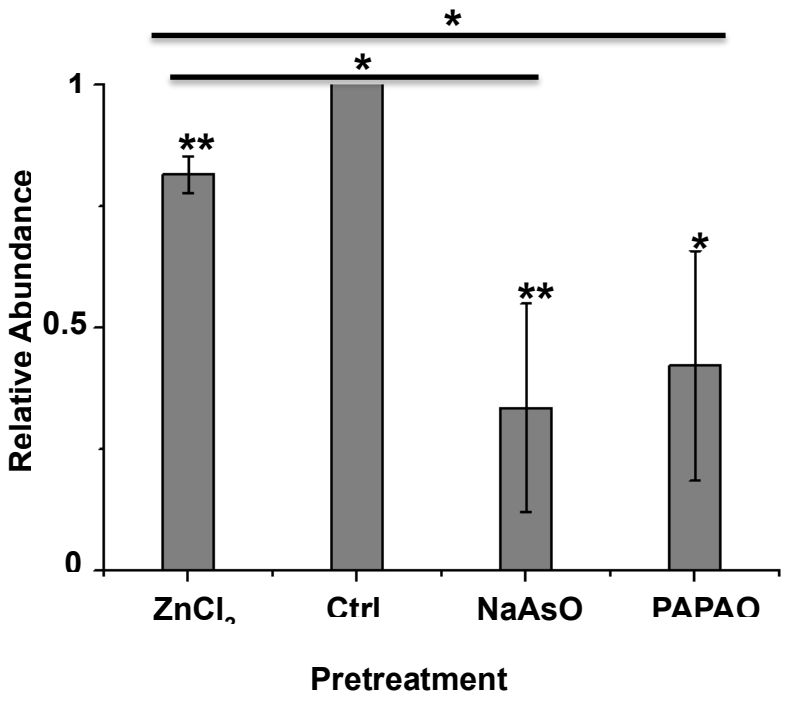

Figure 4.4 a) Streptavidin agarose affinity assay revealed the interaction between As^{3+} and Rbx1 protein in HEK293T cells. The interaction was substantially diminished upon pretreatment with 10 μM $NaAsO_2$, PAPAO, and to a less extent, 10 μM Zn^{2+}. b) Quantitative analysis of relative abundance of panel a.

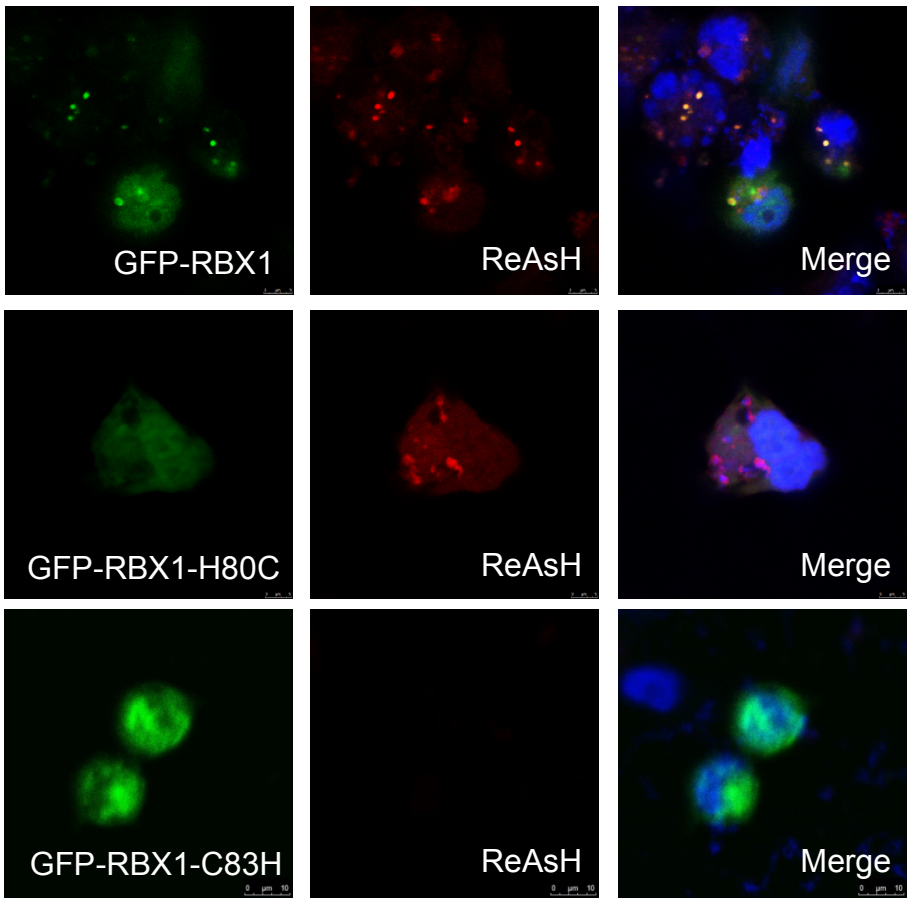

Figure 4.5 Fluorescence microscopy results revealed the co-localization between ReAsH-EDT$_2$ and ectopically expressed GFP-Rbx1. Mutation of histidine to cysteine in the RING finger domain of Rbx1 enhanced the co-localization, whereas mutation of cysteine to histidine diminished the co-localization.

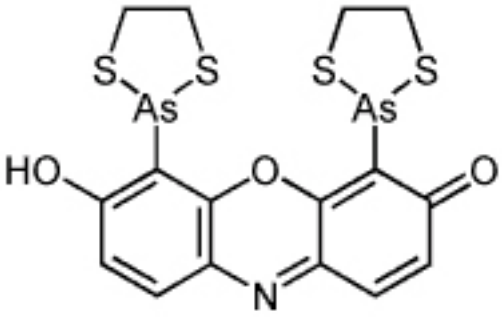

ReAsH-EDT$_2$

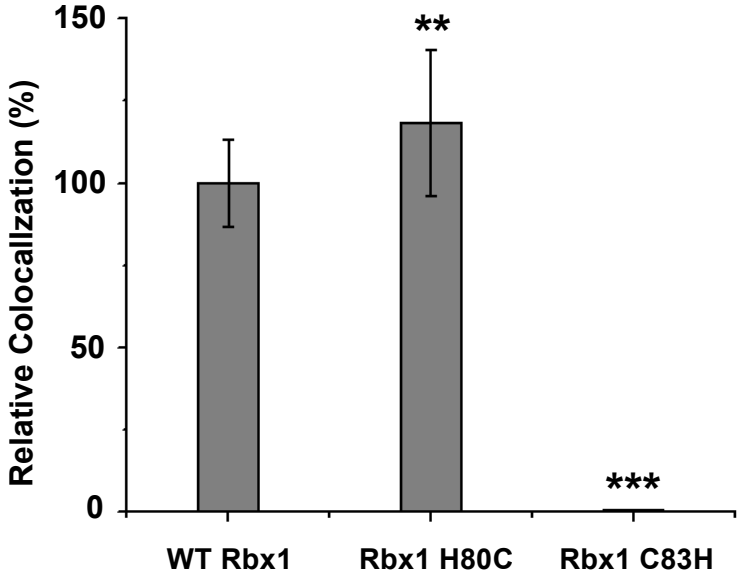

Figure 4.6 Statistical analysis of the extents of co-localization between ReAsH-EDT$_2$ and wild-type Rbx1, Rbx1-H80C and Rbx1-C83H. The signal intensities of each fluorescence channel were measured using ImageJ. The ratios were calculated by dividing the signal intensity of ReAsH-EDT$_2$ with that of GFP. The data represented the mean and standard deviation of the ratios obtained from 30 individual cells. The *P* values were calculated using unpaired two-tailed student's *t*-test (, *P*< 0.005;***, *P*< 0.001). Shown in the inset is the structure of ReAsH-EDT$_2$.**

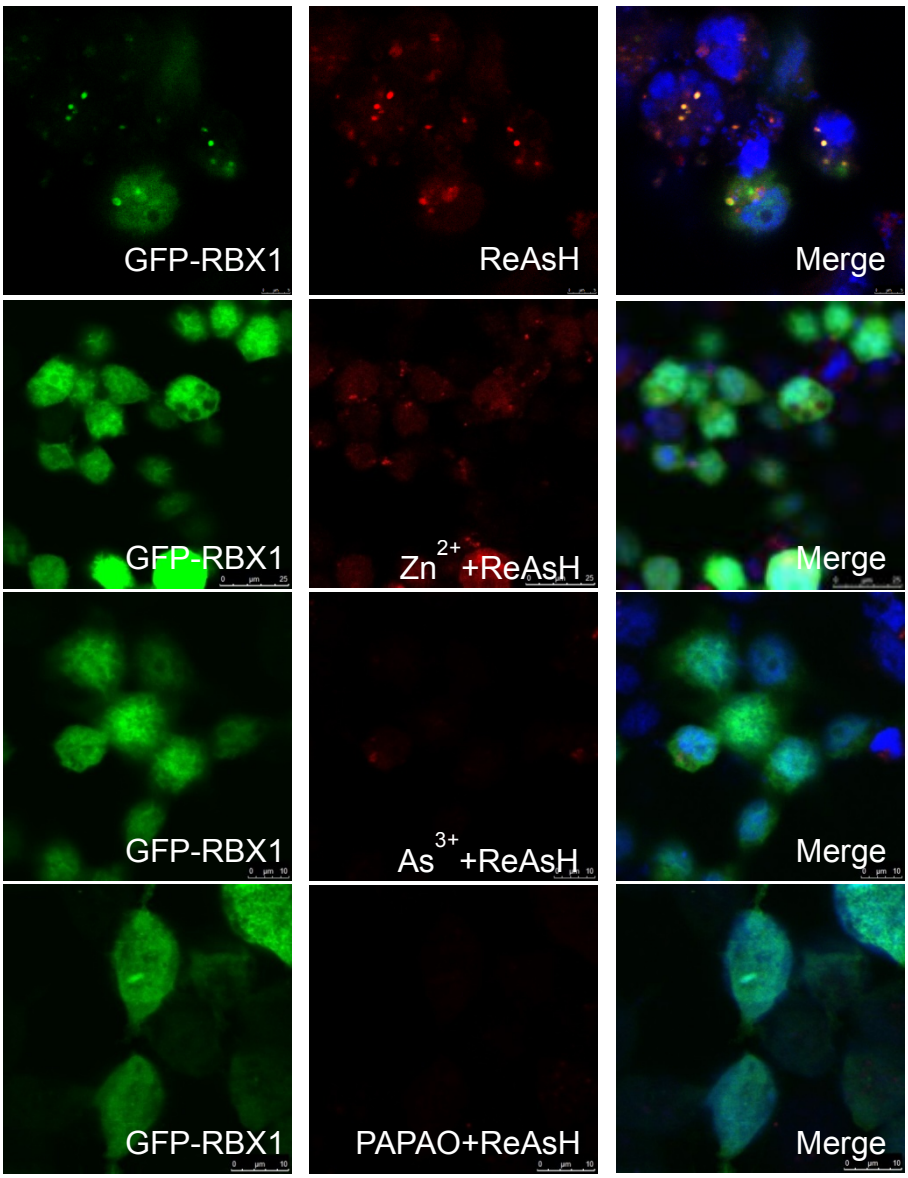

Figure 4.7 Fluorescence microscopy results revealed the co-localization between ReAsH-EDT_2 and ectopically expressed GFP-Rbx1. The co-localization was significantly diminished in cells pretreated with 10 μM $NaAsO_2$ or PAPAO, but not Zn^{2+}.

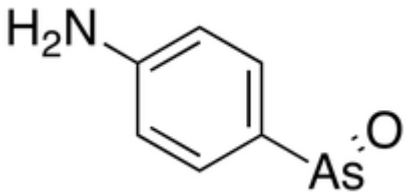

p-aminophenyl arsenoxide (PAPAO)

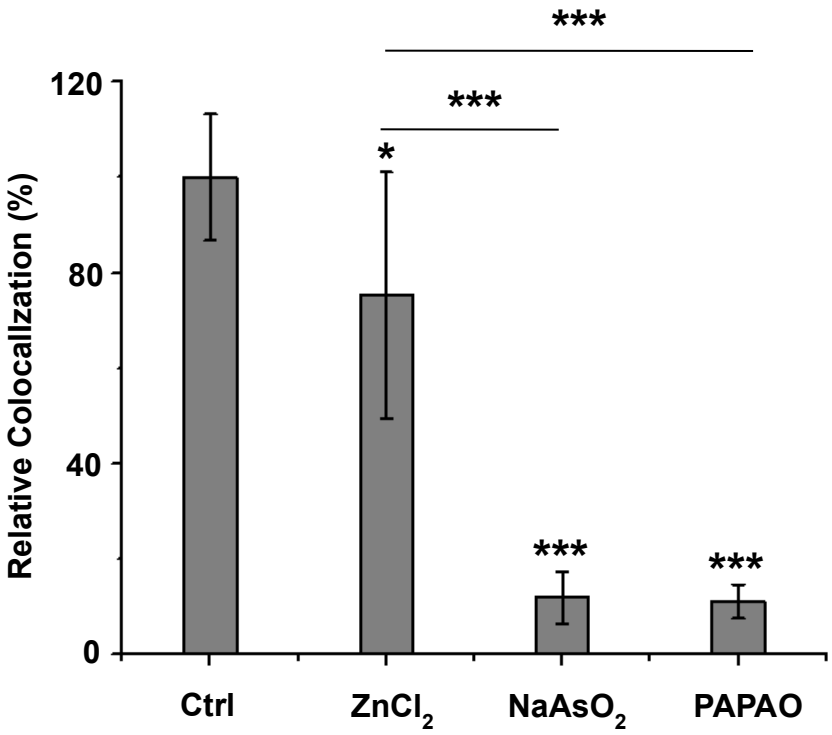

Figure 4.8 Quantitative analysis of the frequencies of co-localization between ReAsH-EDT$_2$ and Rbx1. The data represent the mean and standard deviation of results obtained from images of 30 different cells. The *P* values were calculated using two-tailed, unpaired Student's t test (*, *P*< 0.05; *, *P*< 0.001). Shown the insert is the structure of p-aminophenyl arsenoxide (PAPAO).**

a)

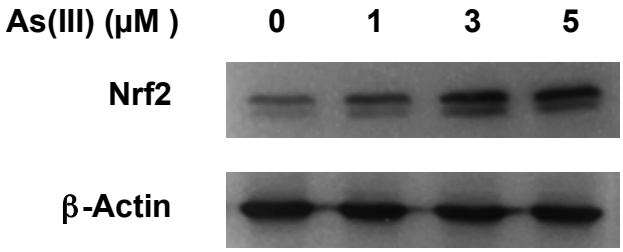

b)

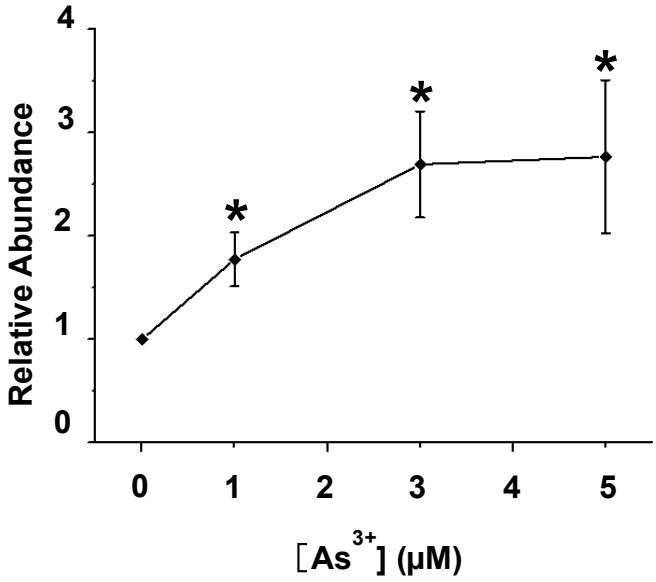

Figure 4.9 a) Arsenite exposure stabilized Nrf2 protein in cells. HEK293T cells were transfected with FLAG-Nrf2 treated with increasing concentrations of As^{3+}. After MG132 treatment, the levels of Nrf2 and β-actin were detected by using anti-Nrf2 and anti-β-actin primary antibody. b) Relative protein levels of Nrf2 in cells exposed to arsenite. The data represent the means and standard deviations of each group acquired from 3 biological replicates. The *P* values were calculated using unpaired two-tailed student's *t*-test (*, *P*< 0.05).

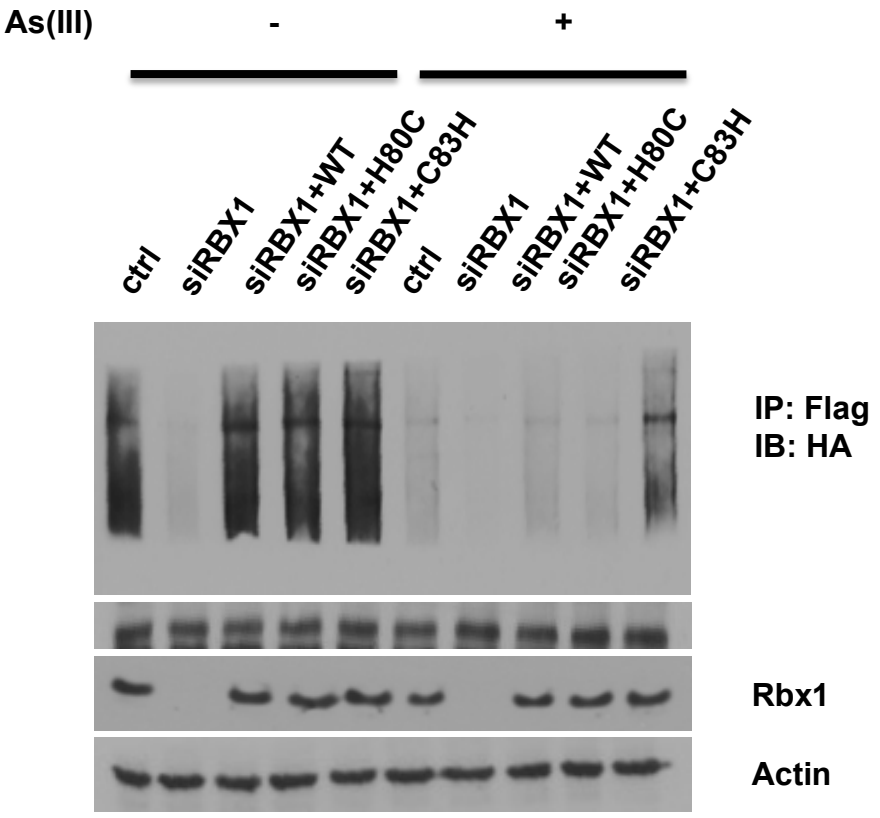

Figure 4.10 HEK293T cells were either transfected with control, non-targeting siRNA (lane 1 and 6) or siRbx1 (lane 2-5 and 7-10), complemented with wild-type Rbx1 (lanes 3 and 8), Rbx1-H80C (lanes 4 and 9), or Rbx1-C83H (lanes 5 and 10), and transfected with FLAG-Nrf2 and ubiquitin-HA, followed by treatment with 5 μM As^{3+} (lanes 6-10) and 5 μM MG132 (lanes 1-10). Anti-FLAG M2 beads were used to immunoprecipitate the FLAG-Nrf2 protein, and the ubiquitination of Nrf2 was detected by Western blot using anti-HA antibody.

Chapter 5. Conclusions and Future Research

The study in this dissertation is mainly focused on discovering arsenite-targeted E3 ubiquitin ligases that play functional roles in mammalian cells. In this respect, I conducted an LC-MS/MS-based quantitative assessment of arsenite-regulated ubiquitin proteome, and was able to identify and quantify ~1500 ubiquitinated peptides in a site-specific manner. Digging into the peptide list, I found that arsenite could bind to three E3 ubiquitin ligases, FANCL, TRC8 and Rbx1, to suppress the ubiquitination of FANCD2, HMGCR and Nrf2, to modulate DNA interstrand crosslink repair, cholesterol biosynthesis and antioxidant response, respectively.

In Chapter 2, arsenite was found to target the E3 ubiquitin ligase FANCL to inhibit FANCD2 ubiquitination. The cysteine residues at the RING finger was found to be important for the arsenite-protein interaction, while mutations of those cysteine residues compromised the interaction between arsenite and FANCL. The monoubiquitination of FANCD2 at K561 was found to be decreased by half upon arsenite exposure in GM00637 and HEK293T cells. The perturbation of this ubiquitination event by arsenite led to an impaired chromatin localization of FANCD2 to the damage sites, which abolished the DNA interstrand crosslink repair pathway and sensitized cells to crosslinking reagents.

In Chapter 3, I identified TRC8 as a main E3 ubiquitin ligase that can be targeted by arsenite, thus inhibiting ubiquitination and proteasome-mediated degradation of HMGCR in HEK293T cells. I uncovered the role of arsenite in stabilizing HMGCR by suppressing its ubiquitination, and this suggests that

arsenite may affect cholesterol biosynthesis pathway. More studies need to be carried out to investigate if arsenite could negatively regulate cholesterol level in HEK293T cells, to further demonstrate the effect of arsenite in this area.

In Chapter 4, it was found that arsenite could bind to the RING finger domain of Rbx1 E3 ubiquitin ligase, which is responsible for the ubiquitination and proteasomal degradation of Nrf2, a key transcription factor involved in regulation of oxidative stress. Taken together, the research in this thesis uncovers several RING-finger-containing E3 ubiquitin ligases as novel targets of arsenite, and the role of arsenite in multiple cell signaling pathways was further expanded.

In total, we identified 277 ubiquitinated peptides from 197 proteins that are downregulated upon arsenite treatment in GM00637 cells by LC-MS/MS analysis. In the future, we will explore other protein targets that play important roles in cells from these 197 proteins, identify the corresponding E3 ubiquitin ligases, and examining their interactions with arsenite. This will further expand the mechanisms underlying arsenite toxicity and carcinogenesis.

References

1. Shankar, S., Shanker, U., and Shikha. (2014) Arsenic contamination of groundwater: a review of sources, prevalence, health risks, and strategies for mitigation. *ScientificWorldJournal* **2014**, 304524

2. Jiang, J. Q., Ashekuzzaman, S. M., Jiang, A., Sharifuzzaman, S. M., and Chowdhury, S. R. (2012) Arsenic contaminated groundwater and its treatment options in Bangladesh. *Int J Environ Res Public Health* **10**, 18-46

3. Chung, J. Y., Yu, S. D., and Hong, Y. S. (2014) Environmental source of arsenic exposure. *J Prev Med Public Health* **47**, 253-257

4. Martinez, V. D., Vucic, E. A., Becker-Santos, D. D., Gil, L., and Lam, W. L. (2011) Arsenic exposure and the induction of human cancers. *J Toxicol* **2011**, 431287

5. Steinmaus, C. M., Ferreccio, C., Romo, J. A., Yuan, Y., Cortes, S., Marshall, G., Moore, L. E., Balmes, J. R., Liaw, J., Golden, T., and Smith, A. H. (2013) Drinking water arsenic in northern chile: high cancer risks 40 years after exposure cessation. *Cancer Epidemiol Biomarkers Prev* **22**, 623-630

6. Guo, H. R. (2007) Cancer risks associated with arsenic in drinking water. *Environ Health Perspect* **115**, A339-340; author reply A340-331

7. Smith, A. H., Hopenhayn-Rich, C., Bates, M. N., Goeden, H. M., Hertz-Picciotto, I., Duggan, H. M., Wood, R., Kosnett, M. J., and Smith, M. T. (1992) Cancer risks from arsenic in drinking water. *Environ Health Perspect* **97**, 259-267

8. Farzan, S. F., Chen, Y., Rees, J. R., Zens, M. S., and Karagas, M. R. (2015) Risk of death from cardiovascular disease associated with low-level arsenic exposure among long-term smokers in a US population-based study. *Toxicol Appl Pharmacol* **287**, 93-97

9. Wade, T. J., Xia, Y., Mumford, J., Wu, K., Le, X. C., Sams, E., and Sanders, W. E. (2015) Cardiovascular disease and arsenic exposure in Inner Mongolia, China: a case control study. *Environ Health* **14**, 35

10. Navas-Acien, A., Sharrett, A. R., Silbergeld, E. K., Schwartz, B. S., Nachman, K. E., Burke, T. A., and Guallar, E. (2005) Arsenic exposure and cardiovascular disease: a systematic review of the epidemiologic evidence. *Am J Epidemiol* **162**, 1037-1049

11. Focazio, M. J., United States. Environmental Protection Agency. Office

of Ground Water and Drinking Water., and Geological Survey (U.S.). (2000) *A retrospective analysis on the occurrence of arsenic in ground-water resources of the United States and limitations in drinking-water-supply characterizations*, U.S. Dept. of the Interior Information Services distributor, Reston, Va. Denver, CO

12. Takamatsu, T., Aoki, H., and Yoshida, T. (1982) Determination of Arsenate, Arsenite, Monomethylarsonate, and Dimethylarsinate in Soil Polluted with Arsenic. *Soil Sci* **133**, 239-246

13. Chen, C. J., Chen, C. W., Wu, M. M., and Kuo, T. L. (1992) Cancer Potential in Liver, Lung, Bladder and Kidney Due to Ingested Inorganic Arsenic in Drinking-Water. *Brit J Cancer* **66**, 888-892

14. Ramesh, A., Hasegawa, H., Maki, T., and Ueda, K. (2007) Adsorption of inorganic and organic arsenic from aqueous solutions by polymeric Al/Fe modified montmorillonite. *Sep Purif Technol* **56**, 90-100

15. Shibata, Y., and Morita, M. (1992) Characterization of Organic Arsenic Compounds in Bivalves. *Appl Organomet Chem* **6**, 343-349

16. Vahter, M. (2000) Genetic polymorphism in the biotransformation of inorganic arsenic and its role in toxicity. *Toxicology Letters* **112**, 209-217

17. Humans, I. W. G. o. t. E. o. C. R. t. (2012) Arsenic, metals, fibres, and dusts. *IARC Monogr Eval Carcinog Risks Hum* **100**, 11-465

18. Ratnaike, R. N. (2003) Acute and chronic arsenic toxicity. *Postgrad Med J* **79**, 391-396

19. Tisler, T., and Zagorc-Koncan, J. (2002) Acute and chronic toxicity of arsenic to some aquatic organisms. *B Environ Contam Tox* **69**, 421-429

20. Lima, A. R., Curtis, C., Hammermeister, D. E., Markee, T. P., Northcott, C. E., and Brooke, L. T. (1984) Acute and Chronic Toxicities of Arsenic(Iii) to Fathead Minnows, Flagfish, Daphnids, and an Amphipod. *Arch Environ Con Tox* **13**, 595-601

21. Hughes, M. F. (2002) Arsenic toxicity and potential mechanisms of action. *Toxicology Letters* **133**, 1-16

22. Rahman, M. M., Chowdhury, U. K., Mukherjee, S. C., Mondal, B. K., Paul, K., Lodh, D., Biswas, B. K., Chanda, C. R., Basu, G. K., Saha, K. C., Roy, S., Das, R., Palit, S. K., Quamruzzaman, Q., and Chakraborti, D. (2001) Chronic arsenic toxicity in Bangladesh and West Bengal,

India - A review and commentary. *J Toxicol-Clin Toxic* **39**, 683-700

23. Mazumder, D. N. G., De, B. K., Santra, A., Dasgupta, J., Ghosh, N., Roy, B. K., Ghoshal, U. C., Saha, J., Chatterjee, A., Dutta, S., Haque, R., Smith, A. H., Chakraborty, D., Angle, C. R., and Centeno, J. A. (1999) Chronic arsenic toxicity: Epidemiology, natural history and treatment. *Arsenic Exposure and Health Effects*, 335-347

24. Alain, G., Tousignant, J., and Rozenfarb, E. (1993) Chronic Arsenic Toxicity. *Int J Dermatol* **32**, 899-901

25. Biswas, U., Sarkar, S., Bhowmik, M. K., Samanta, A. K., and Biswas, S. (2000) Chronic toxicity of arsenic in goats: clinicobiochemical changes, pathomorphology and tissue residues. *Small Ruminant Res* **38**, 229-235

26. Brix, K. V., Cardwell, R. D., and Adams, W. J. (2003) Chronic toxicity of arsenic to the Great Salt Lake brine shrimp, Artemia franciscana. *Ecotox Environ Safe* **54**, 169-175

27. Datta, S., Ghosh, D., Saha, D. R., Bhattacharaya, S., and Mazumder, S. (2009) Chronic exposure to low concentration of arsenic is immunotoxic to fish: Role of head kidney macrophages as biomarkers of arsenic toxicity to Clarias batrachus. *Aquat Toxicol* **92**, 86-94

28. Khandpur, S., Malhotra, A. K., Bhatia, V., Gupta, S., Sharma, V. K., Mishra, R., and Arora, N. K. (2008) Chronic arsenic toxicity from Ayurvedic medicines. *Int J Dermatol* **47**, 618-621

29. Mazumder, D. N. G. (2008) Chronic arsenic toxicity & human health. *Indian J Med Res* **128**, 436-447

30. Hughes, M. F. (2002) Arsenic toxicity and potential mechanisms of action. *Toxicol Lett* **133**, 1-16

31. Rossman, T. G. (2003) Mechanism of arsenic carcinogenesis: an integrated approach. *Mutat Res-Fund Mol M* **533**, 37-65

32. Lynch, H. N., Zu, K., Kennedy, E. M., Lam, T., Liu, X., Pizzurro, D. M., Loftus, C. T., and Rhomberg, L. R. (2017) Quantitative assessment of lung and bladder cancer risk and oral exposure to inorganic arsenic: Meta-regression analyses of epidemiological data (vol 106, pg 178, 2017). *Environ Int* **109**, 195-196

33. Hsu, K. H., Tsui, K. H., Hsu, L. I., Chiou, H. Y., and Chen, C. J. (2017) Dose-Response Relationship between Inorganic Arsenic Exposure and Lung Cancer among Arseniasis Residents with Low Methylation

Capacity. *Cancer Epidem Biomar* **26**, 756-761

34. Boulanger, M., Tual, S., Lemarchand, C., Guizard, A. V., Velten, M., Marcotullio, E., Baldi, I., Clin, B., Lebailly, P., and Registries, F. N. C. (2017) Lung Cancer And Arsenic Exposure In The Agricultural Workplace: Results Of The Agrican Cohort. *Am J Resp Crit Care* **195**

35. Tondel, M., Rahman, M., Magnuson, A., Chowdhury, I. A., Faruquee, M. H., and Ahmad, S. A. (1999) The relationship of arsenic levels in drinking water and the prevalence rate of skin lesions in Bangladesh. *Environ Health Persp* **107**, 727-729

36. HopenhaynRich, C. (1997) Bladder cancer mortality associated with arsenic in drinking water in Argentina (vol 7, pg 117, 1996). *Epidemiology* **8**, 334-334

37. Hopenhayn-Rich, C., Biggs, M. L., and Smith, A. H. (1998) Lung and kidney cancer mortality associated with arsenic in drinking water in Cordoba, Argentina. *International Journal of Epidemiology* **27**, 561-569

38. Uslu, R., Sanli, U. A., Sezgin, C., Karabulut, B., Terzioglu, E., Omay, S. B., and Goker, E. (2000) Arsenic trioxide-mediated cytotoxicity and apoptosis in prostate and ovarian carcinoma cell lines. *Clin Cancer Res* **6**, 4957-4964

39. Cohen, S. M., Ohnishi, T., Arnold, L. L., and Le, X. C. (2007) Arsenic-induced bladder cancer in an animal model. *Toxicol Appl Pharm* **222**, 258-263

40. Kitchin, K. T. (2001) Recent advances in arsenic carcinogenesis: Modes of action, animal model systems, and methylated arsenic metabolites. *Toxicol Appl Pharm* **172**, 249-261

41. Smith, A. H., Biggs, M. L., Moore, L., Haque, R., Steinmaus, C., Chung, J., Hernandez, A., and Lopipero, P. (1999) Cancer risks from arsenic in drinking water: Implications for drinking water standards. *Arsenic Exposure and Health Effects*, 191-199

42. Rossman, T. G., Uddin, A. N., Burns, F. J., and Bosland, M. C. (2001) Arsenite is a cocarcinogen with solar ultraviolet radiation for mouse skin: An animal model for arsenic carcinogenesis. *Toxicol Appl Pharm* **176**, 64-71

43. Simeonova, P. P., Wang, S. Y., Toriuma, W., Kommineni, V., Matheson, J., Unimye, N., Kayama, F., Harki, D., Ding, M., Vallyathan, V., and Luster, M. I. (2000) Arsenic mediates cell proliferation and gene expression in the bladder epithelium: Association with activating

protein-1 transactivation. *Cancer Res* **60**, 3445-3453

44. Zhang, F., Pararnasivam, M., Ca, Q., Dai, X. X., Wang, P. C., Lin, K., Song, J. K., Seidman, M. M., and Wang, Y. S. (2014) Arsenite Binds to the RING Finger Domains of RNF20-RNF40 Histone E3 Ubiquitin Ligase and Inhibits DNA Double-Strand Break Repair. *J Am Chem Soc* **136**, 12884-12887

45. Kitchin, K. T., and Conolly, R. (2010) Arsenic-Induced Carcinogenesis-Oxidative Stress as a Possible Mode of Action and Future Research Needs for More Biologically Based Risk Assessment. *Chem Res Toxicol* **23**, 327-335

46. Kitchin, K. T., and Ahmad, S. (2003) Oxidative stress as a possible mode of action for arsenic carcinogenesis. *Toxicology Letters* **137**, 3-13

47. Gebel, T., Christensen, S., and Dunkelberg, H. (1997) Comparative and environmental genotoxicity of antimony and arsenic. *Anticancer Res* **17**, 2603-2607

48. Aposhian, H. V., Zakharyan, R. A., Avram, M. D., Sampayo-Reyes, A., and Wollenberg, M. L. (2004) A review of the enzymology of arsenic metabolism and a new potential role of hydrogen peroxide in the detoxication of the trivalent arsenic species. *Toxicol Appl Pharm* **198**, 327-335

49. Yin, N. Y., Du, H. L., Zhang, Z. N., Cai, X. L., Li, Z. J., Sun, G. X., and Cui, Y. S. (2016) Variability of arsenic bioaccessibility and metabolism in soils by human gut microbiota using different in vitro methods combined with SHIME. *Sci Total Environ* **566**, 1670-1677

50. Raml, R., Raber, G., Rumpler, A., Bauernhofer, T., Goessler, W., and Francesconi, K. A. (2009) Individual Variability in the Human Metabolism of an Arsenic-Containing Carbohydrate, 2 ',3 '-Dihydroxypropyl 5-deoxy-5-dimethylarsinoyl-beta-D-riboside, a Naturally Occurring Arsenical in Seafood. *Chem Res Toxicol* **22**, 1534-1540

51. Loffredo, C. A., Aposhian, H. V., Cebrian, M. E., Yamauchi, H., and Silbergeld, E. K. (2003) Variability in human metabolism of arsenic. *Environmental Research* **92**, 85-91

52. Violante, A., and Pigna, M. (2002) Competitive sorption of arsenate and phosphate on different clay minerals and soils. *Soil Sci Soc Am J* **66**, 1788-1796

53. Gresser, M. J. (1981) ADP-arsenate. Formation by submitochondrial particles under phosphorylating conditions. *J Biol Chem* **256**, 5981-5983

54. Long, J. W., and Ray, W. J., Jr. (1973) Kinetics and thermodynamics of the formation of glucose arsenate. Reaction of glucose arsenate with phosphoglucomutase. *Biochemistry-Us* **12**, 3932-3937

55. Manning, B. A., and Goldberg, S. (1996) Modeling competitive adsorption of arsenate with phosphate and molybdate on oxide minerals. *Soil Sci Soc Am J* **60**, 121-131

56. Knowles, F. C. (1986) Enzymatic-Reactions Involving Orthoarsenate - Arsenate Is Competitive with Sulfate in the Atp Sulfurylase Reaction. *Arch Biochem Biophys* **251**, 767-770

57. Kitchin, K. T., and Wallace, K. (2006) Arsenite binding to synthetic peptides: The effect of increasing length between two cysteines. *J Biochem Mol Toxic* **20**, 35-38

58. Kitchin, K. T., and Wallace, K. (2005) Arsenite binding to synthetic peptides based on the Zn finger region and the estrogen binding region of the human estrogen receptor-alpha. *Toxicol Appl Pharmacol* **206**, 66-72

59. Petrick, J. S., Jagadish, B., Mash, E. A., and Aposhian, H. V. (2001) Monomethylarsonous acid (MMA(III)) and arsenite: LD50 in hamsters and in vitro inhibition of pyruvate dehydrogenase. *Chem Res Toxicol* **14**, 651-656

60. Samikkannu, T., Chen, C. H., Yih, L. H., Wang, A. S. S., Lin, S. Y., Chen, T. C., and Jan, K. Y. (2003) Reactive oxygen species are involved in arsenic trioxide inhibition of pyruvate dehydrogenase activity. *Chem Res Toxicol* **16**, 409-414

61. Rodriguez, V. M., Del Razo, L. M., Limon-Pacheco, J. H., Giordano, M., Sanchez-Pena, L. C., Uribe-Querol, E., Gutierrez-Ospina, G., and Gonsebatt, M. E. (2005) Glutathione reductase inhibition and methylated arsenic distribution in Cd1 mice brain and liver. *Toxicol Sci* **84**, 157-166

62. Shen, Z. X., Chen, G. Q., Ni, J. H., Li, X. S., Xiong, S. M., Qiu, Q. Y., Zhu, J., Tang, W., Sun, G. L., Yang, K. Q., Chen, Y., Zhou, L., Fang, Z. W., Wang, Y. T., Ma, J., Zhang, P., Zhang, T. D., Chen, S. J., Chen, Z., and Wang, Z. Y. (1997) Use of arsenic trioxide (As2O3) in the treatment of acute promyelocytic leukemia (APL): II. Clinical efficacy and pharmacokinetics in relapsed patients. *Blood* **89**, 3354-3360

63. Silver, A. S., and Wainman, P. L. (1952) Chronic Arsenic Poisoning Following Use of an Asthma Remedy. *Jama-J Am Med Assoc* **150**, 584-585

64. Howard, G., Ahmed, M. F., Teunis, P., Mahmud, S. G., Davison, A., and Deere, D. (2007) Disease burden estimation to support policy decision-making and research prioritization for arsenic mitigation. *J Water Health* **5**, 67-81

65. Farmer, J. G., and Johnson, L. R. (1990) Assessment of Occupational Exposure to Inorganic Arsenic Based on Urinary Concentrations and Speciation of Arsenic. *Brit J Ind Med* **47**, 342-348

66. Pickart, C. M. (2001) Mechanisms underlying ubiquitination. *Annu Rev Biochem* **70**, 503-533

67. Scheffner, M., Nuber, U., and Huibregtse, J. M. (1995) Protein Ubiquitination Involving an E1-E2-E3 Enzyme Ubiquitin Thioester Cascade. *Nature* **373**, 81-83

68. Hurley, J. H., Lee, S., and Prag, G. (2006) Ubiquitin-binding domains. *Biochem J* **399**, 361-372

69. Bienko, M., Green, C. M., Crosetto, N., Rudolf, F., Zapart, G., Coull, B., Kannouche, P., Wider, G., Peter, M., Lehmann, A. R., Hofmann, K., and Dikic, I. (2005) Ubiquitin-binding domains in Y-family polymerases regulate translesion synthesis. *Science* **310**, 1821-1824

70. Hicke, L., Schubert, H. L., and Hill, C. P. (2005) Ubiquitin-binding domains. *Nat Rev Mol Cell Bio* **6**, 610-621

71. Komander, D., and Rape, M. (2012) The Ubiquitin Code. *Annual Review of Biochemistry, Vol 81* **81**, 203-229

72. Valimberti, I., Tiberti, M., Lambrughi, M., Sarcevic, B., and Papaleo, E. (2015) E2 superfamily of ubiquitin-conjugating enzymes: constitutively active or activated through phosphorylation in the catalytic cleft. *Sci Rep-Uk* **5**

73. Polo, S., Sigismund, S., Faretta, M., Guidi, M., Capua, M. R., Bossi, G., Chen, H., De Camilli, P., and Di Fiore, P. P. (2002) A single motif responsible for ubiquitin recognition and monoubiquitination in endocytic proteins. *Nature* **416**, 451-455

74. Spence, J., Sadis, S., Haas, A. L., and Finley, D. (1995) A Ubiquitin Mutant with Specific Defects in DNA-Repair and Multiubiquitination. *Molecular and Cellular Biology* **15**, 1265-1273

75. Meyer, H. J., and Rape, M. (2014) Enhanced Protein Degradation by Branched Ubiquitin Chains. *Cell* **157**, 910-921

76. Tokarev, A. A., Munguia, J., and Guatelli, J. C. (2011) Serine-Threonine Ubiquitination Mediates Downregulation of BST-2/Tetherin and Relief of Restricted Virion Release by HIV-1 Vpu. *J Virol* **85**, 51-63

77. Wang, X. L., Herr, R. A., Chua, W. J., Lybarger, L., Wiertz, E. J. H. J., and Hansen, T. H. (2007) Ubiquitination of serine, threonine, or lysine residues on the cytoplasmic tail can induce ERAD of MHC-I by viral E3 ligase mK3. *J Cell Biol* **177**, 613-624

78. Cadwell, K., and Coscoy, L. (2005) Ubiquitination on nonlysine residues by a viral E3 ubiquitin ligase. *Science* **309**, 127-130

79. Zhang, Y. F., Li, D. Y., Zhang, H. J., Hong, Y. B., Huang, L., Liu, S. X., Li, X. H., Ouyang, Z. G., and Song, F. M. (2015) Tomato histone H2B monoubiquitination enzymes SlHUB1 and SlHUB2 contribute to disease resistance against Botrytis cinerea through modulating the balance between SA- and JA/ET-mediated signaling pathways. *Bmc Plant Biol* **15**

80. Kavathas, P., and Coman, M. (2014) The human CD8 beta isoforms differentially affect signal transduction pathways and monoubiquitination of the M4 isoform regulates signaling through the mTORC1/2/pathway. *J Immunol* **192**

81. Sigismund, S., Polo, S., and Di Fiore, P. P. (2004) Signaling through monoubiquitination. *Curr Top Microbiol* **286**, 149-185

82. Silva, G. M., Finley, D., and Vogel, C. (2015) K63 polyubiquitination is a new modulator of the oxidative stress response. *Nat Struct Mol Biol* **22**, 116-123

83. Deng, L., Wang, C., Spencer, E., Yang, L., Braun, A., You, J., Slaughter, C., Pickart, C., and Chen, Z. J. (2000) Activation of the IkappaB kinase complex by TRAF6 requires a dimeric ubiquitin-conjugating enzyme complex and a unique polyubiquitin chain. *Cell* **103**, 351-361

84. Marx, C., Held, J. M., Gibson, B. W., and Benz, C. C. (2010) ErbB2 trafficking and degradation associated with K48 and K63 polyubiquitination. *Cancer Res* **70**, 3709-3717

85. Wickliffe, K. E., Williamson, A., Meyer, H. J., Kelly, A., and Rape, M. (2011) K11-linked ubiquitin chains as novel regulators of cell division. *Trends Cell Biol* **21**, 656-663

86. Fang, J., Chen, T. P., Chadwick, B., Li, E., and Zhang, Y. (2004) Ring1b-mediated H2A ubiquitination associates with inactive X chromosomes and is involved in initiation of X inactivation. *J Biol Chem* **279**, 52812-52815

87. Metzger, M. B., Hristova, V. A., and Weissman, A. M. (2012) HECT and RING finger families of E3 ubiquitin ligases at a glance. *J Cell Sci* **125**, 531-537

88. Kamadurai, H. B., Qiu, Y., Deng, A., Harrison, J. S., MacDonald, C., Actis, M., Rodrigues, P., Miller, D. J., Souphron, J., Lewis, S. M., Kurinov, I., Fujii, N., Hammel, M., Piper, R., Kuhlman, B., and Schulman, B. A. (2013) Mechanism of ubiquitin ligation and lysine prioritization by a HECT E3. *Elife* **2**

89. Kumar, S., Kao, W. H., and Howley, P. M. (1997) Physical interaction between specific E2 and Hect E3 enzymes determines functional cooperativity. *J Biol Chem* **272**, 13548-13554

90. Scheffner, M., Huibregtse, J. M., Vierstra, R. D., and Howley, P. M. (1993) The Hpv-16 E6 and E6-Ap Complex Functions as a Ubiquitin-Protein Ligase in the Ubiquitination of P53. *Cell* **75**, 495-505

91. Ingham, R. J., Gish, G., and Pawson, T. (2004) The Nedd4 family of E3 ubiquitin ligases: functional diversity within a common modular architecture. *Oncogene* **23**, 1972-1984

92. Deshaies, R. J., and Joazeiro, C. A. P. (2009) RING Domain E3 Ubiquitin Ligases. *Annu Rev Biochem* **78**, 399-434

93. Ye, Y. H., and Rape, M. (2009) Building ubiquitin chains: E2 enzymes at work. *Nat Rev Mol Cell Bio* **10**, 755-764

94. Brzovic, P. S., Rajagopal, P., Hoyt, D. W., King, M. C., and Klevit, R. E. (2001) Structure of a BRCA1-BARD1 heterodimeric RING-RING complex. *Nat Struct Biol* **8**, 833-837

95. Hashizume, R., Fukuda, M., Maeda, I., Nishikawa, H., Oyake, D., Yabuki, Y., Ogata, F., and Ohta, T. (2001) The RING heterodimer BRCA1-BARD1 is a ubiquitin ligase inactivated by a breast cancer-derived mutation. *J Biol Chem* **276**, 14537-14540

96. Haupt, Y., Maya, R., Kazaz, A., and Oren, M. (1997) Mdm2 promotes the rapid degradation of p53. *Nature* **387**, 296-299

97. Witt, S. H., Granzier, H., Witt, C. C., and Labeit, S. (2005) MURF-1 and MURF-2 target a specific subset of myofibrillar proteins redundantly: Towards understanding MURF-dependent muscle ubiquitination. *J Mol Biol* **350**, 713-722

98. Bhat, K. P., Yan, S., Wang, C. E., Li, S. H., and Li, X. J. (2014) Differential ubiquitination and degradation of huntingtin fragments modulated by ubiquitin-protein ligase E3A. *P Natl Acad Sci USA* **111**, 5706-5711

99. Vodermaier, H. C. (2004) APC/C and SCF: Controlling each other and the cell cycle. *Curr Biol* **14**, R787-R796

100. Sudakin, V., Chan, G. K. T., and Yen, T. J. (2001) Checkpoint inhibition of the APC/C in HeLa cells is mediated by a complex of BUBR1, BUB3, CDC20, and MAD2. *J Cell Biol* **154**, 925-936

101. Petroski, M. D., and Deshaies, R. J. (2005) Function and regulation of Cullin-RING ubiquitin ligases. *Nat Rev Mol Cell Bio* **6**, 9-20

102. Duda, D. M., Scott, D. C., Calabrese, M. F., Zimmerman, E. S., Zheng, N., and Schulman, B. A. (2011) Structural regulation of cullin-RING ubiquitin ligase complexes. *Curr Opin Struc Biol* **21**, 257-264

103. Watanabe, M., Funakoshi, T., Unuma, K., Aki, T., and Uemura, K. (2014) Activation of the ubiquitin-proteasome system against arsenic trioxide cardiotoxicity involves ubiquitin ligase Parkin for mitochondrial homeostasis. *Toxicology* **322**, 43-50

104. Yan, W. S., Jung, Y. S., Zhang, Y. H., and Chen, X. B. (2014) Arsenic Trioxide Reactivates Proteasome-Dependent Degradation of Mutant p53 Protein in Cancer Cells in Part via Enhanced Expression of Pirh2 E3 Ligase. *Plos One* **9**

105. Tatham, M. H., Geoffroy, M. C., Shen, L., Plechanovova, A., Hattersley, N., Jaffray, E. G., Palvimo, J. J., and Hay, R. T. (2008) RNF4 is a poly-SUMO-specific E3 ubiquitin ligase required for arsenic-induced PML degradation. *Nature Cell Biology* **10**, 538-546

106. Erker, Y., Neyret-Kahn, H., Seeler, J. S., Dejean, A., Atfi, A., and Levy, L. (2013) Arkadia, a Novel SUMO-Targeted Ubiquitin Ligase Involved in PML Degradation. *Molecular and Cellular Biology* **33**, 2163-2177

107. Lander, E. S., Linton, L. M., Birren, B., Nusbaum, C., Zody, M. C., Baldwin, J., Devon, K., Dewar, K., Doyle, M., FitzHugh, W., Funke, R., Gage, D., Harris, K., Heaford, A., Howland, J., Kann, L., Lehoczky, J., LeVine, R., McEwan, P., McKernan, K., Meldrim, J., Mesirov, J. P.,

Miranda, C., Morris, W., Naylor, J., Raymond, C., Rosetti, M., Santos, R., Sheridan, A., Sougnez, C., Stange-Thomann, Y., Stojanovic, N., Subramanian, A., Wyman, D., Rogers, J., Sulston, J., Ainscough, R., Beck, S., Bentley, D., Burton, J., Clee, C., Carter, N., Coulson, A., Deadman, R., Deloukas, P., Dunham, A., Dunham, I., Durbin, R., French, L., Grafham, D., Gregory, S., Hubbard, T., Humphray, S., Hunt, A., Jones, M., Lloyd, C., McMurray, A., Matthews, L., Mercer, S., Milne, S., Mullikin, J. C., Mungall, A., Plumb, R., Ross, M., Shownkeen, R., Sims, S., Waterston, R. H., Wilson, R. K., Hillier, L. W., McPherson, J. D., Marra, M. A., Mardis, E. R., Fulton, L. A., Chinwalla, A. T., Pepin, K. H., Gish, W. R., Chissoe, S. L., Wendl, M. C., Delehaunty, K. D., Miner, T. L., Delehaunty, A., Kramer, J. B., Cook, L. L., Fulton, R. S., Johnson, D. L., Minx, P. J., Clifton, S. W., Hawkins, T., Branscomb, E., Predki, P., Richardson, P., Wenning, S., Slezak, T., Doggett, N., Cheng, J. F., Olsen, A., Lucas, S., Elkin, C., Uberbacher, E., Frazier, M., Gibbs, R. A., Muzny, D. M., Scherer, S. E., Bouck, J. B., Sodergren, E. J., Worley, K. C., Rives, C. M., Gorrell, J. H., Metzker, M. L., Naylor, S. L., Kucherlapati, R. S., Nelson, D. L., Weinstock, G. M., Sakaki, Y., Fujiyama, A., Hattori, M., Yada, T., Toyoda, A., Itoh, T., Kawagoe, C., Watanabe, H., Totoki, Y., Taylor, T., Weissenbach, J., Heilig, R., Saurin, W., Artiguenave, F., Brottier, P., Bruls, T., Pelletier, E., Robert, C., Wincker, P., Smith, D. R., Doucette-Stamm, L., Rubenfield, M., Weinstock, K., Lee, H. M., Dubois, J., Rosenthal, A., Platzer, M., Nyakatura, G., Taudien, S., Rump, A., Yang, H., Yu, J., Wang, J., Huang, G., Gu, J., Hood, L., Rowen, L., Madan, A., Qin, S., Davis, R. W., Federspiel, N. A., Abola, A. P., Proctor, M. J., Myers, R. M., Schmutz, J., Dickson, M., Grimwood, J., Cox, D. R., Olson, M. V., Kaul, R., Raymond, C., Shimizu, N., Kawasaki, K., Minoshima, S., Evans, G. A., Athanasiou, M., Schultz, R., Roe, B. A., Chen, F., Pan, H., Ramser, J., Lehrach, H., Reinhardt, R., McCombie, W. R., de la Bastide, M., Dedhia, N., Blocker, H., Hornischer, K., Nordsiek, G., Agarwala, R., Aravind, L., Bailey, J. A., Bateman, A., Batzoglou, S., Birney, E., Bork, P., Brown, D. G., Burge, C. B., Cerutti, L., Chen, H. C., Church, D., Clamp, M., Copley, R. R., Doerks, T., Eddy, S. R., Eichler, E. E., Furey, T. S., Galagan, J., Gilbert, J. G., Harmon, C., Hayashizaki, Y., Haussler, D., Hermjakob, H., Hokamp, K., Jang, W., Johnson, L. S., Jones, T. A., Kasif, S., Kaspryzk, A., Kennedy, S., Kent, W. J., Kitts, P., Koonin, E. V., Korf, I., Kulp, D., Lancet, D., Lowe, T. M., McLysaght, A., Mikkelsen, T., Moran, J. V., Mulder, N., Pollara, V. J., Ponting, C. P., Schuler, G., Schultz, J., Slater, G., Smit, A. F., Stupka, E., Szustakowki, J., Thierry-Mieg, D., Thierry-Mieg, J., Wagner, L., Wallis, J., Wheeler, R., Williams, A., Wolf, Y. I., Wolfe, K. H., Yang, S. P., Yeh, R. F., Collins, F., Guyer, M. S., Peterson, J., Felsenfeld, A., Wetterstrand, K. A., Patrinos, A., Morgan, M. J., de Jong, P., Catanese, J. J., Osoegawa, K., Shizuya, H., Choi, S., Chen, Y. J., Szustakowki, J., and International Human Genome Sequencing, C. (2001) Initial sequencing and analysis of the human genome. *Nature* **409**, 860-921

108. Ran, F. A., Hsu, P. D., Wright, J., Agarwala, V., Scott, D. A., and Zhang, F. (2013) Genome engineering using the CRISPR-Cas9 system. *Nat Protoc* **8**, 2281-2308

109. James, P. (1997) Protein identification in the post-genome era: the rapid rise of proteomics. *Q Rev Biophys* **30**, 279-331

110. Jensen, O. N. (2004) Modification-specific proteomics: characterization of post-translational modifications by mass spectrometry. *Curr Opin Chem Biol* **8**, 33-41

111. Nilsen, T. W., and Graveley, B. R. (2010) Expansion of the eukaryotic proteome by alternative splicing. *Nature* **463**, 457-463

112. Aebersold, R., and Mann, M. (2003) Mass spectrometry-based proteomics. *Nature* **422**, 198-207

113. Stave, J. W. (2002) Protein immunoassay methods for detection of biotech crops: Applications, limitations, and practical considerations. *J Aoac Int* **85**, 780-786

114. Mahmood, T., and Yang, P. C. (2012) Western blot: technique, theory, and trouble shooting. *N Am J Med Sci* **4**, 429-434

115. Engvall, E., and Perlmann, P. (1972) Enzyme-Linked Immunosorbent Assay, Elisa .3. Quantitation of Specific Antibodies by Enzyme-Labeled Anti-Immunoglobulin in Antigen-Coated Tubes. *J Immunol* **109**, 129-&

116. Ong, S. E., Blagoev, B., Kratchmarova, I., Kristensen, D. B., Steen, H., Pandey, A., and Mann, M. (2002) Stable isotope labeling by amino acids in cell culture, SILAC, as a simple and accurate approach to expression proteomics. *Molecular & Cellular Proteomics* **1**, 376-386

117. Wiese, S., Reidegeld, K. A., Meyer, H. E., and Warscheid, B. (2007) Protein labeling by iTRAQ: A new tool for quantitative mass spectrometry in proteome research. *Proteomics* **7**, 340-350

118. Bantscheff, M., Schirle, M., Sweetman, G., Rick, J., and Kuster, B. (2007) Quantitative mass spectrometry in proteomics: a critical review. *Anal Bioanal Chem* **389**, 1017-1031

119. Ho, Y., Gruhler, A., Heilbut, A., Bader, G. D., Moore, L., Adams, S. L., Millar, A., Taylor, P., Bennett, K., Boutilier, K., Yang, L. Y., Wolting, C., Donaldson, I., Schandorff, S., Shewnarane, J., Vo, M., Taggart, J., Goudreault, M., Muskat, B., Alfarano, C., Dewar, D., Lin, Z., Michalickova, K., Willems, A. R., Sassi, H., Nielsen, P. A., Rasmussen, K. J., Andersen, J. R., Johansen, L. E., Hansen, L. H., Jespersen, H.,

Podtelejnikov, A., Nielsen, E., Crawford, J., Poulsen, V., Sorensen, B. D., Matthiesen, J., Hendrickson, R. C., Gleeson, F., Pawson, T., Moran, M. F., Durocher, D., Mann, M., Hogue, C. W. V., Figeys, D., and Tyers, M. (2002) Systematic identification of protein complexes in Saccharomyces cerevisiae by mass spectrometry. *Nature* **415**, 180-183

120. Lambert, J. P., Ivosev, G., Couzens, A. L., Larsen, B., Taipale, M., Lin, Z. Y., Zhong, Q., Lindquist, S., Vidal, M., Aebersold, R., Pawson, T., Bonner, R., Tate, S., and Gingras, A. C. (2013) Mapping differential interactomes by affinity purification coupled with data-independent mass spectrometry acquisition. *Nat Methods* **10**, 1239-+

121. Mann, M., and Jensen, O. N. (2003) Proteomic analysis of post-translational modifications. *Nat Biotechnol* **21**, 255-261

122. Fenn, J. B., Mann, M., Meng, C. K., Wong, S. F., and Whitehouse, C. M. (1989) Electrospray Ionization for Mass-Spectrometry of Large Biomolecules. *Science* **246**, 64-71

123. Shen, Y., Tolic, N., Xie, F., Zhao, R., Purvine, S. O., Schepmoes, A. A., Moore, R. J., Anderson, G. A., and Smith, R. D. (2011) Effectiveness of CID, HCD, and ETD with FT MS/MS for degradomic-peptidomic analysis: comparison of peptide identification methods. *J Proteome Res* **10**, 3929-3943

124. Hart, S. R., Lau, K. W., Gaskell, S. J., and Hubbard, S. J. (2011) Distributions of ion series in ETD and CID spectra: making a comparison. *Methods Mol Biol* **696**, 327-337

125. Kim, S., Mischerikow, N., Bandeira, N., Navarro, J. D., Wich, L., Mohammed, S., Heck, A. J., and Pevzner, P. A. (2010) The generating function of CID, ETD, and CID/ETD pairs of tandem mass spectra: applications to database search. *Mol Cell Proteomics* **9**, 2840-2852

126. Sobott, F., Watt, S. J., Smith, J., Edelmann, M. J., Kramer, H. B., and Kessler, B. M. (2009) Comparison of CID versus ETD based MS/MS fragmentation for the analysis of protein ubiquitination. *J Am Soc Mass Spectrom* **20**, 1652-1659

127. Wu, S. L., Huhmer, A. F., Hao, Z., and Karger, B. L. (2007) On-line LC-MS approach combining collision-induced dissociation (CID), electron-transfer dissociation (ETD), and CID of an isolated charge-reduced species for the trace-level characterization of proteins with post-translational modifications. *J Proteome Res* **6**, 4230-4244

128. Scigelova, M., and Makarov, A. (2006) Orbitrap mass analyzer - Overview and applications in proteomics. *Proteomics*, 16-21

129. (2012) Ion-Trap and Time-of-Flight Mass Analysers. *Lc Gc Eur* **25**, 688-688

130. (2012) Quadrupole Mass Analyzers. *Lc Gc N Am* **30**, 1006-1006

131. Taylor, N., and Austin, D. E. (2012) A simplified toroidal ion trap mass analyzer. *Int J Mass Spectrom* **321**, 25-32

132. Kharchenko, A., Vladimirov, G., Heeren, R. M. A., and Nikolaev, E. N. (2012) Performance of Orbitrap Mass Analyzer at Various Space Charge and Non-Ideal Field Conditions: Simulation Approach. *J Am Soc Mass Spectr* **23**, 977-987

133. Kaur, S., Kamli, M. R., and Ali, A. (2011) Role of arsenic and its resistance in nature. *Can J Microbiol* **57**, 769-774

134. Kitchin, K. T. (2001) Recent advances in arsenic carcinogenesis: modes of action, animal model systems, and methylated arsenic metabolites. *Toxicol. Appl. Pharmacol.* **172**, 249-261

135. Shen, S., Li, X. F., Cullen, W. R., Weinfeld, M., and Le, X. C. (2013) Arsenic binding to proteins. *Chem Rev* **113**, 7769-7792

136. Zhou, X., Sun, X., Cooper, K. L., Wang, F., Liu, K. J., and Hudson, L. G. (2011) Arsenite interacts selectively with zinc finger proteins containing C3H1 or C4 motifs. *J Biol Chem* **286**, 22855-22863

137. Schwerdtle, T., Walter, I., and Hartwig, A. (2003) Arsenite and its biomethylated metabolites interfere with the formation and repair of stable BPDE-induced DNA adducts in human cells and impair XPAzf and Fpg. *DNA Repair (Amst)* **2**, 1449-1463

138. Asmuss, M., Mullenders, L. H., Eker, A., and Hartwig, A. (2000) Differential effects of toxic metal compounds on the activities of Fpg and XPA, two zinc finger proteins involved in DNA repair. *Carcinogenesis* **21**, 2097-2104

139. Ding, W., Liu, W., Cooper, K. L., Qin, X. J., de Souza Bergo, P. L., Hudson, L. G., and Liu, K. J. (2009) Inhibition of poly(ADP-ribose) polymerase-1 by arsenite interferes with repair of oxidative DNA damage. *J Biol Chem* **284**, 6809-6817

140. Zhang, F., Paramasivam, M., Cai, Q., Dai, X., Wang, P., Lin, K., Song, J., Seidman, M. M., and Wang, Y. (2014) Arsenite binds to the RING finger domains of RNF20-RNF40 histone E3 ubiquitin ligase and inhibits DNA double-strand break repair. *J Am Chem Soc* **136**, 12884-12887

141. Fierz, B., Chatterjee, C., McGinty, R. K., Bar-Dagan, M., Raleigh, D. P., and Muir, T. W. (2011) Histone H2B ubiquitylation disrupts local and higher-order chromatin compaction. *Nat Chem Biol* **7**, 113-119

142. Liu, S., Jiang, J., Li, L., Amato, N. J., Wang, Z., and Wang, Y. (2015) Arsenite targets the zinc finger domains of Tet proteins and inhibits Tet-mediated oxidation of 5-methylcytosine. *Environ. Sci. Technol.* **49**, 11923-11931

143. Wang, Z. Y., and Chen, Z. (2008) Acute promyelocytic leukemia: from highly fatal to highly curable. *Blood* **111**, 2505-2515

144. Zhang, X. W., Yan, X. J., Zhou, Z. R., Yang, F. F., Wu, Z. Y., Sun, H. B., Liang, W. X., Song, A. X., Lallemand-Breitenbach, V., Jeanne, M., Zhang, Q. Y., Yang, H. Y., Huang, Q. H., Zhou, G. B., Tong, J. H., Zhang, Y., Wu, J. H., Hu, H. Y., de The, H., Chen, S. J., and Chen, Z. (2010) Arsenic trioxide controls the fate of the PML-RARalpha oncoprotein by directly binding PML. *Science* **328**, 240-243

145. Kim, H., and D'Andrea, A. D. (2012) Regulation of DNA cross-link repair by the Fanconi anemia/BRCA pathway. *Genes Dev* **26**, 1393-1408

146. Wang, W. (2007) Emergence of a DNA-damage response network consisting of Fanconi anaemia and BRCA proteins. *Nat. Rev. Genet.* **8**, 735-748

147. Duxin, J. P., and Walter, J. C. (2015) What is the DNA repair defect underlying Fanconi anemia? *Curr. Opin. Cell Biol.* **37**, 49-60

148. Dao, K. H., Rotelli, M. D., Brown, B. R., Yates, J. E., Rantala, J., Tognon, C., Tyner, J. W., Druker, B. J., and Bagby, G. C. (2013) The PI3K/Akt1 pathway enhances steady-state levels of FANCL. *Mol Biol Cell* **24**, 2582-2592

149. Zhang, X., Yang, F., Shim, J. Y., Kirk, K. L., Anderson, D. E., and Chen, X. (2007) Identification of arsenic-binding proteins in human breast cancer cells. *Cancer Lett* **255**, 95-106

150. Kalef, E., and Gitler, C. (1994) Purification of vicinal dithiol-containing proteins by arsenical-based affinity chromatography. *Methods Enzymol* **233**, 395-403

151. Aygun, O., Svejstrup, J., and Liu, Y. (2008) A RECQ5-RNA polymerase II association identified by targeted proteomic analysis of human chromatin. *Proc Natl Acad Sci U S A* **105**, 8580-8584

152. Xiaoxia Dai, Y. W. (2013) Identification of Novel α-N-Methylation of CENP-B That Regulates Its Binding to the Centromeric DNA. *Journal of Proteome Research* **12**, 9

153. Ziv, Y., Bielopolski, D., Galanty, Y., Lukas, C., Taya, Y., Schultz, D. C., Lukas, J., Bekker-Jensen, S., Bartek, J., and Shiloh, Y. (2006) Chromatin relaxation in response to DNA double-strand breaks is modulated by a novel ATM- and KAP-1 dependent pathway. *Nat Cell Biol* **8**, 870-876

154. Martin, B. R., Giepmans, B. N., Adams, S. R., and Tsien, R. Y. (2005) Mammalian cell-based optimization of the biarsenical-binding tetracysteine motif for improved fluorescence and affinity. *Nat Biotechnol* **23**, 1308-1314

155. Muniandy, P. A., Liu, J., Majumdar, A., Liu, S. T., and Seidman, M. M. (2010) DNA interstrand crosslink repair in mammalian cells: step by step. *Crit Rev Biochem Mol Biol* **45**, 23-49

156. McCabe, K. M., Olson, S. B., and Moses, R. E. (2009) DNA interstrand crosslink repair in mammalian cells. *J Cell Physiol* **220**, 569-573

157. Kumaresan, K. R., Ramaswamy, M., and Yeung, A. T. (1992) Structure of the DNA interstrand cross-link of 4,5',8-trimethylpsoralen. *Biochemistry* **31**, 6774-6783

158. Burma, S., Chen, B. P., Murphy, M., Kurimasa, A., and Chen, D. J. (2001) ATM phosphorylates histone H2AX in response to DNA double-strand breaks. *J Biol Chem* **276**, 42462-42467

159. Agre, P., and Kozono, D. (2003) Aquaporin water channels: molecular mechanisms for human diseases. *FEBS Lett* **555**, 72-78

160. Klug, A., and Rhodes, D. (1987) Zinc fingers: a novel protein fold for nucleic acid recognition. *Cold Spring Harb Symp Quant Biol* **52**, 473-482

161. Freemont, P. S., Hanson, I. M., and Trowsdale, J. (1991) A novel cysteine-rich sequence motif. *Cell* **64**, 483-484

162. Lipkowitz, S., and Weissman, A. M. (2011) RINGs of good and evil: RING finger ubiquitin ligases at the crossroads of tumour suppression and oncogenesis. *Nat Rev Cancer* **11**, 629-643

163. D'Andrea, A. D. (2010) Susceptibility pathways in Fanconi's anemia and breast cancer. *N Engl J Med* **362**, 1909-1919

164. Garcia-Higuera, I., Taniguchi, T., Ganesan, S., Meyn, M. S., Timmers, C., Hejna, J., Grompe, M., and D'Andrea, A. D. (2001) Interaction of the fanconi anemia proteins and BRCA1 in a common pathway. *Molecular Cell* **7**, 249-262

165. Knipscheer, P., Raschle, M., Smogorzewska, A., Enoiu, M., Ho, T. V., Scharer, O. D., Elledge, S. J., and Walter, J. C. (2009) The Fanconi anemia pathway promotes replication-dependent DNA interstrand cross-link repair. *Science* **326**, 1698-1701

166. MacKay, C., Declais, A. C., Lundin, C., Agostinho, A., Deans, A. J., MacArtney, T. J., Hofmann, K., Gartner, A., West, S. C., Helleday, T., Lilley, D. M. J., and Rouse, J. (2010) Identification of KIAA1018/FAN1, a DNA Repair Nuclease Recruited to DNA Damage by Monoubiquitinated FANCD2. *Cell* **142**, 65-76

167. Nijman, S. M. B., Huang, T. T., Dirac, A. M. G., Brummelkamp, T. R., Kerkhoven, R. M., D'Andrea, A. D., and Bernards, R. (2005) The deubiquitinating enzyme USP1 regulates the Fanconi anemia pathway. *Molecular Cell* **17**, 331-339

168. Cole, A. R., Lewis, L. P., and Walden, H. (2010) The structure of the catalytic subunit FANCL of the Fanconi anemia core complex. *Nat Struct Mol Biol* **17**, 294-298

169. Jiang, J. Q., Ashekuzzaman, S. M., Jiang, A. L., Sharifuzzaman, S. M., and Chowdhury, S. R. (2013) Arsenic Contaminated Groundwater and Its Treatment Options in Bangladesh. *Int J Env Res Pub He* **10**, 18-46

170. Hastings, E., and Pepper, J. H. (1941) The distribution of sodium arsenite and diluent in the dust cloud. *J Econ Entomol* **34**, 769-772

171. Campos, V. L., Escalante, G., Yanez, J., Zaror, C. A., and Mondaca, M. A. (2009) Isolation of arsenite-oxidizing bacteria from a natural biofilm associated to volcanic rocks of Atacama Desert, Chile. *J Basic Microb* **49**, S93-S97

172. Rodriguez-Freire, L., Moore, S. E., Sierra-Alvarez, R., Root, R. A., Chorover, J., and Field, J. A. (2016) Arsenic remediation by formation of arsenic sulfide minerals in a continuous anaerobic bioreactor. *Biotechnol Bioeng* **113**, 522-530

173. Ramirez-Solis, A., Mukopadhyay, R., Rosen, B. P., and Stemmler, T. L. (2004) Experimental and theoretical characterization of arsenite in water: Insights into the coordination environment of As-O. *Inorg Chem* **43**, 2954-2959

174. Saint-Jacques, N., Brown, P., Nauta, L., Boxall, J., Parker, L., and Dummer, T. J. B. (2018) Estimating the risk of bladder and kidney cancer from exposure to low-levels of arsenic in drinking water, Nova Scotia, Canada. *Environ Int* **110**, 95-104

175. Chen, C. L., Chiou, H. Y., Hsu, L. I., Hsueh, Y. M., Wu, M. M., Wan, Y. H., and Chen, C. J. (2010) Arsenic in Drinking Water and Risk of Urinary Tract Cancer: A Follow-up Study from Northeastern Taiwan. *Cancer Epidem Biomar* **19**, 101-110

176. (2001) Study confirms cancer risk from arsenic in drinking water. *Chem Brit* **37**, 14-14

177. Smith, A., Lopipero, P., Chung, J., Haque, R., Hernandez, A., Moore, L., and Steinmaus, C. (2000) Arsenic in drinking water and cancer risks estimated from epidemiological studies in Argentina, Chile, Taiwan and Japan. *Epidemiology* **11**, S93-S93

178. Smith, A. H., Hopenhaynrich, C., Bates, M. N., Goeden, H. M., Hertzpicciotto, I., Duggan, H. M., Wood, R., Kosnett, M. J., and Smith, M. T. (1992) Cancer Risks from Arsenic in Drinking-Water. *Environ Health Persp* **97**, 259-267

179. Tam, L. M., Jiang, J., Wang, P. C., Li, L., Miao, W. L., Dong, X. J., and Wang, Y. S. (2017) Arsenite Binds to the Zinc Finger Motif of TIP60 Histone Acetyltransferase and Induces Its Degradation via the 26S Proteasome. *Chem Res Toxicol* **30**, 1685-1693

180. Jiang, J., Bellani, M., Li, L., Wang, P. C., Seidman, M. M., and Wang, Y. S. (2017) Arsenite Binds to the RING Finger Domain of FANCL E3 Ubiquitin Ligase and Inhibits DNA Interstrand Crosslink Repair. *Acs Chem Biol* **12**, 1858-1866

181. Kitchin, K. T., and Wallace, K. (2005) Arsenite binding to synthetic peptides based on the Zn finger region and the estrogen binding region of the human estrogen receptor-alpha. *Toxicol Appl Pharm* **206**, 66-72

182. Liu, S., Jiang, J., Li, L., Amato, N. J., Wang, Z., and Wang, Y. S. (2015) Arsenite Targets the Zinc Finger Domains of Tet Proteins and Inhibits Tet-Mediated Oxidation of 5-Methylcytosine. *Environ Sci Technol* **49**, 11923-11931

183. Voutsadakis, I. A. (2012) The ubiquitin-proteasome system and signal transduction pathways regulating Epithelial Mesenchymal transition of cancer. *J Biomed Sci* **19**

184. Lecker, S. H., Goldberg, A. L., and Mitch, W. E. (2006) Protein degradation by the ubiquitin-proteasome pathway in normal and disease states. *J Am Soc Nephrol* **17**, 1807-1819

185. Hochstrasser, M. (1996) Ubiquitin-dependent protein degradation. *Annu Rev Genet* **30**, 405-439

186. Grefen, C., Lalonde, S., and Obrdlik, P. (2007) Split-ubiquitin system for identifying protein-protein interactions in membrane and full-length proteins. *Curr Protoc Neurosci* **Chapter 5**, Unit 5 27

187. Callis, J. (2014) The ubiquitination machinery of the ubiquitin system. *Arabidopsis Book* **12**, e0174

188. Danielsen, J. M., Sylvestersen, K. B., Bekker-Jensen, S., Szklarczyk, D., Poulsen, J. W., Horn, H., Jensen, L. J., Mailand, N., and Nielsen, M. L. (2011) Mass spectrometric analysis of lysine ubiquitylation reveals promiscuity at site level. *Mol Cell Proteomics* **10**, M110 003590

189. Kirkpatrick, D. S., Denison, C., and Gygi, S. P. (2005) Weighing in on ubiquitin: the expanding role of mass-spectrometry-based proteomics. *Nat Cell Biol* **7**, 750-757

190. Huynh, M. L., Russell, P., and Walsh, B. (2009) Tryptic digestion of in-gel proteins for mass spectrometry analysis. *Methods Mol Biol* **519**, 507-513

191. Udeshi, N. D., Mani, D. R., Eisenhaure, T., Mertins, P., Jaffe, J. D., Clauser, K. R., Hacohen, N., and Carr, S. A. (2012) Methods for quantification of in vivo changes in protein ubiquitination following proteasome and deubiquitinase inhibition. *Mol Cell Proteomics* **11**, 148-159

192. Udeshi, N. D., Svinkina, T., Mertins, P., Kuhn, E., Mani, D. R., Qiao, J. W., and Carr, S. A. (2013) Refined Preparation and Use of Anti-diglycine Remnant (K-epsilon-GG) Antibody Enables Routine Quantification of 10,000s of Ubiquitination Sites in Single Proteomics Experiments. *Molecular & Cellular Proteomics* **12**, 825-831

193. Kim, W., Bennett, E. J., Huttlin, E. L., Guo, A., Li, J., Possemato, A., Sowa, M. E., Rad, R., Rush, J., Comb, M. J., Harper, J. W., and Gygi, S. P. (2011) Systematic and Quantitative Assessment of the Ubiquitin-Modified Proteome. *Mol Cell* **44**, 325-340

194. Xu, G. Q., Paige, J. S., and Jaffrey, S. R. (2010) Global analysis of lysine ubiquitination by ubiquitin remnant immunoaffinity profiling. *Nat Biotechnol* **28**, 868-U154

195. Hustoft, H. K., Malerod, H., Wilson, S. R., Reubsaet, L., Lundanes, E., and Greibrokk, T. (2012) A Critical Review of Trypsin Digestion for LC-MS Based Proteomics. *Integrative Proteomics*, 73-92

196. Gill, S., Stevenson, J., Kristiana, I., and Brown, A. (2011) Controlling cholesterol synthesis beyond HMG-CoA reductase. *Chem Phys Lipids* **164**, S6-S6

197. Udeshi, N. D., Mertins, P., Svinkina, T., and Carr, S. A. (2013) Large-scale identification of ubiquitination sites by mass spectrometry. *Nat Protoc* **8**, 1950-1960

198. Cerqueira, N. M. F. S. A., Oliveira, E. F., Gesto, D. S., Santos-Martins, D., Moreira, C., Moorthy, H. N., Ramos, M. J., and Fernandes, P. A. (2016) Cholesterol Biosynthesis: A Mechanistic Overview. *Biochemistry-Us* **55**, 5483-5506

199. Miao, H. H., Jiang, W., Ge, L. A., Li, B. L., and Song, B. L. (2010) Tetra-glutamic acid residues adjacent to Lys248 in HMG-CoA reductase are critical for the ubiquitination mediated by gp78 and UBE2G2. *Acta Bioch Bioph Sin* **42**, 303-310

200. Hwang, S., Hartman, I. Z., Calhoun, L. N., Garland, K., Young, G. A., Mitsche, M. A., McDonald, J., Xu, F., Engelking, L., and DeBose-Boyd, R. A. (2016) Contribution of Accelerated Degradation to Feedback Regulation of 3-Hydroxy-3-methylglutaryl Coenzyme A Reductase and Cholesterol Metabolism in the Liver. *J Biol Chem* **291**, 13479-13494

201. Jiang, W., and Song, B. L. (2014) Ubiquitin ligases in cholesterol metabolism. *Diabetes Metab J* **38**, 171-180

202. Loregger, A., Cook, E. C., Nelson, J. K., Moeton, M., Sharpe, L. J., Engberg, S., Karimova, M., Lambert, G., Brown, A. J., and Zelcer, N. (2015) A MARCH6 and IDOL E3 Ubiquitin Ligase Circuit Uncouples Cholesterol Synthesis from Lipoprotein Uptake in Hepatocytes. *Mol Cell Biol* **36**, 285-294

203. Kikkert, M., Doolman, R., Dai, M., Avner, R., Hassink, G., van Voorden, S., Thanedar, S., Roitelman, J., Chau, V., and Wiertz, E. (2004) Human HRD1 is an E3 ubiquitin ligase involved in degradation of proteins from the endoplasmic reticulum. *J Biol Chem* **279**, 3525-3534

204. Jo, Y., Lee, P. C. W., Sguigna, P. V., and DeBose-Boyd, R. A. (2011) Sterol-induced degradation of HMG CoA reductase depends on interplay of two Insigs and two ubiquitin ligases, gp78 and Trc8. *P Natl Acad Sci USA* **108**, 20503-20508

205. Lee, J. P., Brauweiler, A., Rudolph, M., Hooper, J. E., Drabkin, H. A., and Gemmill, R. M. (2010) The TRC8 Ubiquitin Ligase Is Sterol Regulated and Interacts with Lipid and Protein Biosynthetic Pathways. *Mol Cancer Res* **8**, 93-106

206. Zurn, A., Klenk, C., Zabel, U., Lohse, M. J., and Hoffmann, C. (2010) Site-Specific, Orthogonal Two Color Labeling of Different Proteins with Flash and Reash in Living Cells. *Biophys J* **98**, 392a-392a

207. Irtegun, S., Ramdzan, Y. M., Mulhern, T. D., and Hatters, D. M. (2011) ReAsH/FlAsH Labeling and Image Analysis of Tetracysteine Sensor Proteins in Cells. *Jove-J Vis Exp*

208. Udeshi, N. D., Mertins, P., Svinkina, T., and Carr, S. A. (2013) Large-scale identification of ubiquitination sites by mass spectrometry. *Nat Protoc* **8**, 1950-1960

209. Wagner, S. A., Beli, P., Weinert, B. T., Nielsen, M. L., Cox, J., Mann, M., and Choudhary, C. (2011) A Proteome-wide, Quantitative Survey of In Vivo Ubiquitylation Sites Reveals Widespread Regulatory Roles. *Molecular & Cellular Proteomics* **10**

210. Udeshi, N. D., Mani, D. R., Eisenhaure, T., Mertins, P., Jaffe, J. D., Clauser, K. R., Hacohen, N., and Carr, S. A. (2012) Methods for Quantification of in vivo Changes in Protein Ubiquitination following Proteasome and Deubiquitinase Inhibition. *Molecular & Cellular Proteomics* **11**, 148-159

211. Mertins, P., Qiao, J. W., Patel, J., Udeshi, N. D., Clauser, K. R., Mani, D. R., Burgess, M. W., Gillette, M. A., Jaffe, J. D., and Carr, S. A. (2013) Integrated proteomic analysis of post-translational modifications by serial enrichment. *Nat Methods* **10**, 634-+

212. Krause, M. R., and Regen, S. L. (2014) The Structural Role of Cholesterol in Cell Membranes: From Condensed Bilayers to Lipid Rafts. *Accounts Chem Res* **47**, 3512-3521

213. Rosenheim, O., and Webster, T. A. (1927) The relation of cholesterol to vitamin D. *Biochem J* **21**, 127-129

214. Javitt, N. B. (1994) Bile-Acid Synthesis from Cholesterol - Regulatory and Auxiliary Pathways. *Faseb J* **8**, 1308-1311

215. Qamar, A., and Bhatt, D. L. (2015) Effect of Low Cholesterol on Steroid Hormones and Vitamin E Levels Just a Theory or Real Concern? *Circ Res* **117**, 662-664

216. Buhaescu, I., and Izzedine, H. (2007) Mevalonate pathway: A review of clinical and therapeutical implications. *Clin Biochem* **40**, 575-584

217. Ye, J., and DeBose-Boyd, R. A. (2011) Regulation of Cholesterol and Fatty Acid Synthesis. *Csh Perspect Biol* **3**

218. Tsai, Y. C., Leichner, G. S., Pearce, M. M. P., Wilson, G. L., Wojcikiewicz, R. J. H., Roitelman, J., and Weissman, A. M. (2012) Differential regulation of HMG-CoA reductase and Insig-1 by enzymes of the ubiquitin-proteasome system. *Mol Biol Cell* **23**, 4484-4494

219. Schuhmacher-Wolz, U., Dieter, H. H., Klein, D., and Schneider, K. (2009) Oral exposure to inorganic arsenic: evaluation of its carcinogenic and non-carcinogenic effects. *Crit Rev Toxicol* **39**, 271-298

220. Lantz, R. C., and Hays, A. M. (2006) Role of oxidative stress in arsenic-induced toxicity. *Drug Metab Rev* **38**, 791-804

221. Kitchin, K. T. (2001) Recent advances in arsenic carcinogenesis: modes of action, animal model systems, and methylated arsenic metabolites. *Toxicol Appl Pharmacol* **172**, 249-261

222. Reichard, J. F., and Puga, A. (2010) Effects of arsenic exposure on DNA methylation and epigenetic gene regulation. *Epigenomics* **2**, 87-104

223. Chasapis, C. T., and Spyroulias, G. A. (2009) RING finger E(3) ubiquitin ligases: structure and drug discovery. *Curr Pharm Des* **15**, 3716-3731

224. Jiang, J., Bellani, M., Li, L., Wang, P., Seidman, M. M., and Wang, Y. (2017) Arsenite Binds to the RING Finger Domain of FANCL E3 Ubiquitin Ligase and Inhibits DNA Interstrand Crosslink Repair. *Acs Chem Biol* **12**, 1858-1866

225. Liu, S., Jiang, J., Li, L., Amato, N. J., Wang, Z., and Wang, Y. (2015) Arsenite Targets the Zinc Finger Domains of Tet Proteins and Inhibits Tet-Mediated Oxidation of 5-Methylcytosine. *Environ Sci Technol* **49**, 11923-11931

226. Ruiz-Ramos, R., Lopez-Carrillo, L., Rios-Perez, A. D., De Vizcaya-Ruiz, A., and Cebrian, M. E. (2009) Sodium arsenite induces ROS generation, DNA oxidative damage, HO-1 and c-Myc proteins, NF-kappaB activation and cell proliferation in human breast cancer MCF-7 cells. *Mutat Res* **674**, 109-115

227. Mittal, M., Siddiqui, M. R., Tran, K., Reddy, S. P., and Malik, A. B. (2014) Reactive oxygen species in inflammation and tissue injury. *Antioxid Redox Signal* **20**, 1126-1167

228. Rahman, M., Mofarrahi, M., Kristof, A. S., Nkengfac, B., Harel, S., and Hussain, S. N. (2014) Reactive oxygen species regulation of autophagy in skeletal muscles. *Antioxid Redox Signal* **20**, 443-459

229. Li, L., Ishdorj, G., and Gibson, S. B. (2012) Reactive oxygen species regulation of autophagy in cancer: implications for cancer treatment. *Free Radic Biol Med* **53**, 1399-1410

230. Ishdorj, G., Li, L., and Gibson, S. B. (2012) Regulation of autophagy in hematological malignancies: role of reactive oxygen species. *Leuk Lymphoma* **53**, 26-33

231. Azad, M. B., Chen, Y., and Gibson, S. B. (2009) Regulation of autophagy by reactive oxygen species (ROS): implications for cancer progression and treatment. *Antioxid Redox Signal* **11**, 777-790

232. Eblin, K. E., Hau, A. M., Jensen, T. J., Futscher, B. W., and Gandolfi, A. J. (2008) The role of reactive oxygen species in arsenite and monomethylarsonous acid-induced signal transduction in human bladder cells: acute studies. *Toxicology* **250**, 47-54

233. Huang, H. S., Chang, W. C., and Chen, C. J. (2002) Involvement of reactive oxygen species in arsenite-induced downregulation of phospholipid hydroperoxide glutathione peroxidase in human epidermoid carcinoma A431 cells. *Free Radic Biol Med* **33**, 864-873

234. Li, B., Li, X., Zhu, B., Zhang, X., Wang, Y., Xu, Y., Wang, H., Hou, Y., Zheng, Q., and Sun, G. (2013) Sodium arsenite induced reactive oxygen species generation, nuclear factor (erythroid-2 related) factor 2 activation, heme oxygenase-1 expression, and glutathione elevation in Chang human hepatocytes. *Environ Toxicol* **28**, 401-410

235. Kansanen, E., Kuosmanen, S. M., Leinonen, H., and Levonen, A. L. (2013) The Keap1-Nrf2 pathway: Mechanisms of activation and dysregulation in cancer. *Redox Biol* **1**, 45-49

236. Taguchi, K., Motohashi, H., and Yamamoto, M. (2011) Molecular mechanisms of the Keap1-Nrf2 pathway in stress response and cancer evolution. *Genes Cells* **16**, 123-140

237. Ma, Q. (2013) Role of nrf2 in oxidative stress and toxicity. *Annu Rev Pharmacol Toxicol* **53**, 401-426

238. Hu, C., Eggler, A. L., Mesecar, A. D., and van Breemen, R. B. (2011) Modification of keap1 cysteine residues by sulforaphane. *Chem Res Toxicol* **24**, 515-521

239. Zhang, D. D., and Hannink, M. (2003) Distinct cysteine residues in Keap1 are required for Keap1-dependent ubiquitination of Nrf2 and for stabilization of Nrf2 by chemopreventive agents and oxidative stress. *Mol Cell Biol* **23**, 8137-8151

240. Lau, A., Whitman, S. A., Jaramillo, M. C., and Zhang, D. D. (2013) Arsenic-mediated activation of the Nrf2-Keap1 antioxidant pathway. *J Biochem Mol Toxicol* **27**, 99-105

241. Wang, X. J., Sun, Z., Chen, W., Li, Y., Villeneuve, N. F., and Zhang, D. D. (2008) Activation of Nrf2 by arsenite and monomethylarsonous acid is independent of Keap1-C151: enhanced Keap1-Cul3 interaction. *Toxicol Appl Pharmacol* **230**, 383-389

242. Lau, A., Zheng, Y., Tao, S., Wang, H., Whitman, S. A., White, E., and Zhang, D. D. (2013) Arsenic inhibits autophagic flux, activating the Nrf2-Keap1 pathway in a p62-dependent manner. *Mol Cell Biol* **33**, 2436-2446

243. Wei, D., and Sun, Y. (2010) Small RING Finger Proteins RBX1 and RBX2 of SCF E3 Ubiquitin Ligases: The Role in Cancer and as Cancer Targets. *Genes Cancer* **1**, 700-707

244. Prasad, S., Mandal, I., Singh, S., Paul, A., Mandal, B., Venkatramani, R., and Swaminathan, R. (2017) Near UV-Visible electronic absorption originating from charged amino acids in a monomeric protein. *Chem Sci* **8**, 5416-5433

245. Heredia-Moya, J., and Kirk, K. L. (2008) An improved synthesis of arsenic-biotin conjugates. *Bioorg Med Chem* **16**, 5743-5746

246. Chivers, C. E., Koner, A. L., Lowe, E. D., and Howarth, M. (2011) How the biotin-streptavidin interaction was made even stronger: investigation via crystallography and a chimaeric tetramer. *Biochemical Journal* **435**, 55-63

247. Zhang, D. D., Lo, S. C., Cross, J. V., Templeton, D. J., and Hannink, M. (2004) Keap1 is a redox-regulated substrate adaptor protein for a Cul3-dependent ubiquitin ligase complex. *Molecular and Cellular Biology* **24**, 10941-10953

248. He, X., and Ma, Q. (2009) NRF2 cysteine residues are critical for oxidant/electrophile-sensing, Kelch-like ECH-associated protein-1-dependent ubiquitination-proteasomal degradation, and transcription activation. *Mol Pharmacol* **76**, 1265-1278

249. Hayes, J. D., McMahon, M., Chowdhry, S., and Dinkova-Kostova, A. T. (2010) Cancer Chemoprevention Mechanisms Mediated Through the Keap1-Nrf2 Pathway. *Antioxidants & Redox Signaling* **13**, 1713-1748

250. Kensler, T. W., Wakabayash, N., and Biswal, S. (2007) Cell survival responses to environmental stresses via the Keap1-Nrf2-ARE pathway. *Annual Review of Pharmacology and Toxicology* **47**, 89-116

251. Motohashi, H., and Yamamoto, M. (2004) Nrf2-Keap1 defines a physiologically important stress response mechanism. *Trends in Molecular Medicine* **10**, 549-557

252. Ma, Q., and He, X. Q. (2012) Molecular Basis of Electrophilic and Oxidative Defense: Promises and Perils of Nrf2. *Pharmacological Reviews* **64**, 1055-1081

253. Chan, K. M., Han, X. D., and Kan, Y. W. (2001) An important function of Nrf2 in combating oxidative stress: Detoxification of acetaminophen. *Proceedings of the National Academy of Sciences of the United States of America* **98**, 4611-4616

254. Klaassen, C. D., and Reisman, S. A. (2010) Nrf2 the rescue: Effects of the antioxidative/electrophilic response on the liver. *Toxicology and Applied Pharmacology* **244**, 57-65

255. He, X. Q., Chen, M. G., Lin, G. X., and Ma, Q. (2006) Arsenic induces NAD(P)H-quinone oxidoreductase I by disrupting the Nrf2 center dot Keap1 center dot Cul3 complex and recruiting Nrf2 center dot Maf to the antioxidant response element enhancer. *Journal of Biological Chemistry* **281**, 23620-23631

256. Kobayashi, A., Kang, M. I., Okawa, H., Ohtsuji, M., Zenke, Y., Chiba, T., Igarashi, K., and Yamamoto, M. (2004) Oxidative stress sensor Keap1 functions as an adaptor for Cul3-based E3 ligase to regulate for proteasomal degradation of Nrf2. *Molecular and Cellular Biology* **24**, 7130-7139

257. Lo, S. C., and Hannink, M. (2006) CAND1-mediated substrate adaptor recycling is required for efficient repression of Nrf2 by Keap1. *Molecular and Cellular Biology* **26**, 1235-1244

258. Eggler, A. L., Luo, Y., van Breemen, R. B., and Mesecar, A. D. (2007) Identification of the highly reactive cysteine 151 in the chemopreventive agent-sensor Keap1 protein is method-dependent. *Chemical Research in Toxicology* **20**, 1878-1884

259. Luo, Y., Eggler, A. L., Liu, D. T., Liu, G. W., Mesecar, A. D., and van Breemen, R. B. (2007) Sites of alkylation of human Keap1 by natural Chemoprevention agents. *Journal of the American Society for Mass Spectrometry* **18**, 2226-2232

260. McMahon, M., Lamont, D. J., Beattie, K. A., and Hayes, J. D. (2010) Keap1 perceives stress via three sensors for the endogenous signaling molecules nitric oxide, zinc, and alkenals. *Proceedings of the National Academy of Sciences of the United States of America* **107**, 18838-18843

261. Rusten, T. E., and Stenmark, H. (2010) p62, an autophagy hero or culprit? *Nat Cell Biol* **12**, 207-209

262. Chen, W. M., Sun, Z., Wang, X. J., Jiang, T., Huang, Z. P., Fang, D. Y., and Zhang, D. D. (2009) Direct Interaction between Nrf2 and p21(Cip1/WAF1) Upregulates the Nrf2-Mediated Antioxidant Response. *Molecular Cell* **34**, 663-673

263. Lo, S. C., and Hannink, M. (2008) PGAM5 tethers a ternary complex containing Keap1 and Nrf2 to mitochondria. *Experimental Cell Research* **314**, 1789-1803